US-CE-C

70-2

CONTRACT REPORT N-70-2

STRESS WAVES IN A SOIL-FILLED CYLINDRICAL SHELL

by

J. Kovarna, H. H. Bleich

LIBRARY
US ARMY ENGINEER WATERWAYS EXPERIMENT STATION
VICKSBURG, MISSISSIPPI

May 1970

Sponsored by Defense Atomic Support Agency

Conducted by U. S. Army Engineer Waterways Experiment Station, Vicksburg, Mississippi

Under Contract No. DACA39-67-C-0021

By Paul Weidlinger, Consulting Engineer, New York, New York

This document has been approved for public release and sale; its distribution is unlimited

CONTRACT REPORT N-70-2

STRESS WAVES IN A SOIL-FILLED CYLINDRICAL SHELL

by

J. Kovarna, H. H. Bleich

May 1970

Sponsored by Defense Atomic Support Agency

Conducted by U. S. Army Engineer Waterways Experiment Station, Vicksburg, Mississippi

Under Contract No. DACA39-67-C-0021

By Paul Weidlinger, Consulting Engineer, New York, New York

ARMY-MRC VICKSBURG, MISS.

This document has been approved for public release and sale; its distribution is unlimited

TA7
W34c
no. N-70-2
Cop. B

FOREWORD

This report was prepared by the firm of Paul Weidlinger, Consulting Engineer, of New York, New York, as an independent study under Contract DACA39-67-C-0021 with the U. S. Army Engineer Waterways Experiment Station under the sponsorship of the Defense Atomic Support Agency.

The contract was monitored technically by Mr. R. E. Walker, Project Manager, under the direction of Mr. W. J. Flathau, Chief of the Protective Structures Branch, and under the general direction of Mr. G. L. Arbuthnot, Jr., Chief of the Nuclear Weapons Effects Division, Waterways Experiment Station.

Contracting officers were COL John R. Oswalt, Jr., CE, and COL Levi A. Brown, CE, Directors of the Waterways Experiment Station.

75358

ABSTRACT

An approximate solution to the problem of transient longitudinal wave propagation in a semi-infinite cylindrical body of elasto-plastic material restrained radially by a stacked-ring shell and subjected to a normal pressure at the end is obtained by a Galerkin technique using the radial coordinate as an expansion parameter. In order to get equations applicable to numerical computations the expansions are truncated to the leading term in each variable. This truncation creates a mathematical problem when elastic and plastic regions occur along the same radial line.

A finite-difference scheme is used to solve the differential equations resulting from application and truncation of the Galerkin expansion. A special method for handling the boundary between elastic and plastic regions along the same radial line is developed in conjunction with this numerical solution.

Numerical results of the finite-difference scheme are presented for several variations in such parameters as shell stiffness and material constants.

For the purpose of evaluating the results of the truncation to the leading term in each expansion, the analogous problem is formulated for a linear inviscid fluid and solved twice, once with a truncation to the first term and once carrying two terms in each expansion. The numerical results are presented for these two solutions so that the change in the solution caused by the truncation can be evaluated.

TABLE OF CONTENTS

		Page
List of Major Symbols.		i
I	Introduction.	1
II	Formulation of Differential Equations	6
	a) Constitutive Relations	6
	b) Differential Equations in Plastic Regions. .	9
	c) Differential Equations in Elastic Regions. .	11
	d) Boundary Conditions.	11
III	Formulation of Integro-Differential Equations . .	15
IV	Removal of the Independent Variable r Through Use of the Galerkin Method.	22
	a) Application of Galerkin Method	23
	b) Special Case of Truncation to n=0.	26
	c) Boundaries between Elastic and Plastic Solutions.	28
V	Finite Difference Formulation	31
	a) Difference Equations	31
	b) Correction Algorithm at Interior Points j. .	36
	c) Correction Algorithm at the Boundary j=1 . .	39
VI	Discussion of Typical Numerical Results and Conclusion.	43
	a) Material Case 1.	43
	b) Comparison of Results for Materials of Cases 1 and 2 and of a Test.	46
	c) Considerations Concerning Truncation	48
	d) Conclusion	50

Page

Appendix A - Linear Inviscid Fluid - Influence of Truncation. 61

a) Equations for a Linear Inviscid Fluid. . . . 61

b) Nondimensional Governing Equations 63

c) Truncations. 64

d) Finite Difference Equations. 65

e) Discussion of Results. 67

Appendix B - Estimate for the Magnitude of the Material Constants. 73

a) Triaxial Test. 75

b) Uniaxial Test. 76

1) Elastic Phase $p < p_y$ 76

2) Compressive Yield Point 77

3) Plastic Phase (for k=0) 79

4) Elastic Point 80

5) Initial Tangent Modulus 81

6) Plastic Shock Velocity. 81

c) Discussion of the Fit Obtained 82

Appendix C - Selection of the Value of C_D in the Numerical Integration 89

References 93

LIST OF MAJOR SYMBOLS*)

$A = \rho_s h$	Shell mass parameter, Eq. (II-15).
$\bar{A} = \frac{A}{\rho r_o}$	Dimensionless shell mass parameter.
$\bar{A}_{mi} = \frac{A}{\rho r_o} + \frac{1}{2i+m+5}$	Dimensionless mass parameters generated by Galerkin method, Eqs. (A-10).
$a = \alpha\sqrt{3}$	Material parameter related to angle of internal friction, Eq. (B-11b).
$B = \frac{E_s h}{r_o^2}$	Shell stiffness parameter, Eq. (II-15).
$\bar{B} = \frac{B r_o}{K_o}$	Dimensionless shell stiffness parameter.
C	Viscosity parameter in axial boundary condition, Eq. (II-16).
C_D	Weighting coefficient in finite difference formulation, Eq. (V-3).
C_{11} , C_{12} , C_{21} , C_{22}	Dimensionless mass parameters defined in two term truncation for fluid, Eqs. (A-15).
$\bar{c}$	Plastic shock velocity, Eq. (B-21).
E_s	Young's modulus of shell material.
e_{ij}	Components of strain deviator.
e^E_{ij} , e^P_{ij}	Elastic and plastic parts of strain deviator.
F, $F(\sigma_{ij})$	Yield function and plastic potential, Eq. (II-1a).
$\bar{F}_c(p)$	Yield function for compressive range in uniaxial strain, Eq. (B-10).
$f(p)$	Integrated bulk modulus function, Eq. (B-7).
G	Shear modulus.
h	Shell thickness, Fig. 1.

*) Other symbols are defined as they are used in the text.

$J_1 = \sigma_{kk}$	First invariant of stress, Eqs. (II-2).
$J_2 = \frac{1}{2} s_{ij} s_{ij}$	Second invariant of stress deviator, Eqs. (II-2).
$K(p)$	Bulk modulus function, Eqs. (II-7).
$K_D = \frac{\Delta\bar{z}^2}{(2 + C_D)\,\Delta t}$	Coefficient of diffusion term in finite difference formulation.
K_o	Bulk modulus at zero pressure, Eq. (B-1a).
k	Material parameter defining cohesion, Eq. (II-1a).
M_{co}	Initial modulus in uniaxial strain, Eq. (B-20).
M_{To}	Initial modulus in triaxial test, Eq. (B-3a).
P_a , P_b	Zeros of yield function at the boundary in one term truncation, Eq. (V-26).
$P_i(z,t)$	Undetermined functions defining pressure in Galerkin method, Eqs. (IV-2).
$\bar{P}_i(\zeta,t)$	Dimensionless undetermined functions defining pressure in Galerkin method, Eqs. (A-5).
$p = -\frac{1}{3} J_1$	Mean pressure.
$\bar{p}$	Parameter in bulk modulus function, Eq. (B-1a).
p_c	Confining pressure in triaxial test.
p_E	Pressure defining elastic point in uniaxial strain, Eq. (B-18).
p_y	Pressure defining yield point in uniaxial strain.
$p_c(t)$	Applied surface pressure, Fig. 1.
$\bar{p}_o(\tau)$	Dimensionless surface pressure, Eqs. (A-5).
$R_i(z,t)$	Undetermined functions defining radial stress deviator in Galerkin method, Eqs. (IV-2).
r	Radial coordinate, Fig. 1.
r_o	Radius of shell, Fig. 1.

s_{ij}	Components of stress deviator.
$\bar{s}_{rz} = s_{rz}/r$	Quantity representing shear, Eqs. (II-18).
$T_i(z,t)$	Undetermined functions defining shear stress in Galerkin method, Eqs. (IV-2).
t	Time.
$U_i(z,t)$	Undetermined functions defining radial velocity in Galerkin method, Eqs. (IV-2).
$\bar{U}_i(\zeta,\tau)$	Dimensionless undetermined functions defining radial velocity in Galerkin method, Eqs. (A-5).
u_r	Radial component of displacement, Eq. (II-15).
$V_i(z,t)$	Undetermined functions defining axial velocity in Galerkin method, Eqs. (IV-2).
$\bar{V}_i(\zeta,\tau)$	Dimensionless undetermined functions defining axial velocity in Galerkin method, Eqs. (A-5).
v_r , v_z	Radial and axial components of velocity.
$\bar{v}_r = v_r/r$	Quantity representing radial velocity, Eqs. (II-18).
$Z_i(z,t)$	Undetermined functions defining axial stress deviator in Galerkin method, Eqs. (IV-2).
z	Axial coordinate, Fig. 1.
α	Material parameter related to angle of internal friction, Eq. (II-1a).
$\beta = \frac{3K_o}{2G}$	Dimensionless material parameter, Eq. (B-3b).
Δt, Δz	Coordinate increments in finite difference formulation, Fig. 2.
$\Delta\zeta$, $\Delta\tau$	Dimensionless coordinate increments in finite difference formulation.
ϵ	Arbitrarily small quantity used in limit process.
ϵ_{ij}	Components of strain.
ϵ^E_{ij} , ϵ^P_{ij}	Elastic and plastic parts of strain.
ζ	Dimensionless axial coordinate, Eqs. (A-5).

κ_{mj}	Functions generated from bulk modulus by Galerkin method, Eq. (IV-10).
$\kappa_j^n = K(P_j^n)$	Bulk modulus function in finite difference formulation of one term truncation, Eq. (V-12).
$\Lambda_i(z,t)$	Undetermined functions defining the function λ in Galerkin method, Eqs. (IV-2).
$\Lambda_{1\,a}^{n+1}$, $\Lambda_{1\,b}^{n+1}$	Roots of yield condition on the boundary in finite difference formulation of one term truncation, Eqs. (V-29a,b).
$\lambda \geq 0$	Function related to inelastic behavior, Eqs. (II-8a,b).
ξ	Dummy variable of integration.
ρ	Density of elasto-plastic material.
$\bar{\rho} = \rho + \frac{5A}{r_o}$	Combined density of shell and elasto-plastic material in one term truncation, Eq. (IV-19).
ρ_s	Density of shell material.
$\sigma_E = -(1 + 2a)p_E$	Axial stress at elastic point in uniaxial strain, Eq. (B-19).
σ_{ij}	Components of stress.
τ	Dimensionless time, Eqs. (A-5).
Φ	Integrated yield function in one term truncation, Eq. (IV-18).
Φ_b	Integrated yield function at the boundary in one term truncation, Eq. (V-26).

I INTRODUCTION.

To confirm the suitability of mathematical models for the dynamic behavior of materials, it is necessary to compare analytical results with those of tests. As a first step, because of better control and smaller cost, such tests will be laboratory ones. To be able to make comparisons computation procedures for configurations suitable for dynamic tests must be available. It is essential to study multidimensional situations, for which a suitable, yet simple, configuration consists of a cylindrical tube containing and restraining a cylindrical body of the material. The restraining tube is inherently necessary if the material is a soil, but for other materials the use of a restraining tube permits variation of the basic parameters of the tests, from nearly uniaxial strain for very rigid tubes, to multidimensional situations for (radially) extensible tubes. The variation of basic parameters in comparative tests is obviously desirable for confidence in the results. Moreover, a series of tests with different parameters might also be used, not as a confirmation, but to determine the material constants from dynamic tests.

Tests on soils of the nature described above have been undertaken, e.g., Ref. [1], in continuous tubes and also by confining the material by separate "stacked rings", Ref. [2]. The latter arrangement avoids longitudinal wave propagation in the tubes, a highly desirable simplification, and this paper presents an approach to analyzing longitudinal wave propagation

in a homogeneous and isotropic elasto-plastic material (of the Coulomb type) restrained by such rings. The approach can, however, equally be used for other material prescriptions. It is crucial that the approach presented permits the treatment of different material properties in regions with moving, a priori unknown boundaries. In the elasto-plastic case treated, there are regions where at a given instant the changes in strain are described by elastic relations, while in other regions plastic relations apply. The location of these regions is not known and changes with time. (Similar situations occur in materials where loading and unloading of an element of the material follows a different mathematical prescription such as postulated in Ref. [3].)

Problems of transient axisymmetric wave propagation in cylindrical bodies of inelastic or nonlinear materials can be treated only by purely numerical computations, or by approximate approaches. Because of its influence on nearly all subsequent literature, the earliest approximate approach for harmonic wave propagation in an elastic cylindrical bar, Ref. [4], is mentioned. By postulating the radial dependence of the displacements and introducing weighted average stresses, the approach reduces the problem from three independent variables z, r and t to one in the longitudinal coordinate z and the time t. The result is a system of two simultaneous second order partial differential equations containing corrective terms for shear and radial inertia, not present in the conventional single second order

differential equation for one dimensional wave propagation. This paper was later followed, Ref. [5], by an analysis based on a series expansion of the radial dependence of the displacements, permitting higher order theories leading to a larger number of simultaneous partial differential equations in z and t.

While formulated in various ways, available treatments of transient wave propagation in cylindrical bodies may be classified as being first order theories as Ref. [4], or of higher order. First order sclutions are available for the elastic bar, Ref. [6], for a linearly viscoelastic bar, Ref. [7], and for a nonlinearly strain rate dependent material, Ref. [8]. The latter has been generalized, Ref. [9], for the case of stacked rings and by the inclusion of a further term in the axial displacement and the corresponding stress term, so that the theory corresponds to Ref. [5].

The present paper will use the Galerkin approach to obtain approximate solutions which may be carried to first order terms corresponding to Ref. [4] or to a higher approximation. It should be mentioned that an alternate approach by power series expansion of both displacements and stresses in the radial coordinate, capable of similar refinement, was used in Ref. [10] for the case of an elastic plastic rod. The use of power series leads inherently to lower accuracy, and is thus less efficient than the use of the Galerkin method employing the same number of terms.

The present approach is as follows. In Section II the differential equations and boundary and initial conditions of the problem are formulated in elastic and plastic regions in three independent variables, the two space variables r and z, and the time t. The Galerkin approach to eliminate the variable r is, however, not directly applied to the differential equations because it is not possible to select functions in r which satisfy the boundary conditions due to the stacked rings at the cylindrical surface of the body. By converting the partial differential equations in z, r and t in Section III into a set of integral equations in r, but retaining partial differential equations in z and t, the boundary conditions on $r=r_o$ no longer appear explicitly. Consequently, appropriate expansion functions can be selected without regard to requirements on the boundary. This leads, Section IV, to a system of hyperbolic partial differential equations in z and t.

Complications arise in Section III when the material in a location z acts elastically for some values of r, plastically in others, i.e., in locations where the interface between elastic and plastic regions intersects the plane z = constant. It is crucial that an approach to overcome this difficulty is developed in conjunction with the finite difference solution of the system of partial differential equations.

A typical example is treated using an elasto-plastic material with a nonlinear (hardening) pressure-volume relation.

The properties of this material are taken from static tests as described in Appendix B. The pressure input at the end of the tube is selected in one case as gradually increasing to a peak value, a situation for which a test is available. As a second example a pressure jump with subsequently decaying pressure is applied. In both examples the computation used only one expansion term for each of the seven dependent variables. To judge the reasonableness of the use of only one term in the examples, Appendix A gives comparative results using one and two terms for a liquid.

II FORMULATION OF DIFFERENTIAL EQUATIONS.

The purpose of this analysis is the study of longitudinal wave propagation in a semi-infinite circular cylindrical body of elasto-plastic material, Fig. 1. It is intended to consider only the rotationally symmetric case where the end surface $z=0$ is subjected to a uniform applied pressure $p_o(t)$, while the cylindrical surface of the body is restrained against radial motion by a thin elastic shell consisting of narrow rings which are (in the z-direction) not in contact with each other. The type of shell described represents an experimental arrangement of stacked rings intended to prevent longitudinal wave propagation in the containing shell. The analysis is based on the premise that the strains and velocities are small enough to justify the use of linearized equations of motion, and of linearized relations between strain rates and velocities.

a) Constitutive Relations.

The elasto-plastic material considered here is described by the yield function and plastic potential

$$F = J_2 - (k - \alpha J_1)^2 \qquad \text{(II-1a)}$$

subject to the requirement

$$k - \alpha J_1 \geq 0 \qquad \text{(II-1b)}$$

both proposed in Ref. [11] for granular materials. The

quantities J_1 and J_2 are the invariants

$$J_1 = \sigma_{kk} \quad , \quad J_2 = \frac{1}{2} s_{ij} s_{ij} \tag{II-2}$$

where σ_{ij} are the stresses and s_{ij} are the stress deviators. The constants k and α are properties of the material, with k a measure of the cohesion and α related to the slip angle. Their values are restricted, Ref. [11], to

$$k > 0 \quad , \quad \frac{1}{\sqrt{12}} > \alpha \geq 0 \tag{II-3}$$

The state of stress in the medium must satisfy not only the inequality (1b) but also the inequality

$$F \leq 0 \tag{II-4}$$

The behavior of the material is then described by the following two statements:

(i) When in an element in space and during an interval in time the inequality sign in Eq. (4) applies, or when the equality sign applies in conjunction with $\dot{F} < 0$, then the medium is acting elastically and the actual strain rates $\dot{\varepsilon}_{ij}$ are equal to those obtained from the elastic relations,

$$\dot{\varepsilon}_{ij} = \dot{\varepsilon}^E_{ij} \tag{II-5}$$

(ii) When, however, the equality sign in Eq. (4) applies while the value of the yield function does not change, F=0, the medium yields or may yield, and the strain rates are the sum of the elastic values $\dot{\varepsilon}^E_{ij}$ and a plastic contribution $\dot{\varepsilon}^P_{ij}$,

$$\dot{\varepsilon}_{ij} = \dot{\varepsilon}^E_{ij} + \dot{\varepsilon}^P_{ij} \qquad \text{(II-6)}$$

The elastic strain rates $\dot{\varepsilon}^E_{ij}$ can be separated into the sum of a volumetric and of a deviatoric part, $\dot{\varepsilon}^E_{kk}$ and $\dot{e}^E_{ij}$. To express the hardening behavior observed in uniaxial tests on soil, the bulk modulus $K = K(p)$ will be considered as an appropriate function of the mean pressure $p = -J_1/3$, while the modulus of rigidity G is a constant. The elastic relations are then

$$\dot{\varepsilon}^E_{kk} = -\frac{1}{K(p)}\,\dot{p} \quad , \quad \dot{e}^E_{ij} = \frac{1}{2G}\,\dot{s}_{ij} \qquad \text{(II-7)}$$

The plastic strain rates are obtained in the conventional manner from the plastic potential,

$$\dot{\varepsilon}^P_{ij} = \lambda\,\frac{\partial F}{\partial \sigma_{ij}}$$

with the result

$$\dot{\varepsilon}^P_{kk} = 6\alpha\lambda(k + 3\alpha p) \quad , \quad \dot{e}^P_{ij} = \lambda s_{ij} \qquad \text{(II-8a)}$$

where λ is an open function of time and space, restricted by

$$\lambda \geq 0 \qquad \text{(II-8b)}$$

The energy dissipation in any element at any instant is proportional to $k\lambda$. The value of k being positive, energy will be actually dissipated only if $\lambda > 0$, the special case when λ vanishes is referred to as neutral.

The behavior of the material in elastic regions is described by Eqs. (5) and (7), while in plastic regions

Eqs. (4), (6), (7) and (8) hold. In the solution to be obtained elastic and plastic regions will, in general, both occur. They are, in general, separated by one or more distinct*) boundary surfaces of a priori unknown and time dependent location. The occurrence of moving boundaries introduces complexities into the solution, a matter to be discussed later.

A comment concerning the inequality (1b), requiring $k - \alpha J_1 \geq 0$ must be made. It should be understood that the constitutive relations given are valid only if the inequality holds, no relations are proposed here which would apply in the excluded region, in which the material has disintegrated. If it is found that a solution begins to violate the inequality at a certain time, the results at subsequent times are meaningless. In such cases the present approach leads to no result. (The situation is quite similar to the one in hydrodynamics, where the conventional solutions lose validity at the onset of cavitation.) Equation (1b) is not part of the equations to be solved, but is only to be applied as a final check to confirm the validity of results obtained without its use.

b) Differential Equations in Plastic Regions.

Due to the axial symmetry there are just four meaningful relations between strain rates and velocities,

*) In special situations not expected in the problem to be treated here, the distinct boundaries may degenerate into neutral regions within which elastic relations, or plastic ones with $\lambda=0$, may be used interchangeably.

$$\left.\begin{aligned} \dot{\varepsilon}_{rr} &= \frac{\partial v_r}{\partial r} \\ \dot{\varepsilon}_{\theta\theta} &= \frac{v_r}{r} \\ \dot{\varepsilon}_{zz} &= \frac{\partial v_z}{\partial z} \\ \dot{\varepsilon}_{rz} &= \frac{1}{2}\left(\frac{\partial v_r}{\partial z} + \frac{\partial v_z}{\partial r}\right) \end{aligned}\right\} \qquad \text{(II-9)}$$

Introduction of the constitutive relations and elimination of $s_{\theta\theta} = -(s_{rr} + s_{zz})$ gives

$$2\frac{\partial v_r}{\partial r} - \frac{v_r}{r} - \frac{\partial v_z}{\partial z} = \frac{3}{2G}\frac{\partial s_{rr}}{\partial t} + 3\lambda s_{rr} \qquad \text{(II-10a)}$$

$$-\frac{\partial v_r}{\partial r} - \frac{v_r}{r} + 2\frac{\partial v_z}{\partial z} = \frac{3}{2G}\frac{\partial s_{zz}}{\partial t} + 3\lambda s_{zz} \qquad \text{(II-10b)}$$

$$\frac{\partial v_r}{\partial r} + \frac{v_r}{r} + \frac{\partial v_z}{\partial z} = -\frac{1}{K(p)}\frac{\partial p}{\partial t} + 6\alpha\lambda(k + 3\alpha p) \qquad \text{(II-10c)}$$

$$\frac{\partial v_r}{\partial z} + \frac{\partial v_z}{\partial r} = \frac{1}{G}\frac{\partial s_{rz}}{\partial t} + 2\lambda s_{rz} \qquad \text{(II-10d)}$$

The relation F=0 which must be satisfied in plastic regions becomes

$$F(\sigma_{ij}) = s_{rr}^2 + s_{rr}s_{zz} + s_{zz}^2 + s_{rz}^2 - (k + 3\alpha p)^2 = 0 \qquad \text{(II-11)}$$

In addition there are two equations of motion,

$$\frac{\partial s_{rr}}{\partial r} + \frac{2s_{rr}}{r} + \frac{\partial s_{rz}}{\partial z} + \frac{s_{zz}}{r} - \frac{\partial p}{\partial r} = \rho\frac{\partial v_r}{\partial t} \qquad \text{(II-12a)}$$

$$\frac{\partial s_{rz}}{\partial r} + \frac{s_{rz}}{r} + \frac{\partial s_{zz}}{\partial z} - \frac{\partial p}{\partial z} = \rho\frac{\partial v_z}{\partial t} \qquad \text{(II-12b)}$$

In plastic regions Eqs. (10), (12) and the time derivative of Eq. (11) may be considered to be a set of seven quasi-linear differential equations on seven dependent variables, the four quantities defining the state of stress, s_{rr} , s_{zz} , s_{rz} and p, the two velocities v_r and v_z and a variable L defined by $\dot{L}=\lambda$. In such a formulation, the yield condition Eq. (11) must be added as an initial condition at the instant t when plastic action starts in a particular location.

c) Differential Equations in Elastic Regions.

In elastic regions the relations

$$F < 0 \qquad \text{(II-13a)}$$

or

$$F = 0 \quad \text{and} \quad \dot{F} < 0 \qquad \text{(II-13b)}$$

apply in lieu of Eq. (11). In such regions the six quasi-linear differential equations (10) and (12) apply provided $\lambda \equiv 0$ is introduced into Eqs. (10).

d) Boundary Conditions.

In the problem to be treated, Fig. 1, a uniform pressure $p_o(t)$ is applied for $t \geq 0$ at the loaded end of the cylindrical body, z=0, while the shear stress at z=0 vanishes,

$$\left.\begin{aligned} [s_{zz} - p]_{z=0} &= -p_o(t) \\ [s_{rz}]_{z=0} &= 0 \end{aligned}\right\} \qquad \text{(II-14)}$$

where $p_o(t) = 0$ if $t < 0$.

The cylindrical surface $r = r_o$ is restrained by a shell consisting of "stacked elastic rings". The latter are assumed not to interact with one another but to be able to move radially and axially in response to the stress exerted by the adjacent material. In the radial direction it will be assumed that contact between the material of the cylindrical body and the rings is maintained, so that the radial displacement of any ring is equal to the displacement $[u_r]_{r=r_o}$ of the adjoining material. The radial motion due to the radial stress $\sigma_{rr} = s_{rr} - p$ is thus described by the differential equation

$$[s_{rr} - p + Bu_r + A\ddot{u}_r]_{r=r_o} = 0 \qquad \text{(II-15)}$$

where

$$A = \rho_s h \quad , \quad B = \frac{E_s h}{r_o^2}$$

ρ_s and E_s being the density and Young's modulus of the material of the rings, respectively, and h their thickness in the radial direction. The relations concerning axial motion given below apply for a shear stress $\left[s_{rz}\right]_{r=r_o}$ caused by viscous friction. If the axial velocity of the shell is v_{sz}, the shear stress is

$$\left[s_{rz}\right]_{r=r_o} = C(v_{sz} - [v_z]_{r=r_o}) \qquad \text{(II-16)}$$

where $C \geq 0$. Using the equation of motion of the rings to eliminate v_{sz} gives finally

$$[\dot{s}_{rz} + \frac{C}{A} s_{rz} + C\,\dot{v}_z]_{r=r_o} = 0 \qquad \text{(II-17)}$$

The two ordinary differential equations (15) and (17) are the required boundary conditions.

In addition to these boundary conditions at z=0 and $r = r_o$, the solution must satisfy requirements at the boundary r=0. In this location all quantities must be finite and, for reasons of continuity, the quantities s_{rz} and v_r must vanish. In view of the manipulation to be performed later, it is convenient to replace s_{rz} and v_r by new variables $\bar{s}_{rz}$ and $\bar{v}_r$,

$$s_{rz} = r\,\bar{s}_{rz} \quad , \quad v_r = r\,\bar{v}_r \qquad \text{(II-18)}$$

This substitution ensures that s_{rz} and v_r vanish at r=0 and thus permits the simpler statement that all unknowns p, s_{rr}, s_{zz}, $\bar{s}_{rz}$, v_z, $\bar{v}_r$ and λ must remain finite at r=0.

The boundary conditions at the external surfaces of the cylindrical body, Eqs. (14), (15) and (17), and the requirements at r=0 apply without regard whether the elastic, or plastic differential equations apply in the adjoining material.

However, additional conditions must be formulated at the internal boundaries separating elastic and plastic regions.

At such boundaries, which in general vary with time, two possibilities must be distinguished. In the first case no discontinuities in stresses, velocities or displacements occur, and the appropriate conditions are simply continuity of these quantities with the added requirement that the stresses at the boundaries satisfy Eq. (11). In the second case, when dis-

continuities occur, the latter may occur only in the components of the direct stress and of the particle velocity normal to the bounding surface, and/or in the components of shear stress and of the particle velocity in the tangent plane to the bounding surface. The respective stresses, particle velocities and the local velocity of propagation of the discontinuity must satisfy appropriate Rankine-Hugoniot relations. The numerical solutions to be obtained later are based on finite difference methods where discontinuities are smoothed out, so that the relations at discontinuities will not be required and the further treatment will consider only continuity of stresses, particle velocities and displacements. (It is noted that the requirement of continuity does not include the quantity λ.)

III FORMULATION OF INTEGRO-DIFFERENTIAL EQUATIONS.

The boundary value problem in the three independent variables z, r and t posed by the equations formulated in the preceding section can be solved numerically by finite difference methods in a routine manner, the only drawback being the necessity for a large enough computer and the required computation time. As an alternative the present paper will proceed with a more approximate numerical solution based on the Galerkin method. By expanding the solution in terms of suitably selected functions of r, the problem will be converted into one with only two independent variables. In comparison with the solution of the equations in three independent variables, this approach is of course of advantage only in situations where one or two expansion functions give sufficient accuracy.

If one could choose simple expansion functions which satisfy the boundary conditions, the operations necessary for the use of the Galerkin method could be performed in a straightforward manner on the differential equations derived in the preceding section. However, the boundary conditions at $r = r_o$, Eqs. (II-15) and (II-17), are differential equations with respect to time, so that expansion functions cannot be chosen in such a manner. Procedures when the expansion functions do not satisfy the boundary conditions of the differential equations are discussed in Ref. [12] for the method of weighted residuals*), but the approach still requires essentially arbitrary decisions by the analyst concerning the weighting.

*) This method is more general than the Galerkin one and contains the latter as a special case.

The complications resulting from expansion functions which do not satisfy boundary conditions disappear if the equations to be solved are integral equations, in which case the boundary conditions required for differential equations no longer appear explicitly. To use this approach the results obtained in Section II are converted into an equivalent system of integral equations with respect to r, retaining differential equations with respect to z and t. The new formulation is obtained by integration of the differential equations over the area of the cross-section and integration by parts, so that derivatives with respect to r disappear. The boundary terms resulting from the integration by parts are then eliminated by use of the boundary conditions at $r = r_o$ and by the requirement of finiteness at r=0. The resulting system in plastic regions is

$$-r(\dot{s}_{rr} - \dot{p} + rB\bar{v}_r + rA\ddot{\bar{v}}_r) = \int_r^{r_o} \{[-\dot{s}_{rr} - \dot{s}_{zz} - \dot{p} - \xi^2\dot{\bar{s}}'_{rz} + \xi^2\rho\ddot{\bar{v}}_r] +$$

$$+ B[2\xi v'_z - \xi \frac{3}{2G}\dot{s}_{zz} - \xi\, 3\lambda\, s_{zz}] +$$

$$+ A[2\xi\ddot{v}'_z - \xi \frac{3}{2G}\dddot{s}_{zz} - \xi\, 3(\ddot{\lambda}\, s_{zz} + 2\dot{\lambda}\,\dot{s}_{zz} + \lambda\,\ddot{s}_{zz})]\}d\xi \qquad \text{(III-1)}$$

$$-r(r\dot{\bar{s}}_{rz} + r\frac{C}{A}\bar{s}_{rz} + C\dot{v}_z) = \int_r^{r_o} \{[-\xi\,\dot{s}'_{zz} + \xi\dot{p}' + \xi\rho\ddot{v}_z] +$$

$$+ \frac{C}{A}[-\xi\, s'_{zz} + \xi p' + \xi\rho\dot{v}_z] +$$

$$+ C\frac{\partial}{\partial t}[v_z - \xi^2\bar{v}'_r + \xi^2\frac{1}{G}\dot{\bar{s}}_{rz} + \xi^2\, 2\lambda\,\bar{s}_{rz}]\}d\xi \qquad \text{(III-2)}$$

$$2r^2\bar{v}_r = \int_0^r (3\xi\ \bar{v}_r + \xi\ v_z' + \xi\ \frac{3}{2G}\ \dot{s}_{rr} + \xi\ 3\lambda\ s_{rr})d\xi \qquad \text{(III-3)}$$

$$r^2\bar{v}_r = \int_0^r (\xi\ 2v_z' - \xi\ \frac{3}{2G}\ \dot{s}_{zz} - \xi\ 3\lambda\ s_{zz})d\xi \qquad \text{(III-4)}$$

$$r^2\bar{v}_r = \int_0^r [-\xi\ v_z' - \xi\ \frac{1}{K(p)}\ \dot{p} + \xi\ 6\alpha\lambda(k + 3\alpha p)]d\xi \qquad \text{(III-5)}$$

$$rv_z = \int_0^r (v_z - \xi^2\bar{v}_r' + \xi^2\ \frac{1}{G}\ \dot{\bar{s}}_{rz} + \xi^2\ 2\lambda\ \bar{s}_{rz})d\xi \qquad \text{(III-6)}$$

Differentiation with respect to z and t are respectively denoted by primes and dots, while ξ is a dummy variable of integration replacing the radial coordinate in the integrands. These six equations apply in conjunction with the yield condition

$$F(\sigma_{ij}) = s_{rr}^2 + s_{rr}s_{zz} + s_{zz}^2 + r^2\bar{s}_{rz}^2 - (k + 3\alpha p)^2 = 0 \qquad \text{(III-7)}$$

and the requirements $\lambda \geq 0$, Eq. (II-8b) and $(k + 3\alpha p) \geq 0$, Eq. (II-1b).

The derivation of Eqs. (1) to (6) is symbolically described by the statements

$$\{III - 1\} = \frac{\partial}{\partial t}\int_{r}^{r_o}\{II - 12a\}\xi\, d\xi + B\int_{r}^{r_o}\{II - 10b\}\xi\, d\xi + A\frac{\partial^2}{\partial t^2}\int_{r}^{r_o}\{II - 10b\}\xi\, d\xi - \frac{\partial}{\partial t}\{II - 15\}$$

$$\{III - 2\} = \frac{\partial}{\partial t}\int_{r}^{r_o}\{II - 12b\}\xi\, d\xi + \frac{C}{A}\int_{r}^{r_o}\{II - 12b\}\xi\, d\xi + C\frac{\partial}{\partial t}\int_{r}^{r_o}\{II - 10d\}\xi\, d\xi - \{II - 17\}$$

$$\{III - 3\} = \int_{0}^{r}\{II - 10a\}\xi\, d\xi$$

$$\{III - 4\} = \int_{0}^{r}\{II - 10b\}\xi\, d\xi$$

$$\{III - 5\} = \int_{0}^{r}\{II - 10c\}\xi\, d\xi$$

$$\{III - 6\} = \int_{0}^{r}\{II - 10d\}\xi\, d\xi$$

where the numbers in braces { } denote the various equations. The expressions (1) to (7) being based on the differential equations in plastic regions, the expressions are naturally

valid only in locations z where the material is plastic for all values of $0 \leq r \leq r_o$.

It can be demonstrated by reversing the process of derivation outlined symbolically that the integral formulation, Eqs. (1) to (6), is entirely equivalent to the earlier differential formulation, provided the integrands are continuous functions of r for $0 \leq r \leq r_o$, and that $\bar{v}_r$ and v_z have finite limits for $r \to 0$.

The above integro-differential equations remain subject to the boundary conditions (II-14) at z=0 and to initial conditions representing a state of rest at t=0.

In elastic regions, i.e., in locations z where in the time interval considered the material acts elastically for all values of r, the appropriate integral equations are obtained from Eqs. (1) to (6) by substitution of $\lambda \equiv 0$. In addition to the previously stated initial conditions for $t \leq 0$ and boundary conditions for z=0, the results must satisfy $(k + 3\alpha p) \geq 0$ and one of the two alternate restrictions $F < 0$, or $F = 0$ and $\dot{F} > 0$.

The derivation of the integro-differential equations (1) to (6) in plastic regions and of the similar but simpler set in elastic regions, apply respectively, only if the material in the particular location z and in the interval of time considered acts plastically or elastically, respectively for all

values of r. It is thus necessary to consider the situation where the material acts plastically for some range of r and elastically in the remainder of the range $0 \leq r \leq r_o$. To make a valid statement in such situations it is noted that the differential equations in Section II are hyperbolic, so that the solution, i.e., the values of the stresses and velocities at any time t define the continuation of the solution during the subsequent (differential) interval dt. It is further noted that this continuation of the solution does not explicitly depend on the question of plastic or elastic action of the material for earlier values of the time. The numerical solution of the problem will be based on finite difference procedures in z and t, the latter being of consequence here. Assume that the solution up to some value of t has been found. Using the values of the stresses and velocities at this time t as initial values, one can find a preliminary "plastic" solution [P] for $t + \Delta t$ based on Eqs. (1) to (7). Similarly, one can find a preliminary "elastic" solution [E] for $t + \Delta t$ based on Eqs. (1) to (6) with $\lambda \equiv 0$. These two preliminary solutions are each actually valid in locations r where the respective secondary requirements are satisfied. The solution [P] is valid only in locations r where Eq. (II-8b) holds, while [E] is valid only for values r where one of the two restrictions, Eqs. (II-13a,b), is satisfied. In the expectation that the problem treated has a unique solution*) the ranges in r for the solutions [P] and [E] should cover all values $0 \leq r \leq r_o$ completely and without overlap. However, this

*) While an approach to a proof of uniqueness may be found in Ref. [13], no theorem on existence of solutions in dynamic elasto-plastic problems is available.

ideal requirement is not likely to be satisfied in an approximate analysis using finite steps and a truncated expansion. This detail which requires an approximation will be discussed later in Section IV. Using portions of the solutions [P] and [E] an approximate numerical solution can, however, be obtained for all values of r, even when the material acts plastically in some locations, elastically in others.

The procedure outlined above can be simplified by making the assumption that the separation of elastic and plastic regions is always along a plane normal to the z-axis. As discussed at the very end of Section IV this simplification is appropriate if a very simple analysis is made where only one term of the expansion for each unknown is used when applying the Galerkin method.

IV REMOVAL OF THE INDEPENDENT VARIABLE r THROUGH USE OF THE GALERKIN METHOD.

The removal of the independent variable r by the Galerkin method is achieved by expanding the unknowns in terms of appropriate functions of r, leading to partial differential equations for the expansion coefficients, which are functions of z and t. The expansion functions selected are even powers of r, i.e., r^0, r^2, ... The reason for the omission of odd powers is the fact that the differential equations (II-10) and (II-12) after substitution of $s_{rz} = r\bar{s}_{rz}$ and $v_r = r\bar{v}_r$ permit a solution for all unknowns in form of power series*) in even powers of r. Such a solution is suitable when the boundary conditions at z=0 are even in r, which is the case in the present problem. It is thus expected that immediate omission of the odd powers of r in the Galerkin approach will give better results for the limited number of terms used.

It must be stressed here that the elimination of the variable r by the Galerkin method can only be applied to equalities, such as Eqs. (III-1) to (III-7), but that the secondary conditions expressed by the inequalities, Eqs. (II-1b), (II-8b) and (II-13a,b), must be retained as functions of r unless one is willing to accept a further approximation with some potential error in the results. Consider as an example the inequality $\lambda \geq 0$, using the set of expansion functions r^{2i}, i = 0, 1, 2, ... While $\lambda \geq 0$ permits the conclusion

---

*) Due to the well behaved nature of the problem such a series can be expected to be convergent.

$$\int_0^{r_o} \lambda(r) r^{2i+1} \, dr \geq 0 \qquad \text{(IV-1)}$$

one cannot draw the conclusion that the existence of the inequalities (1) insures $\lambda \geq 0$, even in the limit when Eq. (1) hold for all values of $i = 0, 1, 2, \ldots, \infty$.

a) Application of Galerkin Method.

To remove the variable r, the truncated expansions

$$\left.\begin{aligned}
p(r,z,t) &= \sum_{i=0}^{n} r^{2i} \, P_i(z,t) \\
s_{rr}(r,z,t) &= \sum_{i=0}^{n} r^{2i} \, R_i(z,t) \\
s_{zz}(r,z,t) &= \sum_{i=0}^{n} r^{2i} \, Z_i(z,t) \\
\bar{s}_{rz}(r,z,t) &= \sum_{i=0}^{n} r^{2i} \, T_i(z,t) \\
v_z(r,z,t) &= \sum_{i=0}^{n} r^{2i} \, V_i(z,t) \\
\bar{v}_r(r,z,t) &= \sum_{i=0}^{n} r^{2i} \, U_i(z,t) \\
\lambda(r,z,t) &= \sum_{i=0}^{n} r^{2i} \, \Lambda_i(z,t)
\end{aligned}\right\} \qquad \text{(IV-2)}$$

are introduced into Eqs. (III-1) to (III-7) in fully plastic locations z and into Eqs. (III-1) to (III-6) with $\lambda \equiv 0$ in fully elastic locations z. The equations defining the new unknowns P_i , R_i , Z_i , T_i , V_i , U_i and Λ_i are obtained by multiplying

the respective equations by r^m and integrating over the area $dA = rdr$ of the cross section, the values of m being 0, 2, 4, ..., 2n. The resulting system in plastic locations is

$$\sum_{i=0}^{n} \frac{r_o^{2i}}{(2i+m+3)} \{(m+1)\dot{R}_i - \dot{Z}_i - (m+3)\dot{P}_i + \frac{r_o^2(2i+m+3)}{(2i+m+5)}(-\dot{T}_i' + \rho\ddot{U}_i) + \frac{r_o(2i+m+3)}{(2i+m+4)}(B + A\frac{\partial^2}{\partial t^2})[(m+2)U_i + 2V_i' - \frac{3}{2G}\dot{Z}_i - 3\sum_{j=0}^{n}\frac{r_o^{2j}(2i+m+4)}{(2i+2j+m+4)}\Lambda_i Z_j]\} = 0 \qquad \text{(IV-3)}$$

$$\sum_{i=0}^{n} \frac{r_o^{2i}}{(2i+m+5)} \{\frac{2i+m+5}{2i+m+4}(\frac{C}{A} + \frac{\partial}{\partial t})[(m+2)T_i - Z_i' + P_i' + \rho\dot{V}_i] + r_o C\frac{\partial}{\partial t}[\frac{(m+3)(2i+m+5)}{(2i+m+3)r_o^2}V_i + \frac{1}{G}\dot{T}_i - U_i' + 2\sum_{j=0}^{n}\frac{r_o^{2j}(2i+m+5)}{(2i+2j+m+5)}\Lambda_i T_j]\} = 0 \qquad \text{(IV-4)}$$

$$\sum_{i=0}^{n} \frac{r_o^{2i}}{(2i+2)(2i+m+4)} \{(4i+1)U_i - V_i' - \frac{3}{2G}\dot{R}_i - 3\sum_{j=0}^{n}\frac{r_o^{2j}(2i+2)(2i+m+4)}{(2i+2j+2)(2i+2j+m+4)}\Lambda_i R_j\} = 0 \qquad \text{(IV-5)}$$

$$\sum_{i=0}^{n} \frac{r_o^{2i}}{(2i+2)(2i+m+4)} \{(2i+2)U_i - 2V_i' + \frac{3}{2G}\dot{Z}_i + 3\sum_{j=0}^{n}\frac{r_o^{2j}(2i+2)(2i+m+4)}{(2i+2j+2)(2i+2j+m+4)}\Lambda_i Z_j\} = 0 \qquad \text{(IV-6)}$$

$$\sum_{i=0}^{n} \frac{r_o^{2i}}{(2i+2)(2i+m+4)} \left\{(2i+2)\, U_i + V_i' + \frac{1}{\kappa_{mi}} \dot{P}_i - \right.$$

$$\left. - 6\alpha \sum_{j=0}^{n} \frac{r_o^{2j}(2i+2)(2i+m+4)}{(2i+2j+2)(2i+2j+m+4)} \Lambda_i (k\delta_{oj} + 3\alpha P_j) \right\} = 0 \qquad \text{(IV-7)}$$

$$\sum_{i=0}^{n} \frac{r_o^{2i}}{(2i+3)(2i+m+5)} \left\{ \frac{(2i+3)(2i+m+5)2i}{(2i+1)(2i+m+3) r_o^2} V_i + U_i' - \frac{1}{G} \dot{T}_i - \right.$$

$$\left. - 2 \sum_{j=0}^{n} \frac{r_o^{2j}(2i+3)(2i+m+5)}{(2i+2j+3)(2i+2j+m+5)} \Lambda_i T_j \right\} = 0 \qquad \text{(IV-8)}$$

$$\sum_{i=0}^{n} \sum_{j=0}^{n} \frac{r_o^{2i+2j}}{(2i+2j+m+2)} \left\{ R_i R_j + R_i Z_j + Z_i Z_j + \frac{r_o^2 (2i+2j+m+2)}{(2i+2j+m+4)} T_i T_j - \right.$$

$$\left. - (k\delta_{oi} + 3\alpha P_i)(k\delta_{oj} + 3\alpha P_j) \right\} = 0 \qquad \text{(IV-9)}$$

where

$$\frac{1}{\kappa_{mj}} = \frac{(2j+2)(2j+m+4)}{r_o^{2j+m+4}} \int_0^{r_o} r^{m+1} \left\{ \int_0^{r} \frac{\xi^{2j+1}}{K(x = \sum_{i=0}^{n} \xi^{2i} P_i)} \, d\xi \right\} dr \qquad \text{(IV-10)}$$

The boundary conditions are

$$[Z_i - P_i]_{z=0} = -p_o(t)\, \delta_{oi} \qquad \text{(IV-11a)}$$

$$[T_i]_{z=0} = 0 \qquad \text{(IV-11b)}$$

where δ_{oi} is Kronecker's delta, while the initial conditions require that all unknowns and their partial derivatives of all orders vanish for $t \leq 0$, $z > 0$.

75358

The appropriate equations in elastic regions are Eqs. (IV-3) to (IV-8) with $A_i \equiv 0$.

Solutions obtained from the respective equations in plastic or elastic locations are valid only if the appropriate secondary requirements are satisfied. Thus, the plastic solution is valid only in locations z where Eqs. (IV-2) give $\lambda \geq 0$ for all values of r, while the elastic solution applies only in locations z where the solution satisfies Eq. (II-13a) or Eqs. (II-13b) for all values of r. As discussed in the last two paragraphs of Section III there will in general be locations z where neither of the above two requirements is satisfied. In such locations z the plastic and elastic solutions are each valid in parts of the range in r, the range to be determined after each time step Δt of the numerical integration. Further, as noted in Section II, results are only meaningful if they satisfy the requirement $k + 3\alpha p \geq 0$, which follows from Eq. (II-1b).

b) Special Case of Truncation to n=0.

The simplest solution is obtained if only one term of the expansion is used for each unknown. The solution on this simple basis gives the exact solution for an infinitely rigid containing tube and may therefore be considered reasonable if the tube is sufficiently rigid, a suitable criterion to be developed later. After simplification, the following equations are obtained in plastic locations:

$$5\dot{R}_o - 5\dot{P}_o - r_o^2 \dot{T}_o' + 5r_o BU_o + r_o^2 \bar{\rho}\ddot{U}_o = 0 \qquad \text{(IV-12)}$$

$$\left(\frac{C}{A} + \frac{\partial}{\partial t}\right)(2T_o + 2R_o' + P_o' + \rho\dot{V}_o) + \frac{4C}{r_o}\dot{V}_o = 0 \qquad \text{(IV-13)}$$

$$\frac{3}{2G}\dot{R}_o + V_o' - U_o + 3\Lambda_o R_o = 0 \qquad \text{(IV-14)}$$

$$\frac{1}{K(P_o)}\dot{P}_o + V_o' + 2U_o - 6\alpha\Lambda_o(k + 3\alpha P_o) = 0 \qquad \text{(IV-15)}$$

$$\frac{1}{G}\dot{T}_o - U_o' + 2\Lambda_o T_o = 0 \qquad \text{(IV-16)}$$

$$Z_o + 2R_o = 0 \qquad \text{(IV-17)}$$

$$\Phi \equiv 6R_o^2 + r_o^2 T_o^2 - 2(k + 3\alpha P_o)^2 = 0 \qquad \text{(IV-18)}$$

where

$$\bar{\rho} = \rho + \frac{5A}{r_o} \qquad \text{(IV-19)}$$

The manipulations leading from Eqs. (3) to (9) to Eqs. (12) to (18) are indicated below. Each equation is reduced to the first term by the substitution m=n=0. The result of the elimination of U_o and V_o' between Eqs. (5) and (6) is integrated with respect to time and noting the original state of rest, leads to Eq. (17). It is noted that this equation implies that in this approximation $s_{zz} + 2s_{rr} = 0$, which is exactly true if the restraining tube is absolutely rigid. This result is due to the low order of the truncation, but should be a good approximation for the case of very strong restraint. The remaining operations, including the use of Eq. (17) to eliminate Z_o, are represented symbolically by:

$$\{IV - 12\} = [5\{IV - 3\} + 10r_o(B + A\frac{\partial^2}{\partial t^2})\{IV - 6\}]_{Z_o} = -2R_o$$

$$\{IV - 13\} = [4\{IV - 4\} + 12r_o C\frac{\partial}{\partial t}\{IV - 8\}]_{Z_o} = -2R_o$$

$$\{IV - 14\} = -8\{IV - 5\}$$

$$\{IV - 15\} = 8\{IV - 7\}$$

$$\{IV - 16\} = -15\{IV - 8\}$$

$$\{IV - 18\} = [4\{IV - 9\}]_{Z_o} = -2R_o$$

The system of equations (12) to (18) is subject to the boundary conditions

$$[2R_o + P_o]_{z=0} = p_o(t) \qquad \text{(IV-20a)}$$

$$[T_o]_{z=0} = 0 \qquad \text{(IV-20b)}$$

and to initial conditions corresponding to a state of rest at t=0.

In elastic regions Eqs. (12) to (17) apply with $\Lambda_o = 0$, while the secondary conditions, Eq. (II-13a) or Eqs. (II-13b), must be satisfied, the function F being in this case:

$$F = 3R_o^2 + r^2T_o^2 - (k + 3\alpha P_o)^2 \qquad \text{(IV-21)}$$

c) Boundaries between Elastic and Plastic Solutions.

As a result of the truncation, the extent of elastic and plastic regions obtained from the elastic and from the plastic equations does not quite agree. This requires

discussion to resolve the inconsistency by a suitable approximate procedure. For the particularly important case when only the terms n=0 are used, suitability of the elastic solution obtained by forward integration for a given value t in a location z is to be checked by Eq. (21). This check may indicate that the yield relation is satisfied for some values of r, but not for others, because Eq. (21) contains a term depending on r. On the other hand, the value λ obtained from the plastic analysis in this approximation is necessarily a constant, $\lambda \equiv \Lambda_o$, so that the plastic analysis in this location z would seem to be acceptable for all values of r if $\Lambda_o \geq 0$, or not at all if $\Lambda_o < 0$. This difficulty can be resolved regardless of the order of the truncation, n=0 or n > 0, by accepting the elastic solution [E] wherever Eq. (II-13a) or Eqs. (II-13b) are satisfied and using the plastic one, [P], in all other locations, regardless of the sign of λ. The arbitrary preference given to the result of the elastic solution [E] is motivated by convenience, caused by the fact that numerical solutions derived in Section V furnish the plastic solution as the elastic solution followed by a corrective step. If the procedure recommended above leads in a location z and at a time t to an elastic solution for some range of r and to a plastic one in the remainder, series with different coefficients will apply for the unknowns defined by Eqs. (2). To continue the forward integration in time, the series for each of the quantities in [E] and [P] must be reconciled by expansion of the result. For example, if the pressure $p^{[E]}$, $p^{[P]}$ in the elastic and inelastic regions, respectively, in a two term

expansion at a point z, t are found to be

$$p^{[E]} = P_o^{[E]} + r^2 P_1^{[E]} \qquad 0 \leq r < r^{[P]} \qquad \text{(IV-22a)}$$

$$p^{[P]} = P_o^{[P]} + r^2 P_1^{[P]} \qquad r^{[P]} \leq r \leq r_o \qquad \text{(IV-22b)}$$

then a new expansion for the pressure

$$p = P_o + r^2 P_1 \qquad 0 \leq r \leq r_o \qquad \text{(IV-23)}$$

is to be obtained by appropriate fitting of P_o and P_1. The coefficients P_o, P_i in the last equation are then to be used in the numerical analysis to find the unknowns at the next time step.

A somewhat simpler procedure can be employed when only the terms n=0 are used. Still basing the decision on the elastic analysis one can decide not to apply Eq. (21) as a function of r as a criterion, but to base the decision on the mean value of F. The elastic solution will then apply if

$$\Phi \equiv 6R_o^2 + r_o^2 T_o^2 - 2(k + 3 P_o)^2 \leq 0 \qquad \text{(IV-24)}$$

This procedure is in the spirit of a one term Galerkin solution and eliminates locations where Eqs. (22) and (23) have to be applied. The moving boundaries between elastic and plastic regions become in this approximation planes at right angles to z. This simplified approach was used in the examples in Section VI.

V FINITE DIFFERENCE FORMULATION.

A finite difference solution of Eqs. (IV-12) to (IV-20) generated by the Galerkin method with n=0 is presented in this section. The computation technique consists of a process of forward integration in time based on the elastic relations, followed by a check on the validity of the stresses obtained at each time step and a correction of these trial values to conform to the plastic relations, where necessary. The differencing scheme is therefore motivated primarily by the elastic relations, with the terms depending on Λ_o represented in such a manner that the correction algorithm becomes simple and convenient.

a) Difference Equations.

In elastic regions the problem is fully hyperbolic with real characteristics and the correct number of linearly independent characteristic vectors. In such a case, for a system in two independent variables governing stress wave propagation, a standard technique consists of using a staggered grid with stresses and velocities evaluated at alternate points in time and space and central differences used to approximate derivatives. To this end, the first quadrant of the z-t plane is divided by a double rectangular grid, evenly spaced in the z and t directions by $\frac{\Delta z}{2}$ and $\frac{\Delta t}{2}$, as shown in Figure 2. The superscript n is used to indicate a time level and the subscript j a point in space with n=½

corresponding to t=0 and j=1 to z=0, so that for a generic dependent variable D(z,t),

$$D_j^n = D[(j-1)\Delta z, (n-\tfrac{1}{2})\Delta t] \qquad (V\text{-}1)$$

The stresses are computed at points ($j\Delta z$, $n\Delta t$) and the velocities at points $[(j+\tfrac{1}{2})\Delta z, (n+\tfrac{1}{2})\Delta t]$, j and n representing integral values.

The computation scheme will be applied to a material with a nonlinearity of the hardening type which tends to steepen loading profiles and subsequently generate loading shocks. In a simple centered scheme such as described above, steep fronts are followed by strong numerical oscillations which mask the profile of the true solution. To eliminate these oscillations and render computation with discontinuous loading histories possible, a device similar to that proposed by Lax for equations in conservation form, Ref. [14], is used. The procedure used here consists of replacing the simple centered time difference

$$\left[\frac{\partial D}{\partial t}\right]_j^{n+\frac{1}{2}} = \frac{1}{\Delta t}\,(D_j^{n+1} - D_j^n) + O(\overline{\Delta t}^2) \qquad (V\text{-}2)$$

by the form

$$\left[\frac{\partial D}{\partial t}\right]_j^{n+\frac{1}{2}} = \frac{1}{\Delta t}\left[D_j^{n+1} - \frac{1}{2 + C_D}\,(D_{j+1}^n + C_D D_j^n + D_{j-1}^n)\right] + O\left(\frac{\overline{\Delta z}^2}{\Delta t}\right) \qquad (V\text{-}3)$$

where $C_D > 0$ is an arbitrary parameter. The effect of this modified scheme is to introduce a "diffusion term" proportional to $(\overline{\Delta z}^2/\Delta t)$ into the relations as can be seen from

the Taylor expansion

$$\frac{1}{\Delta t}\left[D_j^{n+1} - \frac{1}{2 + C_D}\left(D_{j+1}^n + C_D D_j^n + D_{j-1}^n\right)\right] = \left[\frac{\partial D}{\partial t}\right]_j^{n+\frac{1}{2}} -$$

$$- \frac{\overline{\Delta z}^2}{\Delta t}\frac{1}{2 + C_D}\left[\frac{\partial^2 D}{\partial z^2}\right]_j^{n+\frac{1}{2}} + O(\overline{\Delta z}^2, \overline{\Delta t}^2) \qquad (V\text{-}4)$$

Using the form, Eq. (3), in the constitutive equations (IV-14) to (IV-16) and deleting the zero subscripts indicating the order of the truncation for the sake of simplicity, the finite difference form of equations (IV-12) to (IV-18) is

$$R_j^{n+1} = R_j^n + \frac{1}{2 + C_D}\left(R_{j+1}^n - 2R_j^n + R_{j-1}^n\right) + \frac{G\Delta t}{3}\left(U_{j+\frac{1}{2}}^{n+\frac{1}{2}} + U_{j-\frac{1}{2}}^{n+\frac{1}{2}}\right) -$$

$$- \frac{2G\Delta t}{3\Delta z}\left(V_{j+\frac{1}{2}}^{n+\frac{1}{2}} - V_{j-\frac{1}{2}}^{n+\frac{1}{2}}\right) - 2G\Delta t\, \Lambda_j^{n+1} R_j^{n+1} \qquad (V\text{-}5)$$

$$P_j^{n+1} = P_j^n + \frac{1}{2 + C_D}\left(P_{j+1}^n - 2P_j^n + P_{j-1}^n\right) - \kappa_j^n \Delta t\left(U_{j+\frac{1}{2}}^{n+\frac{1}{2}} + U_{j-\frac{1}{2}}^{n+\frac{1}{2}}\right) -$$

$$- \frac{\kappa_j^n \Delta t}{\Delta z}\left(V_{j+\frac{1}{2}}^{n+\frac{1}{2}} - V_{j-\frac{1}{2}}^{n+\frac{1}{2}}\right) + 6\alpha\, \kappa_j^n \Delta t\, \Lambda_j^{n+1}\left(k + 3\alpha P_j^{n+1}\right) \qquad (V\text{-}6)$$

$$T_j^{n+1} = T_j^n + \frac{1}{2 + C_D}\left(T_{j+1}^n - 2T_j^n + T_{j-1}^n\right) + \frac{G\Delta t}{\Delta z}\left(U_{j+\frac{1}{2}}^{n+\frac{1}{2}} - U_{j-\frac{1}{2}}^{n+\frac{1}{2}}\right) -$$

$$- 2G\Delta t\, \Lambda_j^{n+1} T_j^{n+1} \qquad (V\text{-}7)$$

$$Z_j^{n+1} = -2R_j^{n+1} \qquad (V\text{-}8)$$

$$U_{j+\frac{1}{2}}^{n+3/2} = \left(2 - \frac{5B\bar{\Delta t}^2}{r_o\bar{\rho}}\right) U_{j+\frac{1}{2}}^{n+\frac{1}{2}} - U_{j+\frac{1}{2}}^{n-\frac{1}{2}} -$$

$$- \frac{5\Delta t}{2r_o^2\bar{\rho}} \left[(R_{j+1}^{n+1} + R_j^{n+1}) - (R_{j+1}^n + R_j^n)\right] +$$

$$+ \frac{5\Delta t}{2r_o^2\bar{\rho}} \left[(P_{j+1}^{n+1} + P_j^{n+1}) - (P_{j+1}^n + P_j^n)\right] +$$

$$+ \frac{\Delta t}{\bar{\rho}\,\Delta z} \left[(T_{j+1}^{n+1} - T_j^{n+1}) - (T_{j+1}^n - T_j^n)\right] \qquad (V\text{-}9)$$

$$V_{j+\frac{1}{2}}^{n+3/2} = \left[1 + \frac{C\Delta t}{2A}\left(1 + \frac{4A}{\rho r_o}\right)\right]^{-1} \left\{2V_{j+\frac{1}{2}}^{n+\frac{1}{2}} - \left[1 - \frac{C\Delta t}{2A}\left(1 + \frac{4A}{\rho r_o}\right)\right] V_{j+\frac{1}{2}}^{n-\frac{1}{2}} -\right.$$

$$- \frac{2\Delta t}{\rho\Delta z}\left[\left(1 + \frac{C\Delta t}{2A}\right)(R_{j+1}^{n+1} - R_j^{n+1}) - \left(1 - \frac{C\Delta t}{2A}\right)(R_{j+1}^n - R_j^n)\right] -$$

$$- \frac{\Delta t}{\rho\Delta z}\left[\left(1 + \frac{C\Delta t}{2A}\right)(P_{j+1}^{n+1} - P_j^{n+1}) - \left(1 - \frac{C\Delta t}{2A}\right)(P_{j+1}^n - P_j^n)\right] -$$

$$\left. - \frac{\Delta t}{\rho}\left[\left(1 + \frac{C\Delta t}{2A}\right)(T_{j+1}^{n+1} + T_j^{n+1}) - \left(1 - \frac{C\Delta t}{2A}\right)(T_{j+1}^n + T_j^n)\right]\right\} \qquad (V\text{-}10)$$

$$\Phi_j^{n+1} \equiv \Phi(R_j^{n+1}, P_j^{n+1}, T_j^{n+1}) = 6(R_j^{n+1})^2 + r_o^2(T_j^{n+1})^2 -$$

$$- 2(k + 3\alpha P_j^{n+1})^2 = 0 \qquad (V\text{-}11)$$

where

$$\kappa_j^n = K(P_j^n) \qquad (V\text{-}12)$$

and $C_D > 0$ is an arbitrary value to be chosen small enough to lead to reasonably smooth numerical results. Consistent with this requirement, C_D should, however, be selected as large as possible, to avoid significant energy losses due to the artificially introduced dissipative terms. For simplicity, the dissipative terms in Eqs. (5), (6) and (7) and the non-linear function κ which depends on the bulk modulus K(p) have been written at (n+1,j) and at (n,j), respectively. This is not consistent with the centered scheme, but is convenient for the computation.

Equations (5) to (11) apply in plastic regions in conjunction with the restrictions, Eqs. (II-1b) and (II-8b), while the first six of these relations, Eqs. (5) to (10) with $\Lambda = 0$ hold in elastic regions subject to the restriction expressing the requirement that the stresses remain below yield. In the present simplified approximation the yield condition will not be used as a function of r, but as indicated in the discussion leading to Eq. (IV-24) only the value Φ defined by this equation will be used as a criterion. The appropriate condition in finite difference form is thus

$$\Phi_j^{n+1} = 6(R_j^{n+1})^2 + r_o^2 (T_j^{n+1})^2 - 2(k + 3\alpha P_j^{n+1})^2 \leq 0 \qquad \text{(V-13)}$$

The process of construction of the solution is as follows. Using the stresses at the time n and velocities at $(n+\frac{1}{2})$ the four equations (5) to (8) for elastic regions (i.e., with $\Lambda_j^{n+1} \equiv 0$) are solved for the stresses at the time (n+1).

For points j where Eq. (13) is satisfied*) the stresses are accepted and Eqs. (9) and (10) are used to find velocities at (n+3/2). If Eq. (13) is not satisfied the correction algorithm indicated**) below is used to find the stresses at the time (n+1).

Equations (5) to (10) with $\Lambda_j^{n+1} \equiv 0$ can be viewed as a (vectorial) finite difference operator at the time level (n+½). Its application requires knowledge of R, P and T at the n^{th} time level and U and V at the $(n+\frac{1}{2})^{th}$ and the $(n-\frac{1}{2})^{th}$ and at all the relevant space points. The operator therefore represents a two-level implicit nonlinear finite difference scheme and a stability analysis according to the methods of Richtmeyer and Morton, Ref. [16], gives the necessary local criteria

$$\frac{\Delta t}{\Delta z}\sqrt{\frac{1}{\rho}\left(\kappa_j^n + \frac{4G}{3}\right)} \leq \sqrt{1 - \frac{2}{2 + C_D}}\,, \quad \frac{\Delta t}{\Delta z}\sqrt{\frac{G}{\rho}} \leq \sqrt{1 - \frac{2}{2 + C_D}} \qquad \text{(V-14)}$$

applicable at each time level and space point.

b) Correction Algorithm at Interior Points j.

At interior stress points (n,j) where the elastic stresses violate Eq. (13) the elastic stresses,

---

*) The secondary requirement $k + 3\alpha P_j^{n+1} \geq 0$ must be satisfied in elastic and plastic regions. If it is not, a situation not further considered here, the above relations do no longer hold, because the material has disintegrated.

**) The manner of correction is a generalization of the approach used in Ref. [15] for the much simpler case of a von Mises material.

$$\bar{R}_j^{n+1} \equiv R_j^n + \frac{1}{2 + C_D} (R_{j+1}^n - 2R_j^n + R_{j-1}^n) + \frac{G\Delta t}{3} (U_{j+\frac{1}{2}}^{n+\frac{1}{2}} + U_{j-\frac{1}{2}}^{n+\frac{1}{2}}) -$$

$$- \frac{2G\Delta t}{3\Delta z} (V_{j+\frac{1}{2}}^{n+\frac{1}{2}} - V_{j-\frac{1}{2}}^{n+\frac{1}{2}}) \qquad (V\text{-}15)$$

$$\bar{P}_j^{n+1} \equiv P_j^n + \frac{1}{2 + C_D} (P_{j+1}^n - 2P_j^n + P_{j-1}^n) - \kappa_j^n \Delta t (U_{j+\frac{1}{2}}^{n+\frac{1}{2}} + U_{j-\frac{1}{2}}^{n+\frac{1}{2}}) -$$

$$- \frac{\kappa_j^n \Delta t}{\Delta z} (V_{j+\frac{1}{2}}^{n+\frac{1}{2}} - V_{j-\frac{1}{2}}^{n+\frac{1}{2}}) \qquad (V\text{-}16)$$

$$\bar{T}_j^{n+1} \equiv T_j^n + \frac{1}{2 + C_D} (T_{j+1}^n - 2T_j^n + T_{j-1}^n) + \frac{G\Delta t}{\Delta z} (U_{j+\frac{1}{2}}^{n+\frac{1}{2}} - U_{j-\frac{1}{2}}^{n+\frac{1}{2}}) \qquad (V\text{-}17)$$

are used as trial values. Substitution of the values $\bar{R}_j^{n+1}$, $\bar{P}_j^{n+1}$, $\bar{T}_j^{n+1}$ into Eqs. (5), (6) and (7) gives the equivalent equations

$$R_j^{n+1} = \frac{1}{1 + 2G\ \Delta t\ \Lambda_j^{n+1}}\ \bar{R}_j^{n+1} \qquad (V\text{-}18)$$

$$T_j^{n+1} = \frac{1}{1 + 2G\ \Delta t\ \Lambda_j^{n+1}}\ \bar{T}_j^{n+1} \qquad (V\text{-}19)$$

$$(k + 3\alpha P_j^{n+1}) = \frac{1}{1 - 18\alpha^2\ \kappa_j^n\ \Delta t\ \Lambda_j^{n+1}} (k + 3\alpha \bar{P}_j^{n+1}) \qquad (V\text{-}20)$$

where R_j^{n+1} , T_j^{n+1} and P_j^{n+1} are the actual stresses allowing for plastic effects. When Eqs. (18), (19) and (20) are substituted into Eq. (11), $\Phi(R_j^{n+1}, P_j^{n+1}, T_j^{n+1}) = 0$, a quadratic equation for Λ_j^{n+1} is obtained. It has two roots

$$\Lambda_j^{n+1} = -\frac{1}{2G\Delta t}\,\frac{1 \mp \sqrt{1 + \dfrac{\Phi(\bar{R}_j^{n+1},\ \bar{P}_j^{n+1},\ \bar{T}_j^{n+1})}{2(k + 3\alpha\,\bar{P}_j^{n+1})^2}}}{1 \pm \dfrac{9\alpha^2\kappa_j^n}{G}\sqrt{1 + \dfrac{\Phi(\bar{R}_j^{n+1},\ \bar{P}_j^{n+1},\ \bar{T}_j^{n+1})}{2(k + 3\alpha\,\bar{P}_j^{n+1})^2}}}$$

where the upper or lower signs are to be used consistently.

The correction procedure is to be used when the elastic values violate Eq. (13), i.e., when $\Phi(\bar{R}_j^{n+1},\ \bar{P}_j^{n+1},\ \bar{T}_j^{n+1}) > 0$. For this case the square roots in the preceding equation are larger than unity so that the upper signs in this equation always furnish a value Λ_j^{n+1} which satisfies the requirement $\Lambda_j^{n+1} > 0$. However, when the term $\dfrac{9\alpha^2\kappa_j^n}{G}$ is larger than unity (or close to unity) the lower signs also furnish a positive value Λ_j^{n+1}. This value is inappropriate and should be disregarded. The inapplicability of the value obtained on the basis of the lower signs can be demonstrated by studying the consequences of decreasing the time step Δt to the limit $\Delta t \to 0$.

As a demonstration consider, for simplicity, Eqs. (15) to (17) with $C_D \to \infty$, and a solution such that the yield condition is just satisfied for (n,j), $\Phi(R_j^n,\ P_j^n,\ T_j^n) = 0$, while $\Phi(\bar{R}_j^{n+1},\ \bar{P}_j^{n+1},\ \bar{T}_j^{n+1}) = \varepsilon > 0$. If the time step is decreased, the value of the yield function at the time (n+1) will become smaller, $\varepsilon = 0(\Delta t)$. Using the upper signs one finds

$$\lim_{\Delta t \to 0} [\Delta t \, \Lambda_j^{n+1}] = \lim_{\varepsilon \to 0} \left[\frac{\varepsilon}{8(9\alpha^2\kappa_j^n + G)(k + 3\alpha P_j^n)^2}\right] = 0$$

while use of the lower signs gives

$$\lim_{\Delta t \to 0} [\Delta t \, \Lambda_j^{n+1}] = \lim_{\varepsilon \to 0} \left[\frac{1}{(9\alpha^2\kappa_j^n - G)} + O(\varepsilon)\right] = \frac{1}{9\alpha^2\kappa_j^n - G}$$

which is a finite positive value if $9\alpha^2\kappa_j^n > G$. Equations (15) to (20) indicate that for $\Delta t \, \Lambda_j^{n+1} \to 0$ the increments $R_j^{n+1} - R_j^n$, $P_j^{n+1} - P_j^n$ and $T_j^{n+1} - T_j^n$ become, in the limit, smaller and smaller as required. If, however, $\Delta t \, \Lambda_j^{n+1}$ in the limit is finite, then $\bar{R}_j^{n+1} - R_j^n$, $\bar{P}_j^{n+1} - P_j^n$ and $\bar{T}_j^{n+1} - T_j^n$ tend to zero, but not $P_j^{n+1} - P_j^n$, etc., because the factors on the right hand sides of Eqs. (18) to (20) differ in the limit from unity.

The corrected stresses are thus to be computed from

$$\Lambda_j^{n+1} = \frac{1}{2G\Delta t} \frac{\sqrt{1 + \dfrac{\Phi(\bar{R}_j^{n+1}, \bar{P}_j^{n+1}, \bar{T}_j^{n+1})}{2(k + 3\alpha \bar{P}_j^{n+1})^2}} - 1}{\dfrac{9\alpha^2\kappa_j^n}{G} \sqrt{1 + \dfrac{\Phi(\bar{R}_j^{n+1}, \bar{P}_j^{n+1}, \bar{T}_j^{n+1})}{2(k + 3\alpha \bar{P}_j^{n+1})^2}} + 1} \qquad \text{(V-21)}$$

c) Correction Algorithm at the Boundary j=1.

At the boundary j=1 (z=0) a similar correction algorithm must be formulated to satisfy the boundary conditions corresponding to Eqs. (IV-20a,b)

$$2R_1^n + P_1^n = p_o^n \tag{V-22a}$$

$$T_1^n = 0 \tag{V-22b}$$

where $p_o^n = p_o[(n-\tfrac{1}{2})\Delta t]$. For this purpose the constitutive equations (5), (6) and (7) with $C_D \to \infty$ and the yield condition, Eq. (11), at j=1 are used and the grid is extended one half-step beyond z=0 to include $j=\tfrac{1}{2}$. Substitution of Eqs. (22a,b) and elimination of $(V_{3/2}^{n+\frac{1}{2}} - V_{\frac{1}{2}}^{n+\frac{1}{2}})$ gives the relation

$$\left(\frac{\kappa_1^n + 4G/3}{\kappa_1^n}\right)(P_1^{n+1} - P_1^n) - (p_o^{n+1} - p_o^n) + 4G\Delta t\, U_{3/2}^{n+\frac{1}{2}} -$$

$$- 2G\Delta t\, \Lambda_1^{n+1}\left[p_o^{n+1} + 4\alpha k - (1 - 12\alpha^2)\, P_1^{n+1}\right] = 0 \tag{V-23}$$

Using an elastic trial value

$$\bar{P}_1^{n+1} \equiv P_1^n - \frac{\kappa_1^n}{(\kappa_1^n + 4G/3)}\left[4G\Delta t\, U_{3/2}^{n+\frac{1}{2}} - (p_o^{n+1} - p_o^n)\right] \tag{V-24}$$

reduces Eq. (23) to the form

$$P_1^{n+1} = \frac{\bar{P}_1^{n+1} + \left(\frac{\kappa_1^n}{\kappa_1^n + 4G/3}\right) 2G\Delta t\, \Lambda_1^{n+1}\,(p_o^{n+1} + 4\alpha k)}{1 + \left(\frac{\kappa_1^n}{\kappa_1^n + 4G/3}\right) 2G\Delta t\, \Lambda_1^{n+1}\,(1 - 12\alpha^2)} \tag{V-25}$$

The yield condition at the boundary becomes

$$\Phi_b^{n+1} \equiv \Phi_b(P_1^{n+1}) = \frac{3}{2}(1 - 12\alpha^2)(P_1^{n+1} - P_a)(P_1^{n+1} - P_b) \leq 0 \tag{V-26}$$

where the quantities

$$P_a = \frac{(3p_o^{n+1} - k\sqrt{12})}{3(1 + \alpha\sqrt{12})} \qquad \text{(V-27a)}$$

$$P_b = \frac{(3p_o^{n+1} + k\sqrt{12})}{3(1 - \alpha\sqrt{12})} \qquad \text{(V-27b)}$$

satisfy the inequality

$$P_b - P_a = \frac{4(3\alpha p_o^{n+1} + k)}{\sqrt{3}(1 - 12\alpha^2)} > 0 \qquad \text{(V-28)}$$

for $(3\alpha p_o^{n+1} + k) > 0$, $\frac{1}{\sqrt{12}} > \alpha \geq 0$. Finally, substitution of Eq. (25) into Eq. (26) gives two roots for Λ_1^{n+1} ,

$$\Lambda_{1\ a}^{n+1} = \frac{1}{G\Delta t} \frac{(\kappa_1^n + 4G/3)}{(1 - 12\alpha^2)\ \kappa_1^n} \frac{(P_a - \bar{P}_1^{n+1})}{(P_b - P_a)} \qquad \text{(V-29a)}$$

$$\Lambda_{1\ b}^{n+1} = \frac{1}{G\Delta t} \frac{(\kappa_1^n + 4G/3)}{(1 - 12\alpha^2)\ \kappa_1^n} \frac{(\bar{P}_1^{n+1} - P_b)}{(P_b - P_a)} \qquad \text{(V-29b)}$$

where use of $\Lambda_{1\ a}^{n+1}$ in Eq. (25) gives $P_1^{n+1} = P_a$, whereas $\Lambda_{1\ b}^{n+1}$ gives $P_1^{n+1} = P_b$.

From the form of Eq. (26) and the inequality Eq. (28) it is seen that only if the elastic trial value computed from Eq. (24) is outside the range $P_a \leq \bar{P}_1^{n+1} \leq P_b$ will the yield condition Eq. (26) be violated, that is $\Phi_b(\bar{P}_1^{n+1}) > 0$ and a correction of the trial value be required. When $\bar{P}_1^{n+1} > P_b$, of the two roots given by Eqs. (29a,b) only $\Lambda_{1\ b}^{n+1}$ is positive and its use in Eq. (25) gives $P_1^{n+1} = P_b$. If $\bar{P}_1^{n+1} < P_a$,

$\Lambda_{1\,a}^{n+1}$ is the positive root and leads to $P_1^{n+1} = P_a$. Thus, in either case, the solution satisfies $\Lambda_1^{n+1} > 0$.

VI DISCUSSION OF TYPICAL NUMERICAL RESULTS AND CONCLUSION.

a) Material Case 1.

Results for a group of situations were obtained using the material properties listed as Case 1 in Appendix B and a gradually rising input pressure

$$p_o(t) = 300[1 - \exp(-1000t)] \qquad \text{(VI-1)}$$

in psi and seconds. The analysis was made in all cases for stacked rings with a radius $r_o = 24$ in., but three radically different values for the parameter B representing the shell stiffness were used,

$$B_1 = 7.95 \times 10^5 \text{ lb/in}^3 \quad , \quad B_2 = 2.93 \times 10^4 \text{ lb/in}^3$$

$$B_3 = 5.35 \times 10^3 \text{ lb/in}^3$$

The mass of the rings was not varied, $\rho_s = 7.5 \times 10^{-4}$ lb.sec^2/in^4.

The analysis was made for the value C=0, defined in Eq. (II-16), implying that there is no longitudinal interaction between rings and filler material. The values of B_2 and ρ_s correspond to steel rings of 9/16 in. thickness and 24 in. radius, a case for which a test, Ref. [1], is available. The value B_1 is very much larger than B_2 , so that transverse strains for the former are severely inhibited and the situation for B_1 can be expected to be very close to uniaxial strain. The value B_3 on the other hand represents a situation where the lateral restraint is an order of magnitude less than for B_2 and longitudinal and transverse strains can be expected to be of comparable magnitude.

Under uniaxial strain, See Figs. B-1 and B-2, the material description implies hardening with increase in pressure. As a result, a progressing shock front occurs in all examples, even for the gradually rising input $p_o(t)$.

When formulating the finite difference scheme a "diffusion term" defined by the arbitrary parameter C_D was introduced. After some experimentation it was found that numerical results in which the shock fronts are steep, while subsequent oscillations (due to the numerical approach) are not excessive, could be obtained for $\Delta t = 5.0 \times 10^{-6}$ sec., $\Delta z = 0.25$ in. if values of C_D on the order of 30 were used. A short discussion of the effect of varying C_D is given in Appendix C.

All results shown used one term of the expansion for each unknown. The matter of adequacy of this truncation is discussed later. As a result of the truncation the axial stress is uniform for all values of r, while the radial velocity, e.g., varies as r, etc.

Numerical computations were made on a CDC 6600. Figures 3, 4 and 5 show the axial stress histories in three locations, z = 15, 25 and 75 in., for the three values B_1, B_2 and B_3, respectively. The shocks are clearly visible and the strength increases with z in Figs. 3 and 4 as expected. This is not so for the weakest shell, Fig. 5, where the shock strength at 75 in. has decreased. (It will be seen later that the truncation used can not be considered adequate for this case and the unexpected decrease may be due to this inadequacy.) In Figs. 4 and 5

oscillations with periods in excess of 1 msec. are clearly visible. Their periods, respectively, agree with estimates for the periods of radial oscillations of the shell filled with the material. These oscillations are thus not caused by the numerical scheme, but are real. The same type of oscillation (while present) is not easily discernible in Fig. 3 for the very stiff shell. Such oscillations do not occur in wave propagation in uniaxial strain and the smallness of the oscillations is due to the fact that the value B_1 is sufficiently large to approximate the uniaxial situation well. In addition to these oscillations there are others of much higher frequencies just after the arrival of the shocks. These oscillations are of purely computational origin. Their magnitude is controlled by the value of C_D .

The time-histories for axial velocities are quite similar to those for the axial stresses and were not shown. Typical results for the radial velocities at $r = r_o$ are shown for the stiffness B_2 in two locations z, Fig. 6. The results show decaying oscillations corresponding to those in Fig. 4.

Typical plots of shear stress for the three values B_i are shown in Fig. 7. Due to the truncation the distribution of the shear stresses is necessarily poorly approximated. They are proportional to the location r, i.e., the boundary condition $s_{rz} = 0$ for $r = r_o$ is not, and can not be satisfied. The result obtained is only a "best fit" of the actual distribution. The shear stresses, which are much smaller than

the radial ones, oscillate with respect to some ultimate, non-vanishing value. As expected, the magnitude of shear stresses and oscillations increases as the rings become softer. The period of oscillation agrees with that in the axial stresses for the values B_2 and B_3. For the stiffness $B_1 = 7.95 \times 10^5$ lb/in^3, Fig. 3 does not show oscillations clearly, while Fig. 7 indicates oscillating shear stresses below 4 lb/in^2. As mentioned before, the corresponding variations in Fig. 3 are too small to be visible.

Situations with an immediate pressure rise in $p_o(t)$, followed by an exponential decay can also be handled. As an example, Fig. 8 shows the applied axial stress $p_o(t)$ and the resulting axial stress at z = 15 in. and 75 in. for $B_2 = 2.93 \times 10^4$ lb/in^3. It must be emphasized that the material model used is for this input entirely unrealistic. The response in this case involves important unloading situations, while the material model was not fitted for unloading. Figure 8 is thus purely academic.

b) Comparisons of Results for Materials of Cases 1 and 2 and of a Test.

A test result giving the axial stress at a distance z = 15 in. is available, Ref. [1], for the tube stiffness $B_2 = 2.93 \times 10^4$ lb/in^3. The measured input pressure and the time-history of $p_o(t)$ according to Eq. (1) are shown in Fig. 9, indicating that the difference is modest. Figure 10 shows the

test result and the computed results at z = 15 in. for the materials of Cases 1 and 2, the properties of which are listed in Appendix B. Both analytical results agree well with the test.

The agreement between the calculations for Cases 1 and 2 at z = 15 in. shows that the results in this location depend essentially on the behavior in uniaxial strain, where both cases lead to nearly identical stress-strain curves, (see Figs. B-1 and B-2). Differences between the materials, however, become apparent in the results further from the loaded end of the tube, at z = 75 in., also shown in Fig. 10. Arrival times and the corresponding jumps in stress differ noticeably, but not radically. This indicates that the effect of differences in triaxial behavior increases with z, a trend which will hold in other cases too.

While the agreement between the test and the computation is gratifying, its importance must not be exaggerated. The fact that both sets of material parameters give good results indicates a lack of sensitivity in this location, provided the behavior in uniaxial strain is well expressed by the parameters. The agreement should also not be used to claim confirmation of the elasto-plastic model used. Any other model representing the uniaxial stress-strain curve well would have given good results too. There is one conclusion of some importance, however, which can be drawn from the agreement of test results and analysis. The latter matched, in Cases 1 and 2, the uniaxial static test. The adequacy of the static test as a basis for a dynamic analysis indicates

that effects of strain rate in this range, and for this material, are not important.

A sharper tool for an experimental decision on the adequacy of any material model could be made by observing not only the axial stress, but also the radial motion of the restraining rings. To demonstrate the strong dependence of the radial motion on the material properties, Fig. 6 shows also a plot of the radial velocity at z = 15 in. and 75 in. for the material of Case 2. The velocities are only about 50% of those for Case 1.

c) Considerations Concerning Truncation.

An obvious, but uneconomical way to determine the sufficiency of a truncation is to make an alternative computation for the actual problem with an increased number of terms.

However, estimates of adequacy can be made with less effort, based on simplifications of the material properties. In Appendix A, the differential equations for a tube filled with a linear elastic inviscid fluid are obtained from the general relations in Sections II, III and IV.

Applying these relatively simple relations and comparing the results from truncations to one and two terms, gives an understanding of the situation. The nondimensional analysis in Appendix A depends on the shape of the input function $\bar{p}_o(\tau)$ and on the two parameters

$$\bar{B} = \frac{B r_o}{K_o} = \frac{E_s h}{K_o r_o}$$

$$\bar{A} = \frac{A}{\rho r_o} = \frac{\rho_s h}{\rho r_o}$$

The last parameter expresses the influence of the mass of the containing rings and is on physical grounds of minor importance, because this mass is a small fraction of the mass of the enclosed material. There is, further, no reason to expect a radical dependence on $\bar{p}_o(\tau)$ when the time constants describing the load histories are of similar order of magnitude. The situation for the fluid, considered in Appendix A, thus depends principally on the nondimensional parameter $\bar{B}$.

To use the result obtained for a fluid in Appendix A as a guide for a nonlinear solid, it is necessary to use an appropriate equivalent value $\bar{B}_e$ for the parameter $\bar{B}$. If a tube is so stiff that the transverse strains ε_r vanish, the truncation to one term inherently gives the exact solution. As the transverse strains increase, or more precisely as the ratio $\varepsilon_r/\varepsilon_z$ increases, the solution using one term will become progressively less accurate. The value $\varepsilon_r/\varepsilon_z$ seems therefore a suitable gage and the equivalent value $\bar{B}_e$ should be selected so that the ratios $\varepsilon_r/\varepsilon_z$ in fluid and solid agree. As there are no strain rate effects only a static comparison is required, but the nonlinearity in the solid requires the selection of a representative stress level. For the material properties designated as Case 1 and a stress level of 200 psi the values

$$\bar{B}_{e1} \sim 718 \quad , \quad \bar{B}_{e2} \sim 26.2 \quad , \quad \bar{B}_{e3} \sim 4.5$$

were obtained for the three shell stiffnesses B_i defined

previously. (The corresponding values $\bar{B}_e$ for the material of Case 2 are somewhat larger, e.g., $\bar{B}_{e2} = 55.$) The knowledge of the values $\bar{B}_e$ permits comparison with the results for the fluid, which were obtained from

$$\bar{B}_1 = 2110 \quad , \quad \bar{B}_2 = 77.7 \quad , \quad \bar{B}_3 = 14.2$$

The results using one term were quite satisfactory for $\bar{B}_1$ and $\bar{B}_2$, while the results for the smallest value $\bar{B}_3 = 14.2$ were meaningful, but not really good, particularly for the largest value of $\zeta = 3.0$. This leads to the conclusion that all results for the stiff tube, $B_1 = 7.95 \times 10^5$ lb/in^3, can be accepted as reliable. For the value $B_2 = 2.93 \times 10^4$ lb/in^3, the results at $z = 15$ in. and 25 in. can be accepted, but the results at 75 in. are likely to deviate appreciably. The results for $B_3 = 5.35 \times 10^3$ lb/in^3 may be inaccurate, but still meaningful at $z = 15$ in., but are questionable at $z = 75$ in. The insufficiency of the truncation may be the cause for the drop in the shock strength from $z = 25$ in. to $z = 75$ in. in Fig. 5.

The value $\bar{B}_{e2}$ for the material of Case 2 being larger than for Case 1, the results shown are at least as good as for the material of Case 1.

d) Conclusion.

A scheme has been presented which permits the analysis of wave propagation problems in tubes filled with an elasto-plastic material. The approach permits the treatment of cases where the

material behaves differently, elastically or plastically, in different regions which move with time in an a priori unknown manner.

The method is applicable to other materials. For example, it is possible to modify the model used to allow for hysteresis by using different pressure-volume relationships for loading and unloading. It is also possible to apply the approach to elasto-plastic materials with different yield conditions, to materials of the type considered in Ref. [3], or to viscous or visco-plastic materials.

The arrangement considered is suitable for tests, so that the analysis proposed permits a check on the appropriateness of material models and corresponding parameters obtained from other tests. It may also be possible to use the analysis in conjunction with dynamic tests to obtain the values of the parameters required for a theoretical description of a material.

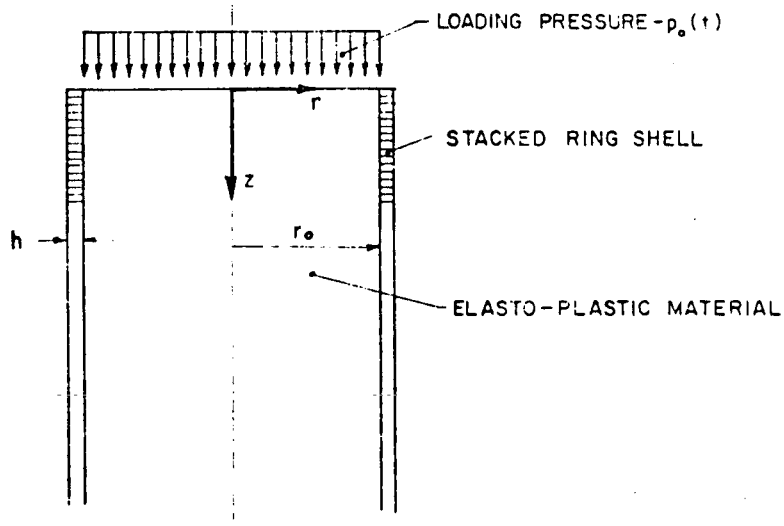

FIG. 1 - CONFIGURATION

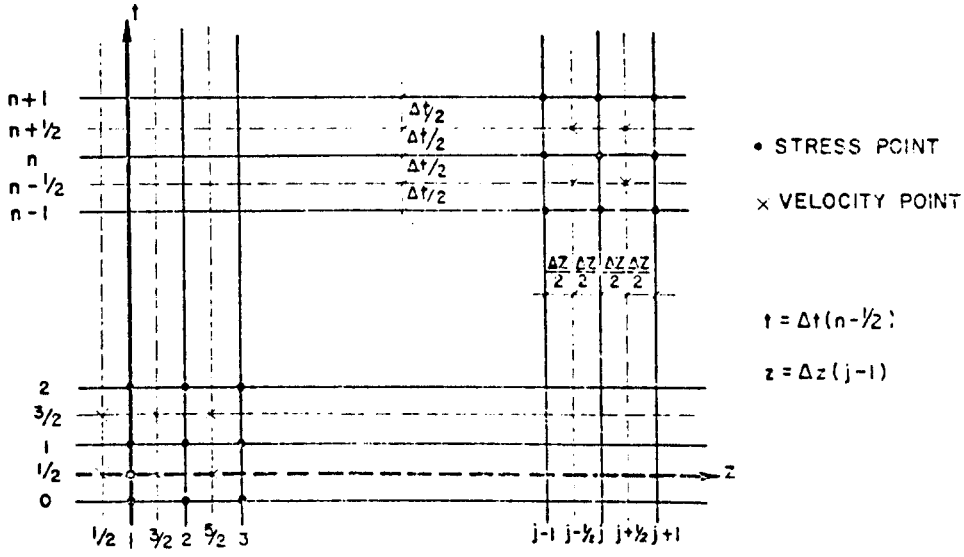

FIG. 2 – FINITE DIFFERENCE GRID

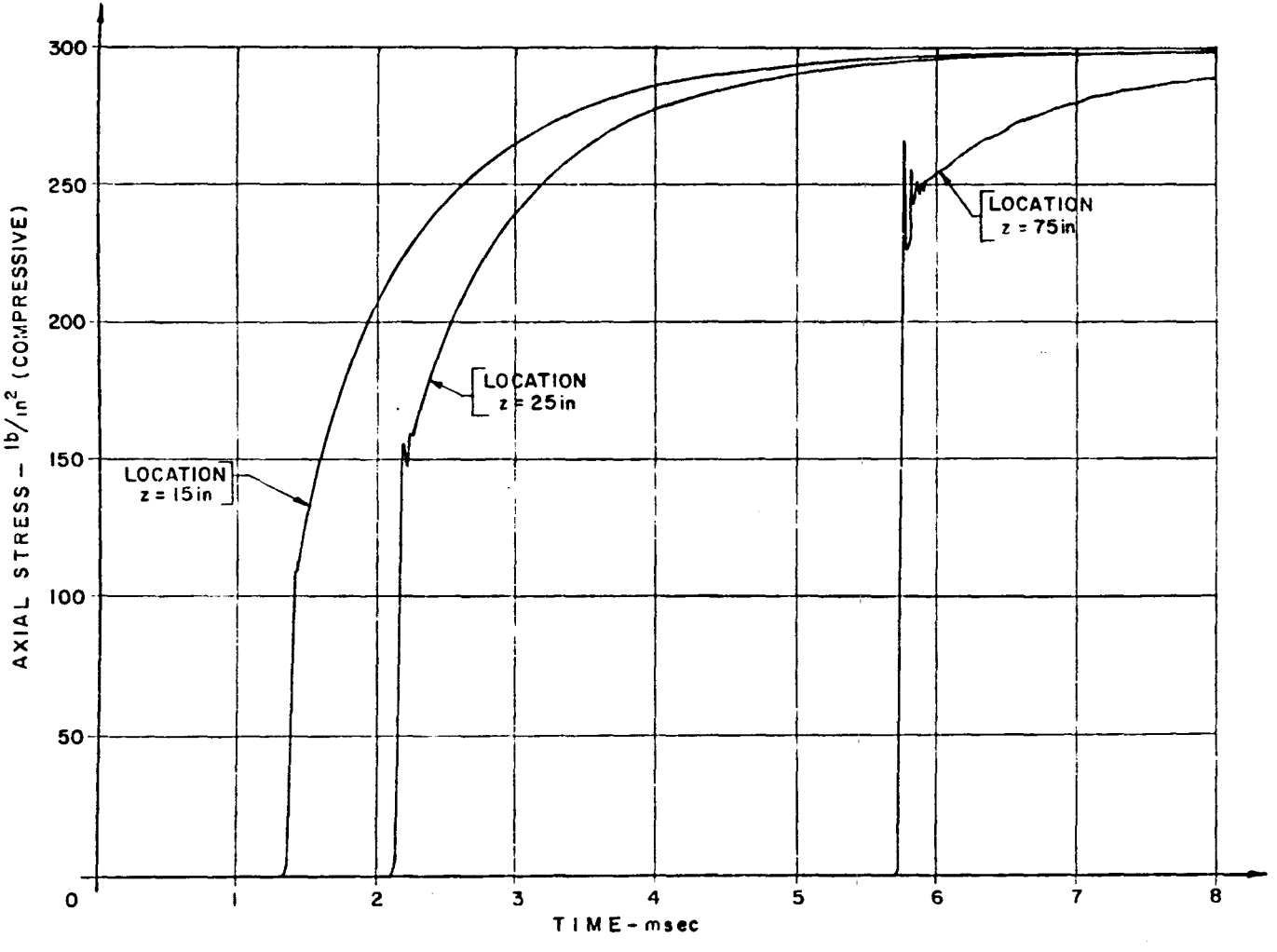

FIG.3– TIME HISTORIES OF AXIAL STRESS
(MATERIAL OF CASE I, SHELL STIFFNESS $B_1 = 7.95 \times 10^5 lb/in^3$)

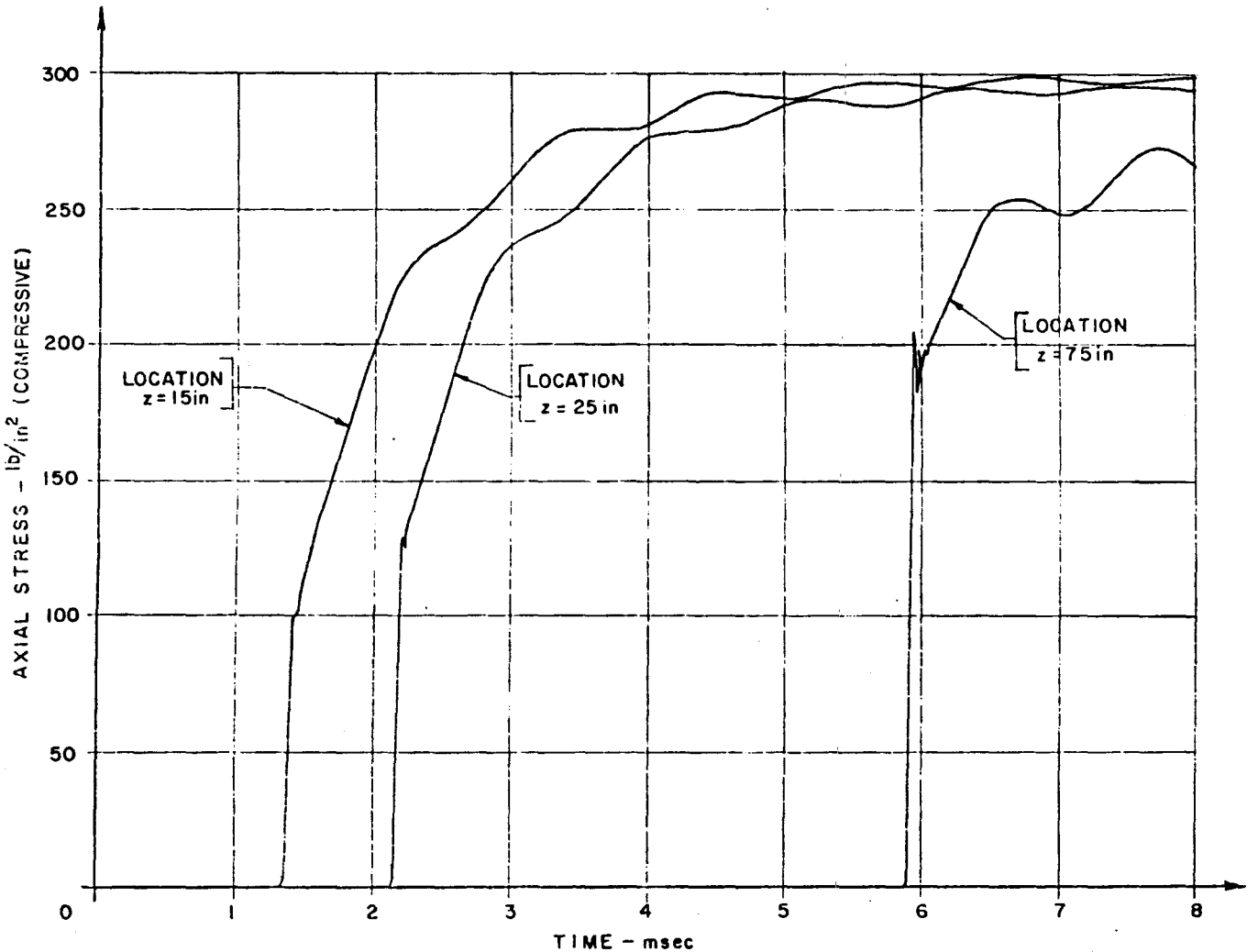

FIG. 4 – TIME HISTORIES OF AXIAL STRESS
(MATERIAL OF CASE I, SHELL STIFFNESS $B_2 = 2.93 \times 10^4$ lb/in³)

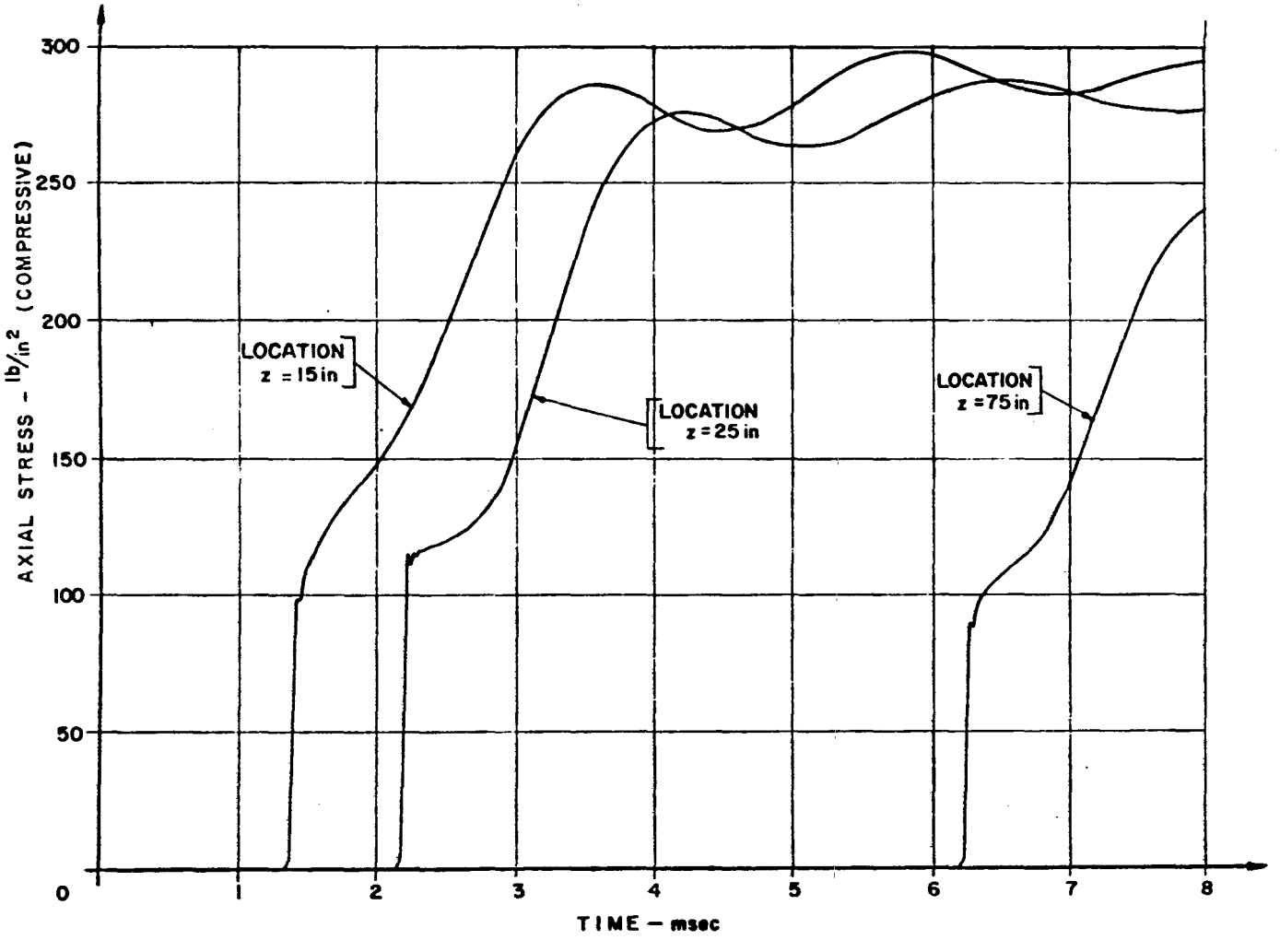

FIG. 5 TIME HISTORIES OF AXIAL STRESS
(MATERIAL OF CASE I, SHELL STIFFNESS $B_3 = 5.35 \times 10^3$ lb/in³)

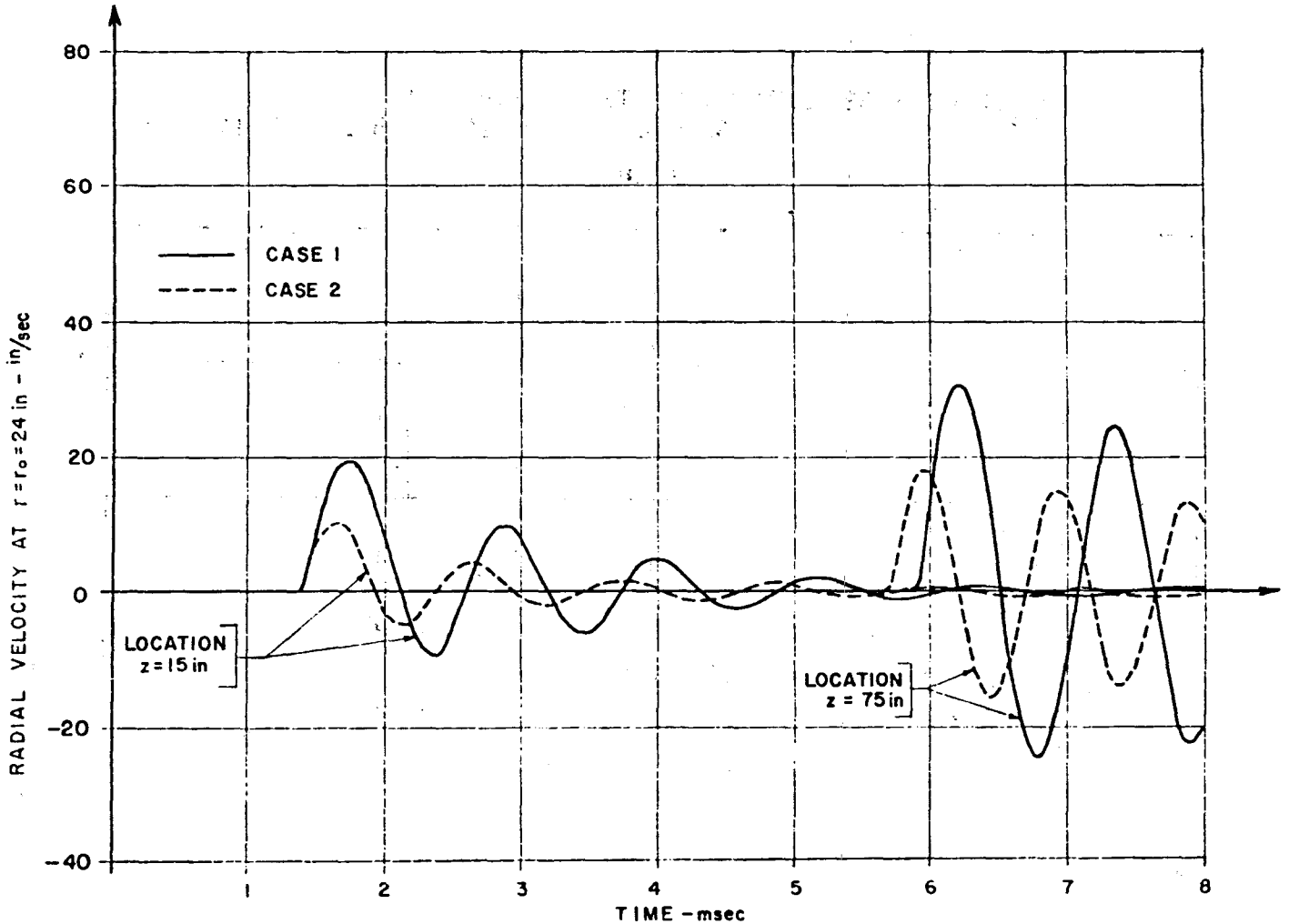

FIG.6 - TIME HISTORIES OF RADIAL VELOCITY AT $r=r_o$
(MATERIAL OF CASE 1 AND 2, SHELL STIFFNESS $B_2 = 2.93 \times 10^4 lb/in^3$)

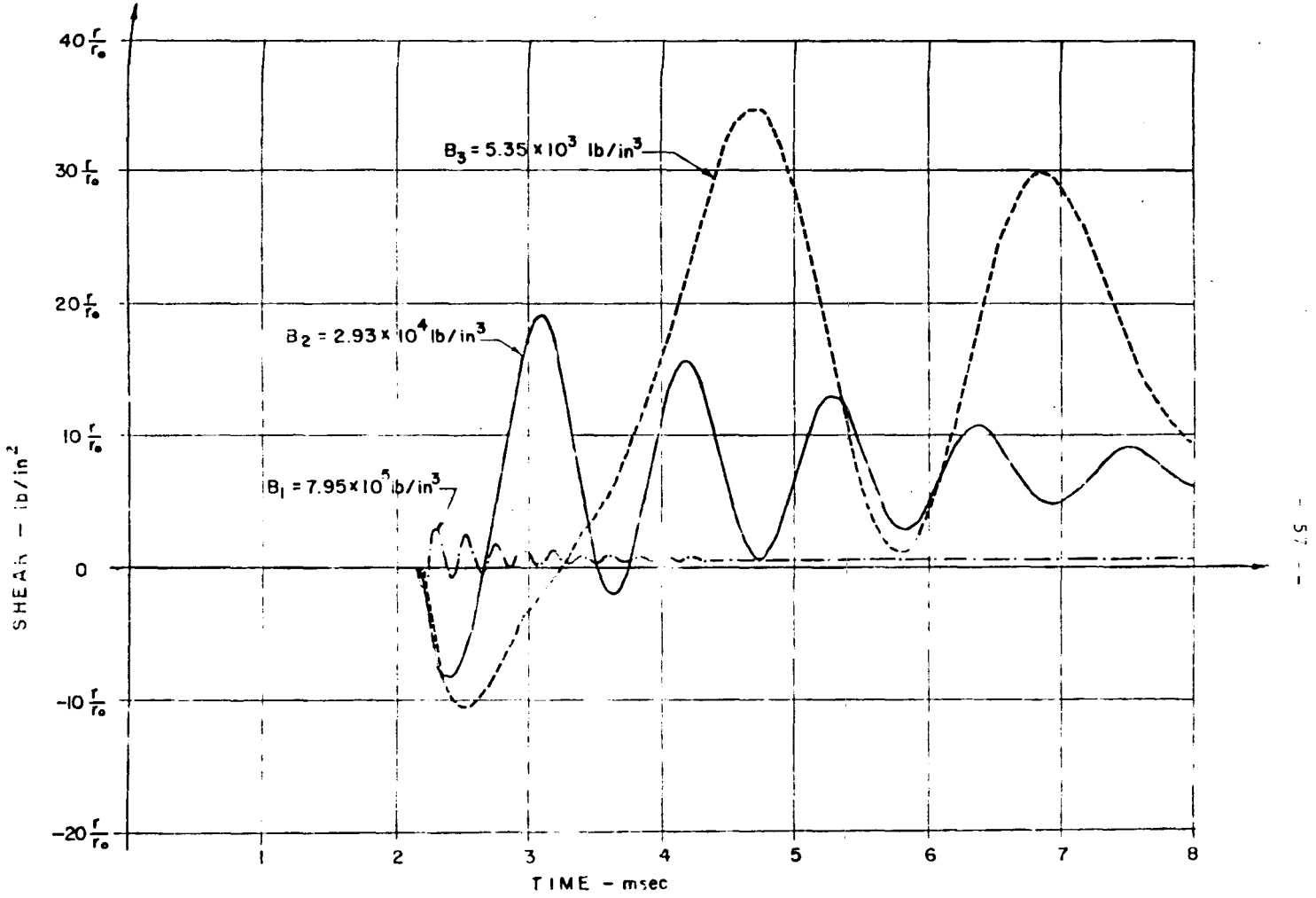

FIG. 7 - TIME HISTORIES OF SHEAR AT $z = 25$ in
(MATERIAL OF CASE I, SHELL STIFFNESSES B_1, B_2, B_3)

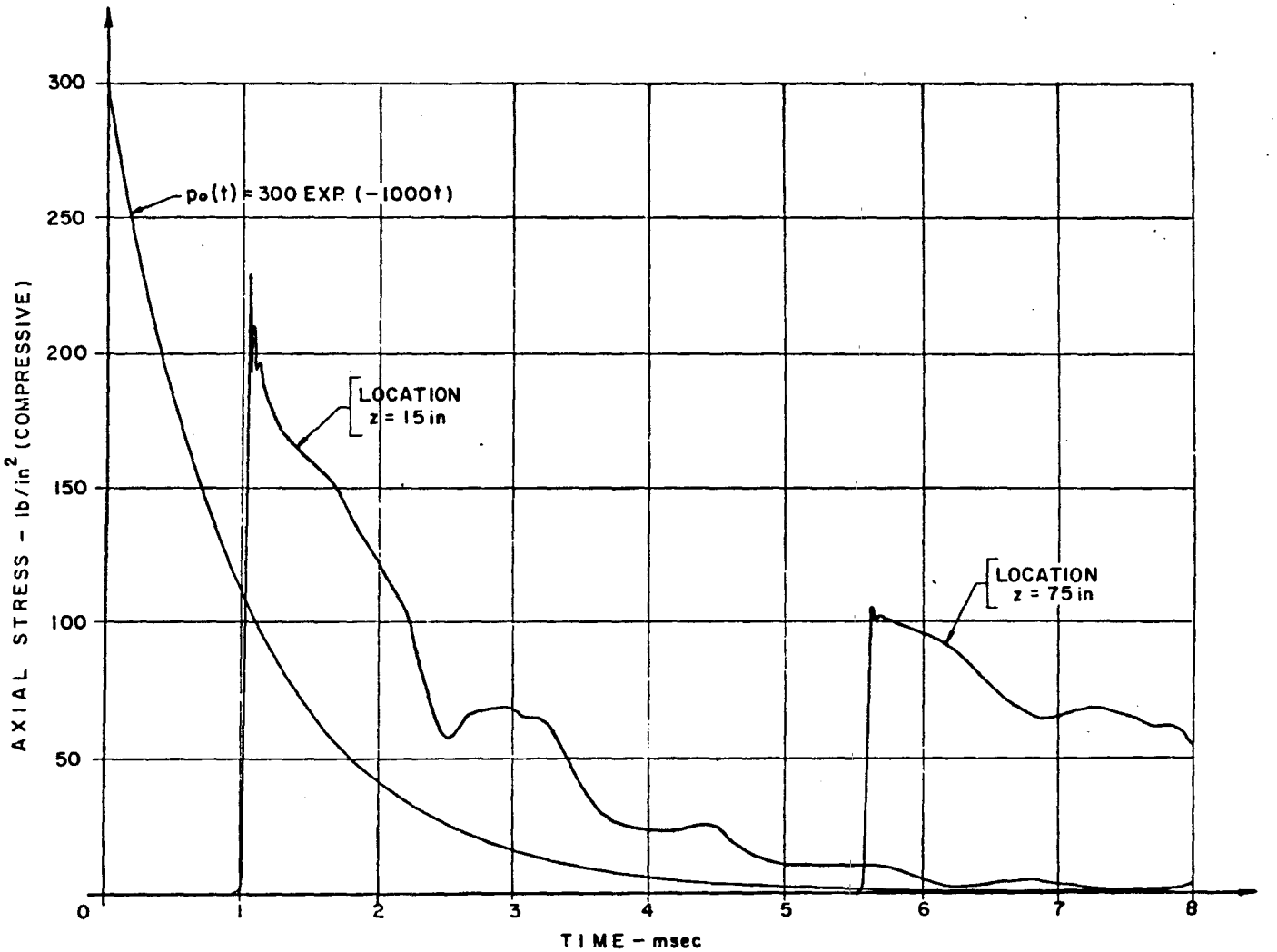

FIG. 8 – INPUT $p_o(t)$ AND TIME HISTORIES OF AXIAL STRESS
(MATERIAL OF CASE I, SHELL STIFFNESS $B_2 = 2.93 \times 10^4$ lb/in^3)

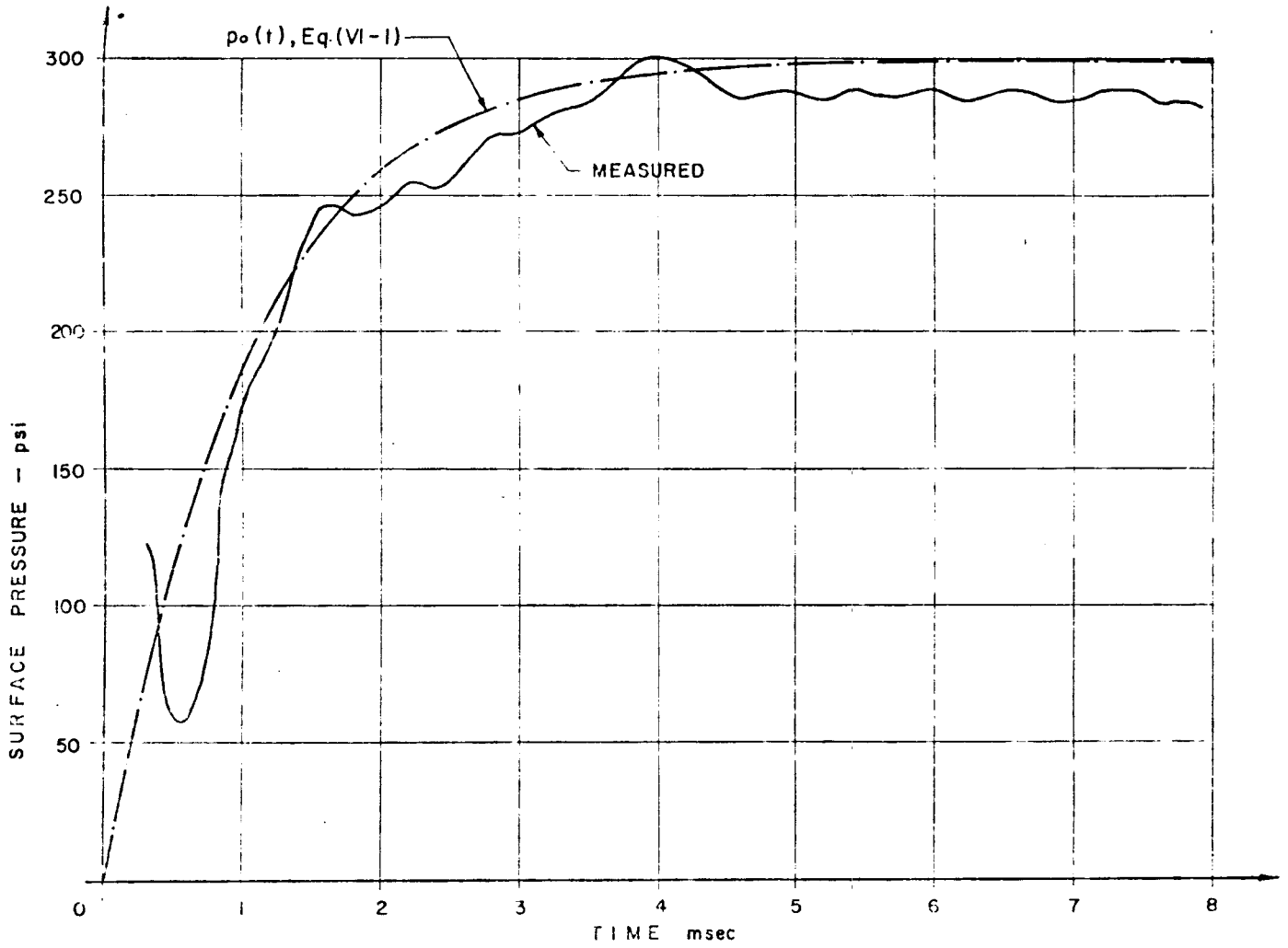

FIG. 9 – COMPARISON OF TIME HISTORY OF $p_o(t)$, AND OF THE SURFACE PRESSURE MEASURED IN THE TEST

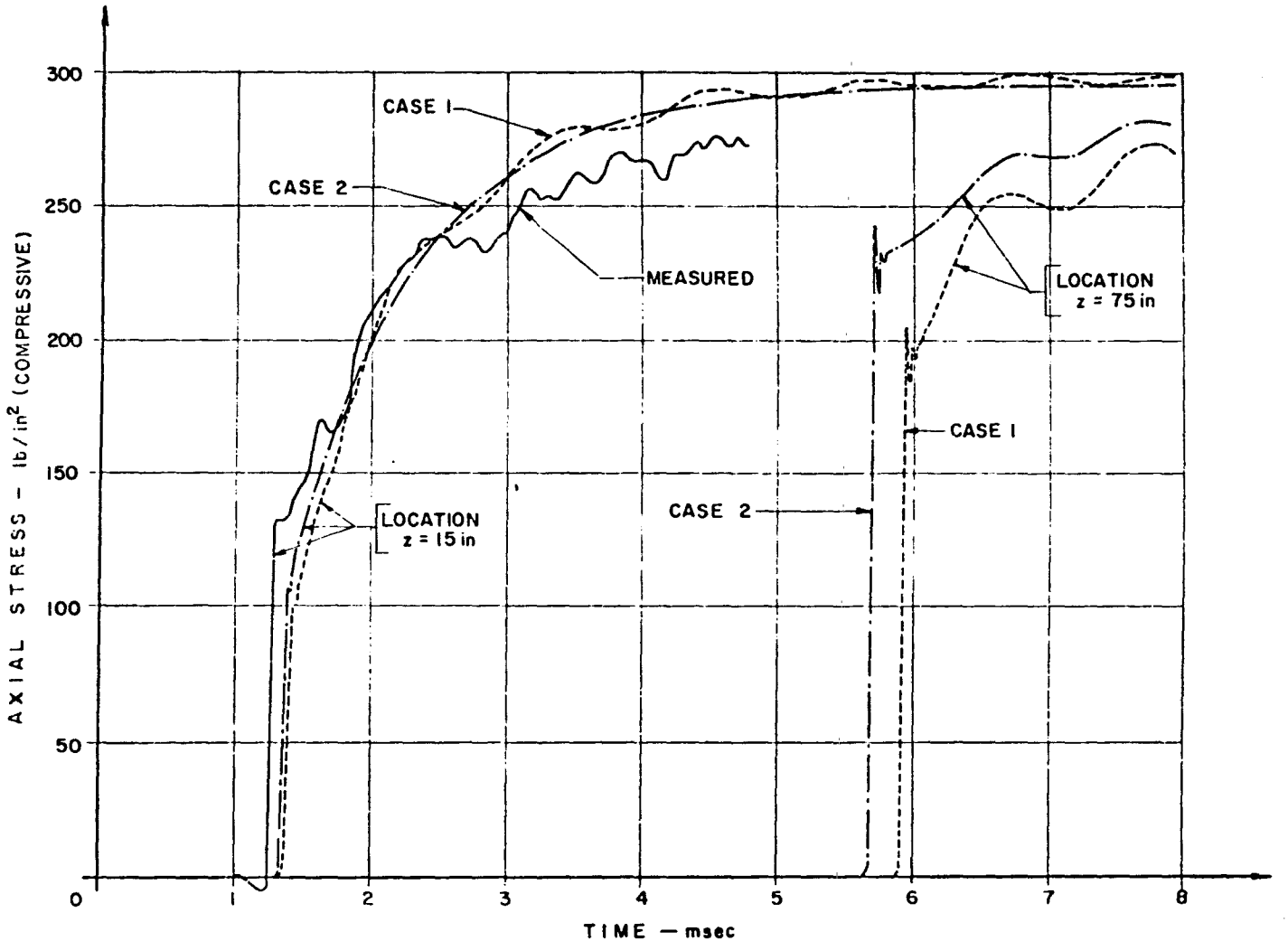

FIG. 10 — COMPARISON OF TEST RESULT AND COMPUTED TIME HISTORIES OF AXIAL STRESS (MATERIALS OF CASE 1 AND 2, SHELL STIFFNESS $B_2 = 2.93 \cdot 10^4$ lb/in^3)

APPENDIX A - Linear Inviscid Fluid - Influence of Truncation.

For the purpose of obtaining a judgment on the validity of the truncation used in the body of the report, this appendix considers the special case of a linear inviscid fluid in the same configuration. For this case, numerical solutions based on truncations with one and with two terms are compared. In this simple case the analysis requires little effort, yet is very helpful. The appropriate equations for a linear inviscid fluid can be obtained as a special case of the relations found in Section IV in elastic regions.

a) Equations for a Linear Inviscid Fluid.

In an inviscid fluid, several of the variables vanish,

$$R_i = Z_i = T_i \equiv 0$$

and the corresponding equations obtained by the Galerkin method will not appear. The value G=0 is to be used for the modulus of rigidity, while the linearity leads to

$$K(p) = K_o = \text{constant}$$

so that Eq. (IV-10) becomes $K_{mj} = K_o$.

As a result of these simplifications, Eq. (IV-7) becomes

$$\sum_{i=0}^{n} \frac{r_o^{2i}}{(2i+2)(2i+m+4)} \left[(2i+2)\, U_i + V_i' + \frac{1}{K_o} \dot{P}_i\right] = 0; \quad m=0,2,\ldots,2n \tag{A-1a}$$

This form can further be simplified by noting that the expression in brackets does not contain the subscript m and the coefficients $\frac{r_o^{2i}}{(2i+2)(2i+m+4)}$ form the elements of a square nonsingular matrix. Consequently, the equations uncouple

$$(2i+2)\ U_i + V_i' + \frac{1}{K_o}\dot{P}_i = 0 \ ;\ i=0,1,2,\ldots,n \qquad \text{(A-1b)}$$

Equation (IV-3) contains the indeterminate quantity $\frac{\dot{Z}_i}{G}$. By the artifice of evaluating this quantity from Eq. (IV-6) and noting that the equations again uncouple, one finds

$$\frac{3}{2G}\dot{Z}_i = 2V_i' - (2i+2)\ U_i$$

Substitution of this relation into Eq. (IV-3) gives

$$\sum_{i=0}^{n} r_o^{2i}\left\{-\frac{(m+3)}{(2i+m+3)}\dot{P}_i + r_o B U_i + \left[r_o A + \frac{\rho r_o^2}{(2i+m+5)}\right]\ddot{U}_i\right\} = 0 \ ;$$

$$m=0,2,\ldots,2n \qquad \text{(A-2)}$$

Finally, in Eq. (IV-4) attention must be given to the constant C, introduced in Section III in the process of incorporating the tangential boundary condition at $r = r_o$ represented by Eq. (II-17). Unless C is taken as zero, Eq. (IV-4) will contain the implication that the fluid at $r = r_o$ and the stacked ring shell have the same axial velocity, which is not a proper boundary condition for an inviscid fluid. When C=0 is introduced, Eqs. (IV-4), which uncouple again, become

$$\frac{\partial}{\partial t}\left(P_i' + \rho \dot{V}_i\right) = 0 \quad ; \quad i = 0, 1, 2, \ldots, n$$

This form can be simplified by integration from an initial state of rest and zero pressure,

$$P_i' + \rho \dot{V}_i = 0 \quad ; \quad i = 0, 1, 2, \ldots, n \qquad \text{(A-3)}$$

The formulation is completed by the specification of an initial stress-free state of rest at t=0 and of the boundary condition,

$$[P_i]_{z=0} = p_o(t)\, \delta_{oi} \quad ; \quad i = 0, 1, 2, \ldots, n \qquad \text{(A-4)}$$

b) Nondimensional Governing Equations.

By the introduction of the dimensionless variables

$$\left.\begin{aligned} \zeta &= z/r_o \\ \tau &= \frac{t}{r_o}\sqrt{K_o/\rho} \\ \bar{P}_i &= r_o^{2i}\, P_i/K_o \\ \bar{V}_i &= r_o^{2i}\, V_i \sqrt{\rho/K_o} \\ \bar{U}_i &= r_o^{2i+1}\, U_i \sqrt{\rho/K_o} \\ \bar{p}_o(\tau) &= \frac{1}{K_o}\, p_o(\tau r_o \sqrt{\rho/K_o}) \end{aligned}\right\} \qquad \text{(A-5)}$$

Equations (1b), (2), (3) and (4) are transformed to

$$\frac{\partial \bar{P}_i}{\partial \tau} + \frac{\partial \bar{V}_i}{\partial \zeta} + (2i+2)\, \bar{U}_i = 0 \; ; \; i = 0, 1, \ldots, n \qquad \text{(A-6)}$$

$$\sum_{i=0}^{n} \left[- \frac{(m+3)}{(2i+m+3)} \frac{\partial \bar{P}_i}{\partial \tau} + \bar{\bar{B}} \bar{U}_i + \bar{A}_{mi} \frac{\partial^2 \bar{U}_i}{\partial \tau^2} \right] = 0 \; ; \; m = 0, 2, \ldots, 2n \tag{A-7}$$

$$\frac{\partial \bar{V}_i}{\partial \tau} + \frac{\partial \bar{P}_i}{\partial \zeta} = 0 \quad ; \quad i = 0, 1, \ldots, n \tag{A-8}$$

$$[\bar{P}_i]_{\zeta=0} = \bar{P}_o(\tau)\, \delta_{oi} \quad ; \quad i = 0, 1, \ldots, n \tag{A-9}$$

where

$$\bar{B} = \frac{r_o B}{K_o} \quad , \quad \bar{A}_{mi} = \frac{A}{\rho r_o} + \frac{1}{(2i+m+5)} \tag{A-10}$$

c) Truncations.

If a truncation to two terms for each variable is desired the equations are obtained from Eqs. (6)-(9) for n=1. The result is

$$\frac{\partial \bar{P}_o}{\partial \tau} = - \frac{\partial \bar{V}_o}{\partial \zeta} - 2\bar{U}_o \tag{A-11a}$$

$$\frac{\partial \bar{P}_1}{\partial \tau} = - \frac{\partial \bar{V}_1}{\partial \zeta} - 4\bar{U}_1 \tag{A-11b}$$

$$\frac{\partial^2 \bar{U}_o}{\partial \tau^2} = C_{11} \frac{\partial \bar{P}_o}{\partial \tau} + C_{12} \frac{\partial \bar{P}_1}{\partial \tau} - \bar{B} C_{11} \bar{U}_o - \bar{B} C_{11} \bar{U}_1 \tag{A-12a}$$

$$\frac{\partial^2 \bar{U}_1}{\partial \tau^2} = C_{21} \frac{\partial \bar{P}_o}{\partial \tau} + C_{22} \frac{\partial \bar{P}_1}{\partial \tau} - \bar{B} C_{21} \bar{U}_o - \bar{B} C_{21} \bar{U}_1 \tag{A-12b}$$

$$\frac{\partial \bar{V}_o}{\partial \tau} = - \frac{\partial \bar{P}_o}{\partial \zeta} \tag{A-13a}$$

$$\frac{\partial \bar{V}_1}{\partial \tau} = - \frac{\partial \bar{P}_1}{\partial \zeta} \tag{A-13b}$$

$$[\bar{P}_o]_{\zeta=0} = \bar{\rho}_o(\tau) \qquad \text{(A-14a)}$$

$$[\bar{P}_1]_{\zeta=0} = 0 \qquad \text{(A-14b)}$$

where

$$\left.\begin{aligned} C_{11} &= (\bar{A}_{21} - \bar{A}_{01})/(\bar{A}_{00}\bar{A}_{21} - \bar{A}_{01}\bar{A}_{20}) \\ C_{12} &= (\tfrac{3}{5}\,\bar{A}_{21} - \tfrac{5}{7}\,\bar{A}_{01})/(\bar{A}_{00}\bar{A}_{21} - \bar{A}_{01}\bar{A}_{20}) \\ C_{21} &= (\bar{A}_{00} - \bar{A}_{20})/(\bar{A}_{00}\bar{A}_{21} - \bar{A}_{01}\bar{A}_{20}) \\ C_{22} &= (\tfrac{5}{7}\,\bar{A}_{00} - \tfrac{3}{5}\,\bar{A}_{20})/(\bar{A}_{00}\bar{A}_{21} - \bar{A}_{01}\bar{A}_{20}) \end{aligned}\right\} \qquad \text{(A-15)}$$

The system for the truncation using one term consists of Eqs. (11a), (12a), (13a) and (14a) in which the terms with $\bar{P}_1$, $\bar{U}_1$ and $\bar{V}_1$ are removed. The definition of C_{1i} becomes $C_{11} = 1/A_{00}$.

d) Finite Difference Equations.

The finite difference form of Eqs. (11) to (14) is generated in the manner described in Section V. A staggered grid in both time and space with constant mesh size is used, with derivatives approximated by central differences except for the time derivatives in the constitutive equations, Eqs. (11a,b), which are approximated by the form Eq. (V-3). The resulting equations for the truncation to two terms are

$$\bar{P}^{n+1}_{o\,j} = \bar{P}^{n}_{o\,j} + \frac{1}{2 + C_D}\left(\bar{P}^{n}_{o\,j-1} - 2\bar{P}^{n}_{o\,j} + \bar{P}^{n}_{o\,j-1}\right) -$$

$$- \frac{\Delta\tau}{\Delta\zeta}\left(\bar{V}^{n+\frac{1}{2}}_{o\,j+\frac{1}{2}} - \bar{V}^{n+\frac{1}{2}}_{o\,j-\frac{1}{2}}\right) - \Delta\tau\left(\bar{U}^{n+\frac{1}{2}}_{o\,j+\frac{1}{2}} + \bar{U}^{n+\frac{1}{2}}_{o\,j-\frac{1}{2}}\right) \qquad \text{(A-16a)}$$

$$\bar{P}^{n+1}_{1\,j} = \bar{P}^{n}_{1\,j} + \frac{1}{2 + C_D}\left(\bar{P}^{n}_{1\,j+1} - 2\bar{P}^{n}_{1\,j} + \bar{P}^{n}_{1\,j-1}\right) -$$

$$- \frac{\Delta\tau}{\Delta\zeta}\left(\bar{V}^{n+\frac{1}{2}}_{1\,j+\frac{1}{2}} - \bar{V}^{n+\frac{1}{2}}_{1\,j-\frac{1}{2}}\right) - 2\Delta\tau\left(\bar{U}^{n+\frac{1}{2}}_{1\,j+\frac{1}{2}} + \bar{U}^{n+\frac{1}{2}}_{1\,j-\frac{1}{2}}\right) \qquad \text{(A-16b)}$$

$$\bar{U}^{n\,+\,3/2}_{o\,j+\frac{1}{2}} = \left(2 - \bar{B}C_{11}\bar{\Delta\tau}^2\right)\bar{U}^{n+\frac{1}{2}}_{o\,j+\frac{1}{2}} - \bar{U}^{n-\frac{1}{2}}_{o\,j+\frac{1}{2}} +$$

$$+ \frac{C_{11}\Delta\tau}{2}\left(\bar{P}^{n+1}_{o\,j+1} - \bar{P}^{n}_{o\,j+1} + \bar{P}^{n+1}_{o\,j} - \bar{P}^{n}_{o\,j}\right) +$$

$$+ \frac{C_{12}\Delta\tau}{2}\left(\bar{P}^{n+1}_{1\,j+1} - \bar{P}^{n}_{1\,j+1} + \bar{P}^{n+1}_{1\,j} - \bar{P}^{n}_{1\,j}\right) -$$

$$- \bar{B}C_{11}\bar{\Delta\tau}^2\bar{U}^{n+\frac{1}{2}}_{1\,j+\frac{1}{2}} \qquad \text{(A-17a)}$$

$$\bar{U}^{n\,+\,3/2}_{1\,j+\frac{1}{2}} = \left(2 - \bar{B}C_{21}\bar{\Delta\tau}^2\right)\bar{U}^{n+\frac{1}{2}}_{1\,j+\frac{1}{2}} - \bar{U}^{n-\frac{1}{2}}_{1\,j+\frac{1}{2}} +$$

$$+ \frac{C_{21}\Delta\tau}{2}\left(\bar{P}^{n+1}_{o\,j+1} - \bar{P}^{n}_{o\,j+1} + \bar{P}^{n+1}_{o\,j} - \bar{P}^{n}_{o\,j}\right)$$

$$+ \frac{C_{22}\Delta\tau}{2}\left(\bar{P}^{n+1}_{1\,j+1} - \bar{P}^{n}_{1\,j+1} + \bar{P}^{n+1}_{1\,j} - \bar{P}^{n}_{1\,j}\right)$$

$$- \bar{B}C_{21}\bar{\Delta\tau}^2\bar{U}^{n+\frac{1}{2}}_{o\,j+\frac{1}{2}} \qquad \text{(A-17b)}$$

$$\bar{V}_{o\ j+\frac{1}{2}}^{n+3/2} = \bar{V}_{o\ j+\frac{1}{2}}^{n+\frac{1}{2}} - \frac{\Delta\tau}{\Delta\zeta}\left(\bar{P}_{o\ j+1}^{n+1} - \bar{P}_{o\ j}^{n+1}\right) \qquad \text{(A-18a)}$$

$$\bar{V}_{1\ j+\frac{1}{2}}^{n+3/2} = \bar{V}_{1\ j+\frac{1}{2}}^{n+\frac{1}{2}} - \frac{\Delta\tau}{\Delta\zeta}\left(\bar{P}_{1\ j+1}^{n+1} - \bar{P}_{1\ j}^{n+1}\right) \qquad \text{(A-18b)}$$

$$\bar{P}_{o\ 1}^{n} = \bar{p}\,[(n-\tfrac{1}{2})\,\Delta\tau] \qquad \text{(A-19a)}$$

$$\bar{P}_{1\ 1}^{n} = 0 \qquad \text{(A-19b)}$$

The equations for the truncation to the leading terms are obtained by the procedure described in the case of the differential equations.

Equations (16a) to (18b) represent a two level implicit linear finite difference operator whose application requires the knowledge of $\bar{P}_o$ and $\bar{P}_1$ at the time level n, $\bar{V}_o$, $\bar{V}_1$, $\bar{U}_o$ and $\bar{U}_1$ at $(n+\frac{1}{2})$ and $\bar{U}_o$ and $\bar{U}_1$ at $(n-\frac{1}{2})$, and at all relevant space points. The stability criterion becomes, Ref. [16],

$$\frac{\Delta\tau}{\Delta\zeta} \leq \sqrt{1 - \frac{2}{2 + C_D}} \qquad \text{(A-20)}$$

e) Discussion of Results.

Figures A-1, A-2 and A-3 show typical time histories of the dimensionless pressure $\bar{P}_o^{(1)}$ obtained for a unit step input if the series are truncated to one term. In this case the values of the pressure at r=0 and at $r=r_o$ are identical, and $\bar{P}_o^{(1)}$ is thus the mean pressure. The values $\bar{P}_c^{(2)}$ and $\bar{P}_{ro}^{(2)}$ are also plotted, representing the dimensionless pressures at

$r=0$ and $r=r_o$, respectively, when two terms in the truncation are retained. The mean value of the pressure, in this case, is $\bar{P}_m^{(2)} = \bar{P}_o^{(2)} + \frac{1}{2}\bar{P}_1^{(2)} = \frac{1}{2}[\bar{P}_o^{(2)} + \bar{P}_{ro}^{(2)}]$. The latter is a suitable basis for comparison with $\bar{P}_o^{(1)}$.

Three sets of results for different values of the non-dimensional stiffness $\bar{B}$ are given. Comparing first the results for the same value of $\bar{B}$, but in different locations, it is seen that the differences increase with ζ, i.e., with distance from the input end. From Fig. A-2 it is also apparent that in each location the oscillations and the differences decay with time.

The order of magnitude of the difference in the same location increases as the stiffness parameter $\bar{B}$ of the shell decreases. It serves no purpose to quote percentages for the various cases. For the stiffest shell, $\bar{B}_1 = 2110$, the truncation using one term is clearly an excellent approximation. For the cases $\bar{B}_2 = 77.7$ and $\bar{B}_3 = 14.2$, the results for $\bar{P}_o^{(1)}$ and $\bar{P}_m^{(2)}$ differ moderately. In these cases, appreciable differences between the pressure at $r=0$ and at $r=r_o$ occur, particularly shortly after arrival of the signal, the situation being particularly unfavorable for $\bar{B}_3$ and for large values of ζ.

The problem of the fluid filled tube for a step velocity input has been treated in Ref. [17] by transform methods,

leading to a series solution. Numerical results were obtained for two cases, corresponding to $\bar{B}=2$ and $\bar{B}=10$. From the Reference it is known that the jump in pressure at arrival time in all locations is equal to the initial pressure, and the location and magnitude of this jump are indicated in Figs. A-1 to A-3 for comparison purposes.

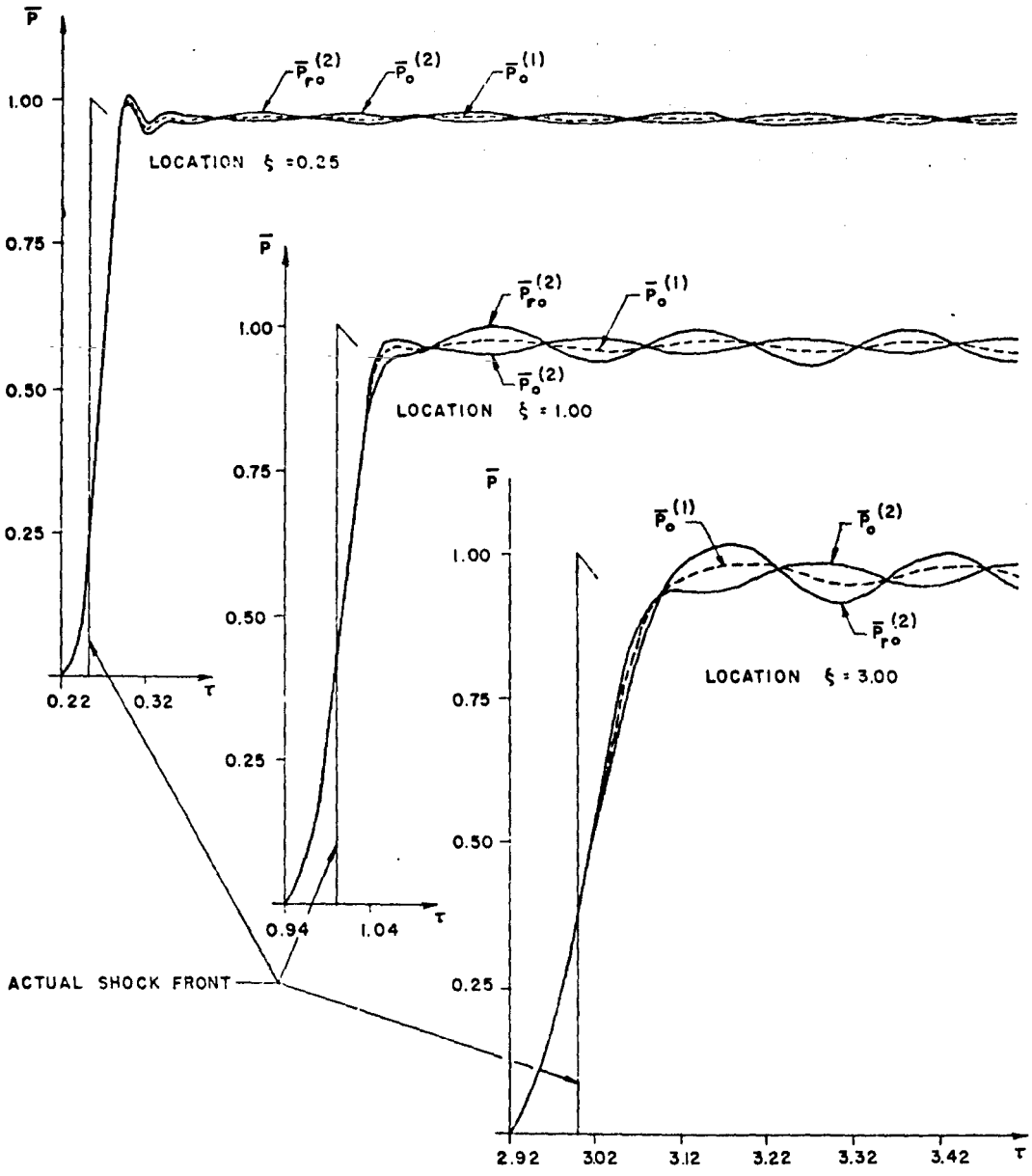

FIG. A-1 PRESSURE - TIME HISTORIES, $\bar{B}$ = 2110

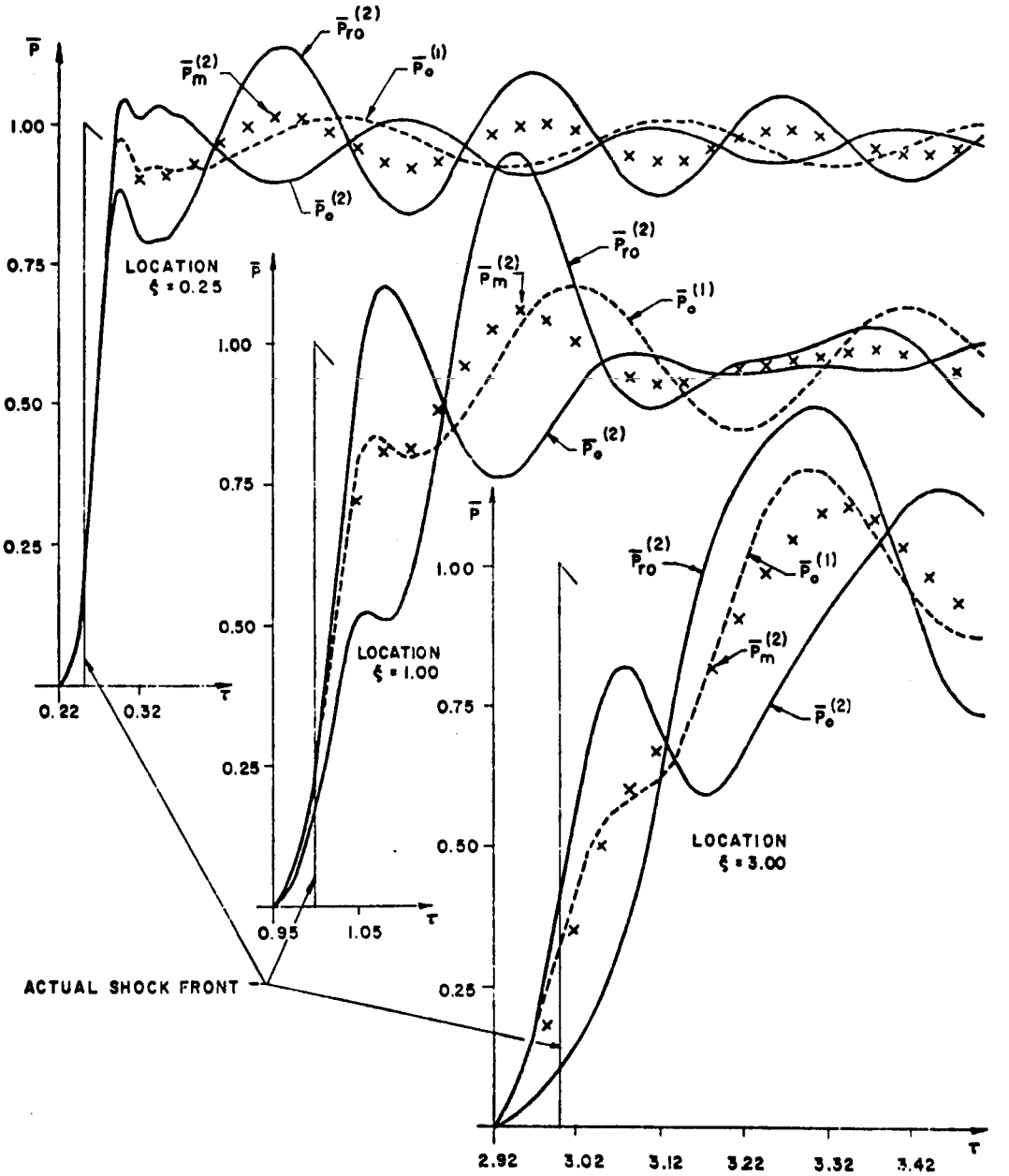

FIG. A-2 PRESSURE-TIME HISTORIES, $\bar{B} = 77.7$

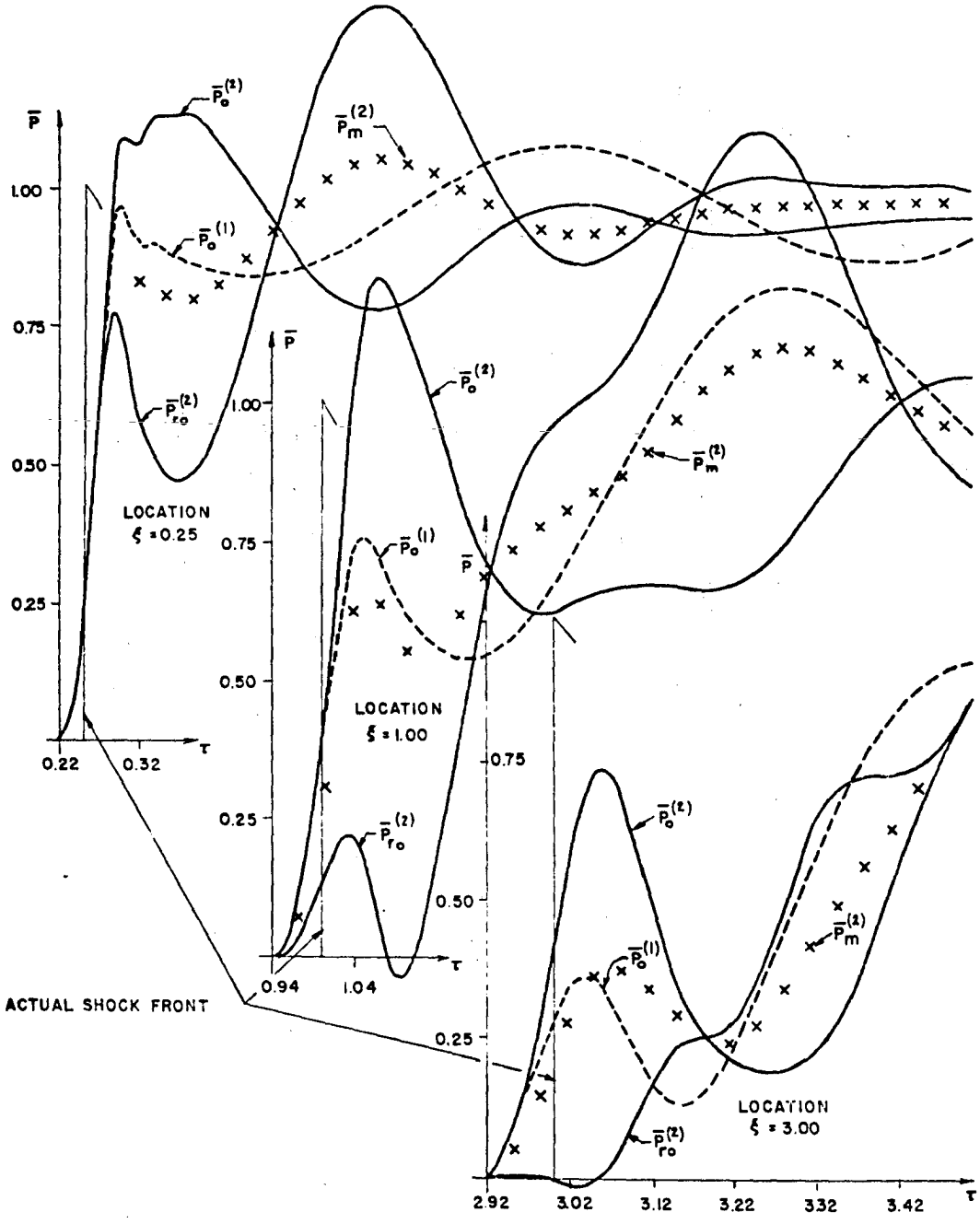

FIG. A-3 PRESSURE-TIME HISTORIES, $\bar{B}$ = 14.2

APPENDIX B - Estimate for the Magnitude of the Material Constants.

In order to select values of material constants to be used in the numerical examples, a fit was made using some available quasi-static test data on sand*). The data used were results of uniaxial and triaxial tests, and measurements of the velocities of the shock waves.

It must be stressed that no claim is made that the sets of values for the material constants given are of consequence in actual situations, which will vary greatly. The fits were made solely to get "reasonable" values for the various properties.

In view of the intended application to situations in which, at least grossly, the stress levels increase with time, only experimental data for initial loading were used for the fit. Further, also because the situation for stiff tubes is closer to uniaxial tests than to triaxial ones, the fit to the former was emphasized.

In addition to the values of k, α and G, the function K(p) is to be selected. For practical applications a function with three open parameters, such as

$$K(p) = K_o(1 + p/\bar{p})^n \qquad \text{(B-1a)}$$

where $K_o > 0$, $\bar{p} > 0$ and $1 > n > 0$ permits an adequate fit. This function leads to an expression for p in terms of ε_{kk} which is a parabola of order 1/(1-n).

---

*) Data on Cook's Bayou No. 1 sand, Refs. [18] and [19], obtained from the U.S. Army Engineer Waterways Experiment Station, Vicksburg, Miss.

Because of the exploratory nature of the present study the value $n=\frac{1}{2}$ was chosen immediately, to simplify the fitting process,

$$K(p) = K_o(1 + p/\bar{p})^{\frac{1}{2}} \qquad \text{(B-1b)}$$

A representative value for the density, $\rho = 1.573 \times 10^{-4}$ lb.sec^2/in^4 was selected. In addition it was assumed that the value of the constant k, representing cohesion, would be sufficiently small compared to the stress level to permit the use of the limiting value $k \to 0$ for the fit.

By trial two sets of material constants were determined, as follows:

Case 1	$\alpha = 3.09 \times 10^{-2}$	$G = 9660$ lb/in^2
	$K_o = 9050$ lb/in^2	$\bar{p} = 8.31$ lb/in^2
Case 2	$\alpha = 0.199$	$G = 18300$ lb/in^2
	$K_o = 2960$ lb/in^2	$\bar{p} = 1.56$ lb/in^2

As will be seen subsequently, Case 1 fits the uniaxial test up to 300 lb/in^2 extremely well, but gives very poor correlation with failure strength in the triaxial tests. Case 2 still fits the uniaxial test quite well. It approaches the triaxial ones somewhat better, but not really well. (This is inherent in the model employed.) The sets of parameters differ appreciably, and some results were run for both cases in order to determine the sensitivity of the results.

The fitting process, and the comparison of the fit obtained require a few analytical relations which are derived below.

a) Triaxial Test.

The triaxial test consists of a hydrostatic loading phase up to some value p_c of the confining pressure, followed by an axial loading phase during which the specimen is loaded axially at a constant confining pressure. If σ denotes the change of axial stress above its value $-p_c$ at the termination of the hydrostatic phase, $\sigma_{zz} = \sigma - p_c$, $\sigma_{rr} = \sigma_{\theta\theta} = -p_c$, or $p = p_c - \sigma/3$, $s_{zz} = -2s_{rr} = -2s_{\theta\theta} = 2\sigma/3$. The elastic constitutive relations, Eqs. (II-7), give the axial strain rate

$$\dot{\varepsilon}_{zz} = \left[\frac{1}{3G} + \frac{1}{9K_o} \left(1 + \frac{3p_c - \sigma}{3\bar{p}} \right)^{-\frac{1}{2}} \right] \dot{\sigma} \qquad \text{(B-2)}$$

In the fitting process the initial triaxial modulus

$$M_{To} = \left[\frac{d\sigma}{d\varepsilon_{zz}} \right]_{\sigma=0}$$

was utilized. Using Eq. (2) gives

$$M_{To} = \frac{3G(1 + p_c/\bar{p})^{\frac{1}{2}}}{\frac{1}{2\beta} + (1 + p_c/\bar{p})^{\frac{1}{2}}} \qquad \text{(B-3a)}$$

where

$$\beta = 3K_o/2G \qquad \text{(B-3b)}$$

b) Uniaxial Test.

The constrained compression test may be ideally considered as a state of purely uniaxial strain. For the assumed model of the material there will be initial elastic behavior for all values of the pressure, or only up to a yield point p_y. In the latter case which is of sole interest here, the elastic phase is followed by a plastic one up to an "elastic point" p_E. Under further loading the material re-elasticizes and a second elastic phase follows.

Elastic behavior for stress levels $p > p_E$ does not occur in the elasto-plastic material with a linear relation between p and ε_{kk} as originally considered in Ref. [11]. The situation here is caused by the fact that the modulus of rigidity, G, is a constant, while the bulk modulus K is stress-dependent, the combination being equivalent to a stress-dependent Poisson's ratio ν. When, for large p, the value ν becomes sufficiently large, an increase in axial stress causes sufficiently large transverse stresses which prevent further yielding.

1) Elastic Phase $p < p_y$.

As a result of the radial constraint and of symmetry $\dot{\varepsilon}_{rr} = \dot{\varepsilon}_{\theta\theta} = 0$, while the rates of change of the stress deviators and of the pressure are related by

$$\dot{s}_{zz} = -2\dot{s}_{rr} = -2\dot{s}_{\theta\theta} = -\frac{4G}{3K(p)}\,\dot{p} \qquad \text{(B-4)}$$

The axial strain rate is therefore

$$\dot{\varepsilon}_{zz} = \frac{1}{2G}\,\dot{s}_{zz} - \frac{1}{3K(p)}\,\dot{p} = -\frac{1}{K(p)}\,\dot{p} \qquad \text{(B-5)}$$

Integration of Eqs. (4) and (5) from an unstrained and unstressed initial state gives

$$s_{zz} = -2s_{rr} = -2s_{\theta\theta} = -\frac{4G}{3}\,f(p) \qquad \text{(B-6a)}$$

$$\varepsilon_{zz} = -f(p) \qquad \text{(B-6b)}$$

where f(p) is the integral

$$f(p) = \int_0^p \frac{1}{K(\xi)}\,d\xi = \frac{2\bar{p}}{K_o}\left[(1 + p/\bar{p})^{\frac{1}{2}} - 1\right] \qquad \text{(B-7)}$$

2) Compressive Yield Point.

Substitution of Eq. (6a) into Eq. (II-4) gives

$$F(\sigma_{ij}) = \frac{4G^2}{3}\,f^2(p) - (k + 3\alpha p)^2 \leq 0; \quad p \geq -\frac{k}{3\alpha} \qquad \text{(B-8)}$$

The yield point is a root p of F=0,

$$\frac{2G}{\sqrt{3}}\,f(p) = \pm(k + 3\alpha p); \quad p \geq -\frac{k}{3\alpha} \qquad \text{(B-9)}$$

For the compressive case $p \geq 0$, $f(p) \geq 0$ so that only the upper sign in Eq. (9) is relevant. Let an auxiliary yield function for the compressive range be defined by

$$\bar{F}_c(p) = \frac{2G}{\sqrt{3}}\,f(p) - (k + 3\alpha p) \qquad \text{(B-10)}$$

For $p \geq 0$, the function $F(\sigma_{ij})$, Eq. (8), has the same sign as $\bar{F}_c$ so that the material remains elastic as long as $\bar{F}_c < 0$.

The compressive yield point p_y is the smaller positive root p_y, if any, of $\bar{F}_c(p) = 0$. To assure yield this root must not be a double root, otherwise $\bar{F}_c < 0$ would not be violated for $p > p_y$. Examination of the coefficients of the equation defining p_y gives the necessary and sufficient condition for the existence of a meaningful compressive yield point,

$$\beta a < \left(1 + \frac{\beta k\sqrt{3}}{6\bar{p}}\right) - \sqrt{\left(1 + \frac{\beta k\sqrt{3}}{6\bar{p}}\right)^2 - 1} \qquad \text{(B-11a)}$$

where

$$a = \alpha\sqrt{3} \qquad \text{(B-11b)}$$

In the limiting case $k \to 0$, the yield point becomes $p_y = 0$ and the restriction, Eq. (11a),

$$\beta a < 1 \qquad \text{(B-11c)}$$

If Eq. (11c) holds, the material in the constrained compression test yields immediately. There is no initial elastic phase, and loading begins in the plastic phase. If $\beta a \geq 1$ the material in the constrained compression test never becomes plastic.

3) Plastic Phase (For k=0).

For reasons of brevity only the case k=0 is considered from here on.

In the plastic phase the elastic strain rates are, Eqs. (II-7),

$$\dot{\varepsilon}^E_{ij} = \dot{e}^E_{ij} + \frac{1}{3}\,\dot{\varepsilon}^E_{kk}\,\delta_{ij} = \frac{1}{2G}\,\dot{s}_{ij} - \frac{1}{3K(p)}\,\dot{p}\,\delta_{ij} \qquad \text{(B-12a)}$$

The plastic strain rates for k=0 are, Eqs. (II-8a),

$$\dot{\varepsilon}^P_{ij} = \dot{e}^P_{ij} + \frac{1}{3}\,\dot{\varepsilon}^P_{kk}\,\delta_{ij} = \lambda\, s_{ij} + 2a^2\,\lambda p\,\delta_{ij} \qquad \text{(B-12b)}$$

so that

$$\dot{\varepsilon}_{ij} = \dot{\varepsilon}^E_{ij} + \dot{\varepsilon}^P_{ij} = \frac{1}{2G}\,\dot{s}_{ij} - \frac{1}{3K(p)}\,\dot{p}\,\delta_{ij} + \lambda\, s_{ij} + 2a^2\,\lambda p\,\delta_{ij} \qquad \text{(B-12c)}$$

Using cylindrical coordinates the constrained compression test implies $\dot{\varepsilon}_{rr} = \dot{\varepsilon}_{\theta\theta} = \dot{\varepsilon}_{r\theta} = \dot{\varepsilon}_{\theta z} = \dot{\varepsilon}_{zr} = 0$, and Eqs. (12c) give

$$\dot{\varepsilon}_{zz} = \frac{1}{2G}\,\dot{s}_{zz} - \frac{1}{3K(p)}\,\dot{p} + \lambda\, s_{zz} + 2a^2\,\lambda p \qquad \text{(B-13a)}$$

$$\dot{\varepsilon}_{rr} = \frac{1}{2G}\,\dot{s}_{rr} - \frac{1}{3K(p)}\,\dot{p} + \lambda\, s_{rr} + 2a^2\,\lambda p = 0 \qquad \text{(B-13b)}$$

Symmetry requires $\dot{s}_{rr} = \dot{s}_{\theta\theta} = -\tfrac{1}{2}\,\dot{s}_{zz}$, $\dot{s}_{r\theta} = \dot{s}_{\theta z} = \dot{s}_{rz} = 0$, which can be integrated, $s_{rr} = s_{\theta\theta} = -\tfrac{1}{2}\,s_{zz}$, $s_{r\theta} = s_{\theta z} = s_{rz} = 0$. The yield condition for k=0 becomes therefore $s_{zz} = \pm\, 2ap$. For the compressive case $s_{zz} < 0$ so that

$$s_{zz} = -2ap \qquad \text{(B-14)}$$

Substitution of Eq. (14) and of $s_{rr} = -\frac{1}{2} s_{zz}$ in Eq. (13b) gives

$$\lambda = - \frac{[a - \frac{2G}{3K(p)}]}{2a(1 + 2a)G} \frac{\dot{p}}{p} \tag{B-15}$$

and substitution of Eq. (15) into Eq. (13a)

$$\dot{\varepsilon}_{zz} = - \frac{3}{G(1 + 2a)} [a^2 + \frac{G}{3K(p)}] \dot{p} \tag{B-16}$$

Integration of Eq. (16) from the yield point, and use of Eq. (14) relating s_{zz} and p results finally in the desired relation between ε_{zz} and σ_{zz}

$$\varepsilon_{zz} = \frac{3}{G(1 + 2a)^2} \left\{ a^2 \sigma_{zz} + \frac{(1 + 2a)\bar{p}}{\beta} \left[1 - \sqrt{1 - \frac{\sigma_{zz}}{(1 + 2a)\bar{p}}} \right] \right\} \tag{B-17}$$

where, as previously defined, $\beta = 3K_o/2G$, $a = \alpha\sqrt{3}$.

4) Elastic Point.

The validity of Eq. (17) is subject to the restriction, Eq. (II-8b), requiring that λ computed from Eq. (15) satisfy

$$\lambda \geq 0$$

Since for compressive loading $\dot{p}/p > 0$ and $a, G > 0$ this restriction is equivalent to

$$p \leq \bar{p} \left[\frac{1}{(a\beta)^2} - 1 \right] \equiv p_E \tag{B-18}$$

where p_E is the pressure defining the elastic point. The corresponding axial stress is

$$\sigma_E = -(1 + 2a)p_E = -(1 + 2a)\bar{p}\ \left[\frac{1}{(a\beta)^2} - 1\right] \qquad \text{(B-19)}$$

For $p > p_E$, Eq. (17) is no longer valid and elastic incremental relations must be used. Note that Eq. (11c) implies $p_E > 0$ so that the plastic range is always of finite extent. For the material constants listed at the beginning of this appendix the plastic range extends up to $\sigma_E \sim 1600$ psi in Case 1 and $\sigma_E \sim 375$ psi in Case 2.

5) Initial Tangent Modulus.

Equation (17) gives the initial tangent modulus

$$M_{co} = \left[\frac{d\sigma_{zz}}{d\varepsilon_{zz}}\right]_{\sigma_{zz} = \varepsilon_{zz} = 0} = \frac{2\beta G(1 + 2a)^2}{3(1 + 2a^2\beta)} \qquad \text{(B-20)}$$

The knowledge of this result is convenient for the fitting process.

6) Plastic Shock Velocity.

Provided the pressure level is below the limit defined by Eq. (18) a plane plastic shock will propagate into the undisturbed material at a velocity $\bar{c}$ obtained from the Rankine-Hugoniot relations,

$$\bar{c}^2 = \frac{1}{\rho}\frac{\sigma^s_{zz}}{\varepsilon^s_{zz}} = \frac{G(1+2a)^2}{3\rho} \quad \frac{\sigma^s_{zz}}{a^2\,\sigma^s_{zz} + \frac{(1+2a)\bar{p}}{\beta}\left[1 - \sqrt{1 - \frac{\sigma^s_{zz}}{(1+2a)\bar{p}}}\right]}$$

(B-21)

where σ^s_{zz} and ε^s_{zz} are the normal stress and strain behind the shock.

c) Discussion of the Fit Obtained.

To demonstrate the fit obtained Figs. B-1 and B-2 show the fit for the uniaxial test. Both fit reasonably well, but Case 1 is superior*) in the stress range up to 300 psi of interest in the dynamic test discussed in Section VI.

Figure B-3 shows curves for the computed values for the initial triaxial tangent modulus M_{To} for both cases, in comparison to three available test points. The test points show large scatter, possibly due to differences in the material tested. Cases 1 and 2 fit respectively the low and high values of M_{To} .

An additional comparison can be made of the triaxial failure predictions from the theoretical models, Fig. B-4. Case 1 is extremely poor, and even Case 2 has a large error. It is a known shortcoming of the plastic model that the failure stresses are not well predicted. It must be stressed, however, that in dynamic situations the material is constrained,

*) In Case 1 the initial slope M_{co} of the test and of the computed curve have been made to agree.

and the deviation near failure may not be important, provided the portions of the triaxial test at lower stresses fit reasonably.

The above reasoning is not intended to make the claim that Case 1 should be used as a realistic model. The case was selected because it gives an excellent fit in Fig. B-1. By use of the more general relation for K(p) given in Eq. (1a) it is possible to obtain a fit as good as in Case 1, and represent the failure stress to the degree obtained for Case 2.

A comparison can also be made of the shock velocities in tests and as computed for Cases 1 and 2. The results for both cases, Fig. B-5, are of the same order of magnitude as found in the tests.

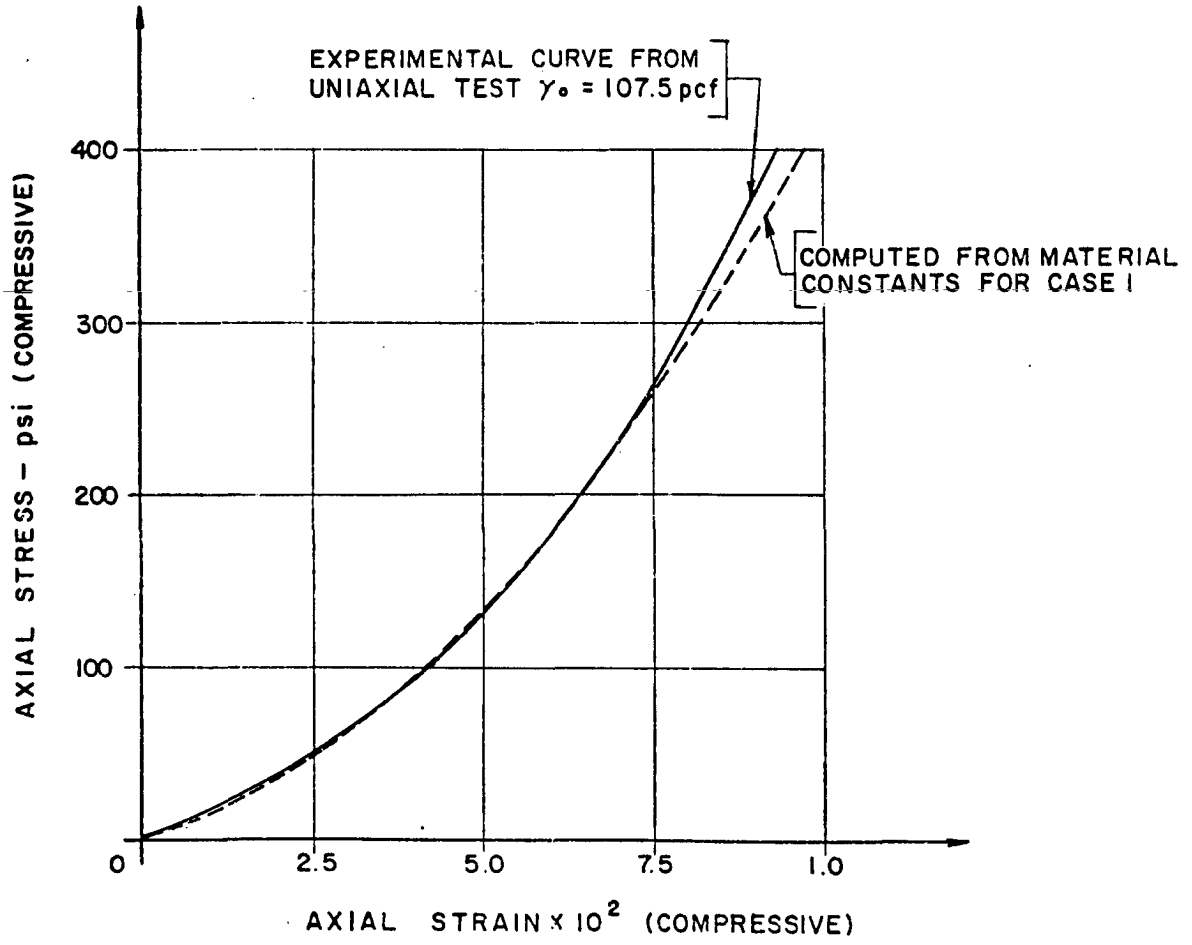

FIG. B-1 – COMPARISON FOR UNIAXIAL TEST-CASE I

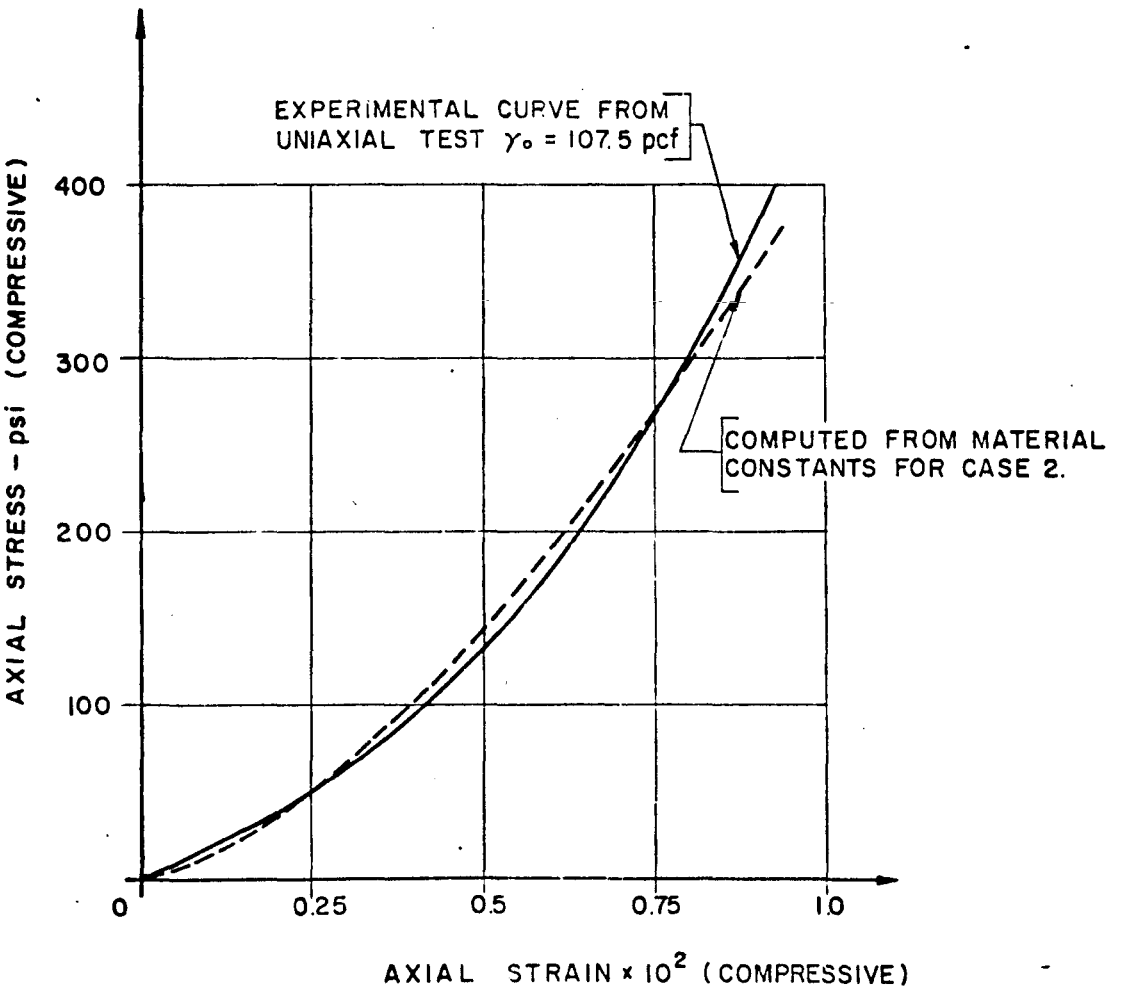

FIG. B-2 – COMPARISON FOR UNIAXIAL TEST-CASE 2

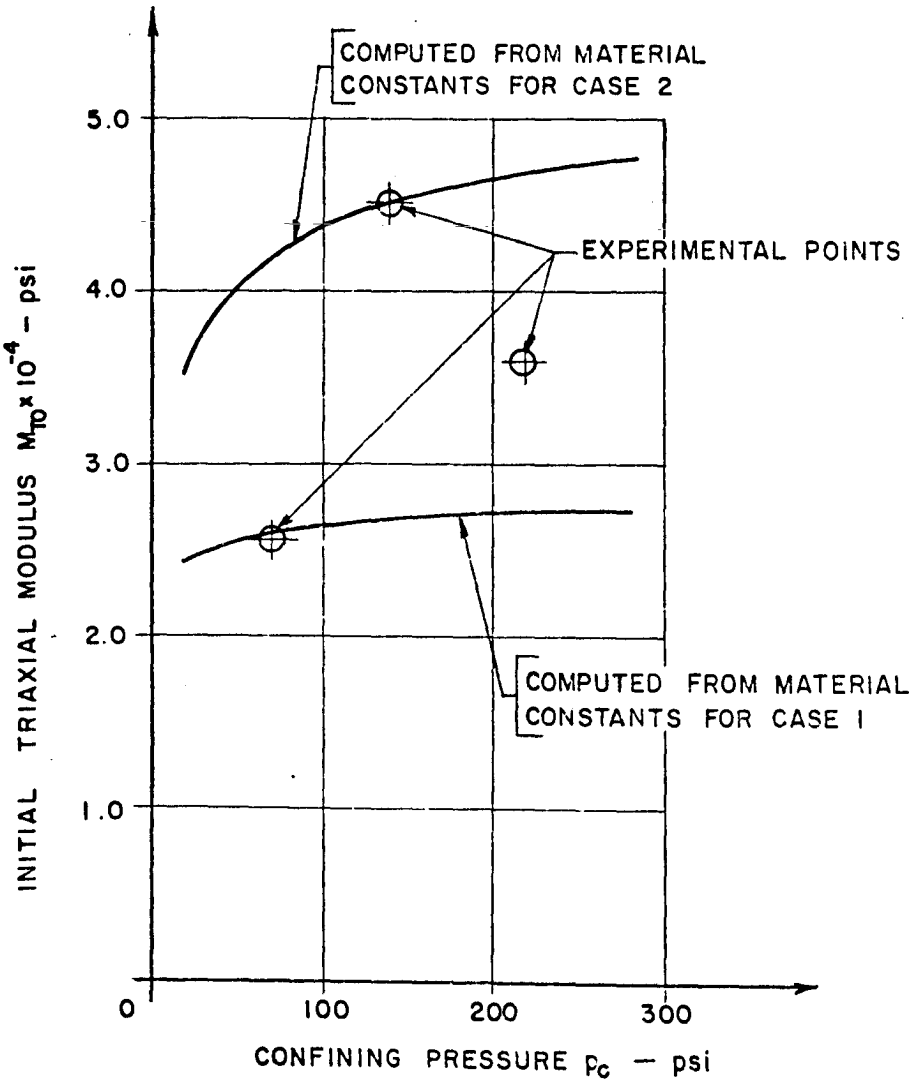

FIG. B-3 - COMPARISON FOR TRIAXIAL TEST INITIAL MODULUS

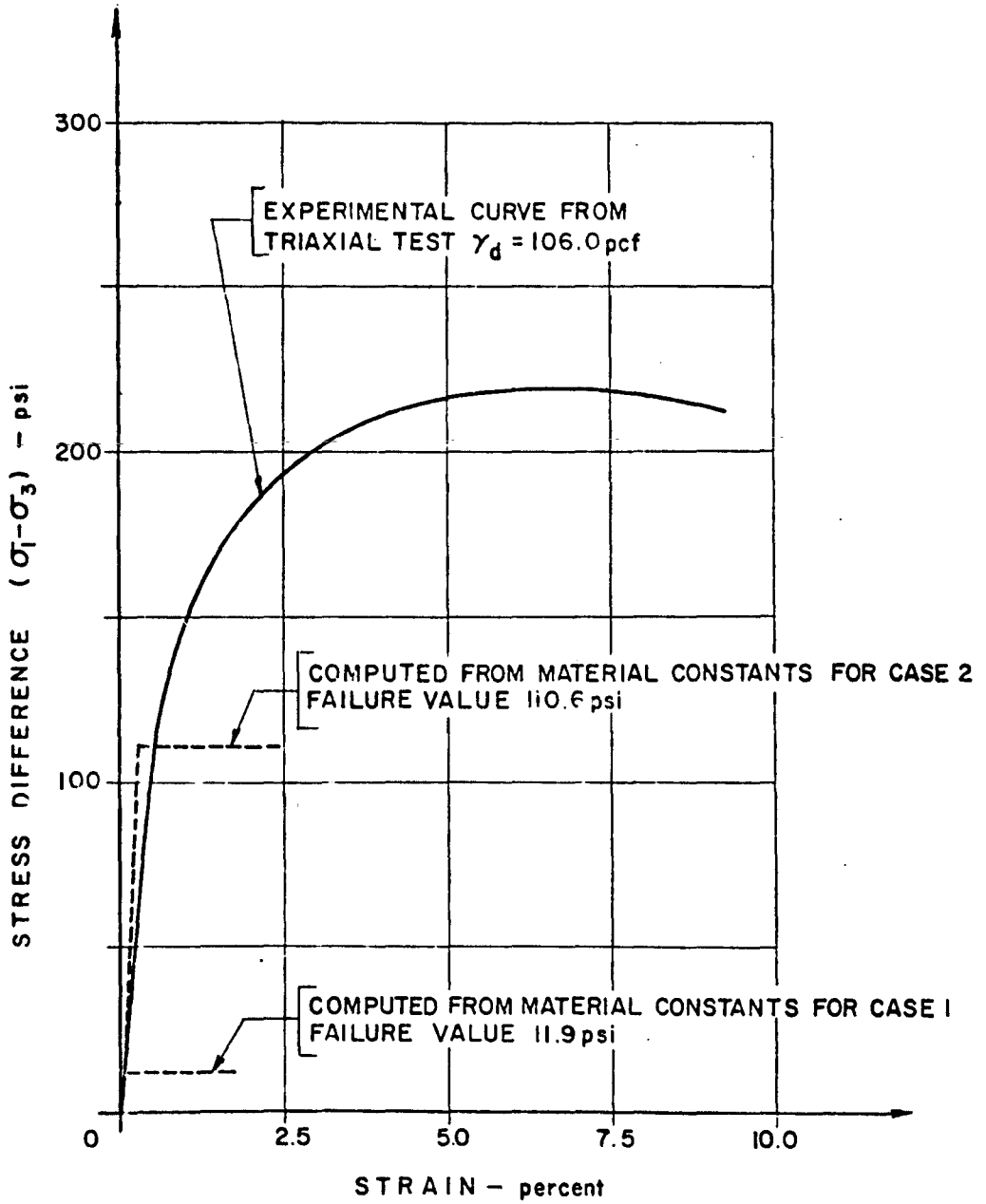

FIG. B-4 - COMPARISON FOR TRIAXIAL TEST - p_c = 70 psi

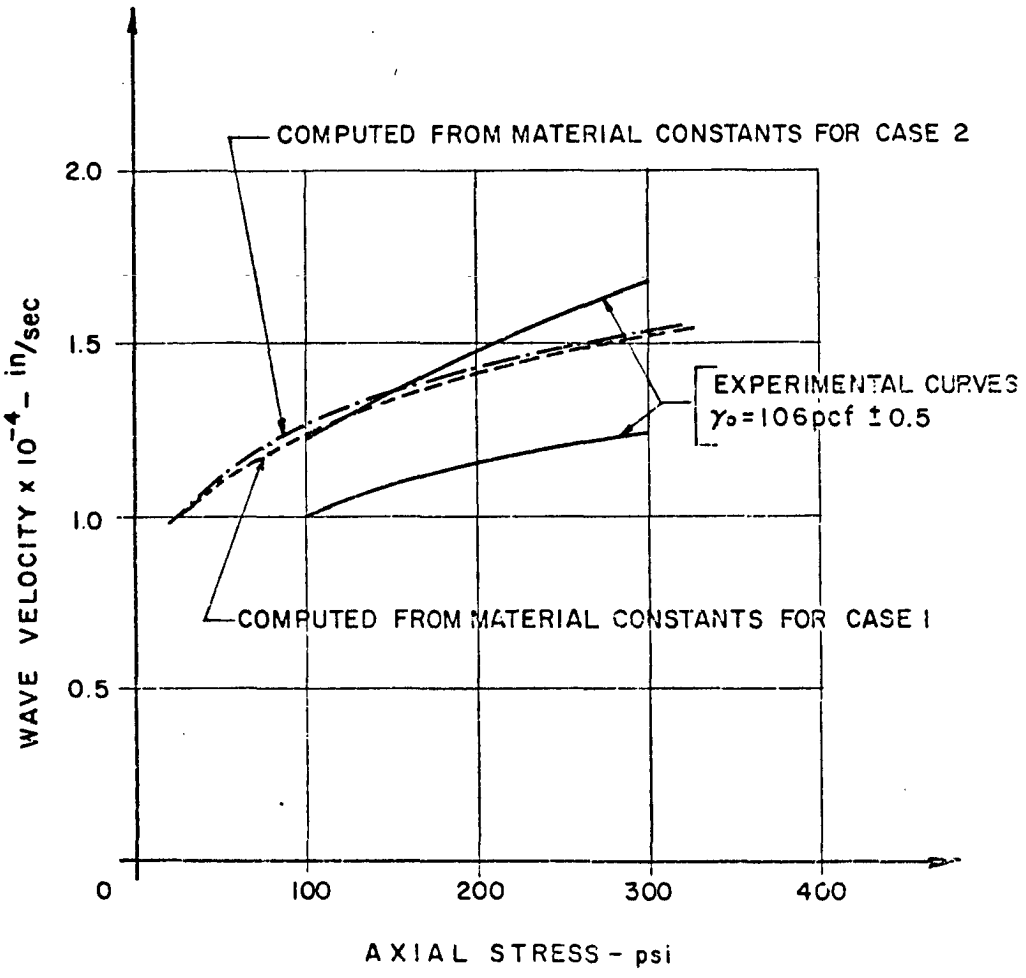

FIG. B-5 – COMPARISON FOR SHOCK-WAVE VELOCITY

APPENDIX C - Selection of the Value of C_D in the Numerical Integration.

If the exact solution contains shocks, the solution by finite differences without artifices usually shows large oscillations, which may be so severe that the results are useless. Figure C-1 shows a typical result of this type obtained from the relations in Section V when the terms with C_D are omitted. To eliminate such situations the scheme presented in Section V uses a diffusion term which reduces the oscillations to an acceptable level. The approach requires the choice of a "suitable" value of the parameter C_D occurring in the relations derived in Section V.

As the terms containing C_D modify the problem, it is necessary to make their effect as inconsequential as possible. Due to the manner in which it enters the relations, C_D should be selected as large as compatible with the purpose of elimination of oscillations caused by the finite difference scheme.

The choice of an appropriate value C_D must be made by trial for each particular set of values Δt and Δz, and may also be influenced by the location z where the results are desired. The dependence of the value of the parameter to be selected on the increments can be reduced by considering the results as a function of the combination

$$K_D = \frac{(\Delta z)^2}{(2 + C_D)\ \Delta t}$$

which occurs in Eq. (V-4). The value K_D should be selected

as small as possible.

The dependence can be seen in Fig. C-2, showing the longitudinal stress σ_{zz} for the two values $K_D \sim 3100$ and 60 $in^2/sec.$, respectively. (For the spacing used the corresponding values C_D were 2 and 50.) For the larger value K_D (smaller C_D) the result is very smooth, but the rise in pressure (which should be a shock) is very gradual, and occurs in about 30 space steps. If K_D is reduced (C_D is increased) the front becomes steeper, but there is a limit. The rise can not be reduced to less than a distance of about 3 space steps. This is roughly the situation for $K_D \sim 60$ ($C_D = 50$) in Fig. C-2. However, as the above mentioned limit is approached, oscillations of computational nature appear, and it is necessary to compromise between the desire for a rapid rise (and small overall effects of the artificial terms) and the desire for smooth results.

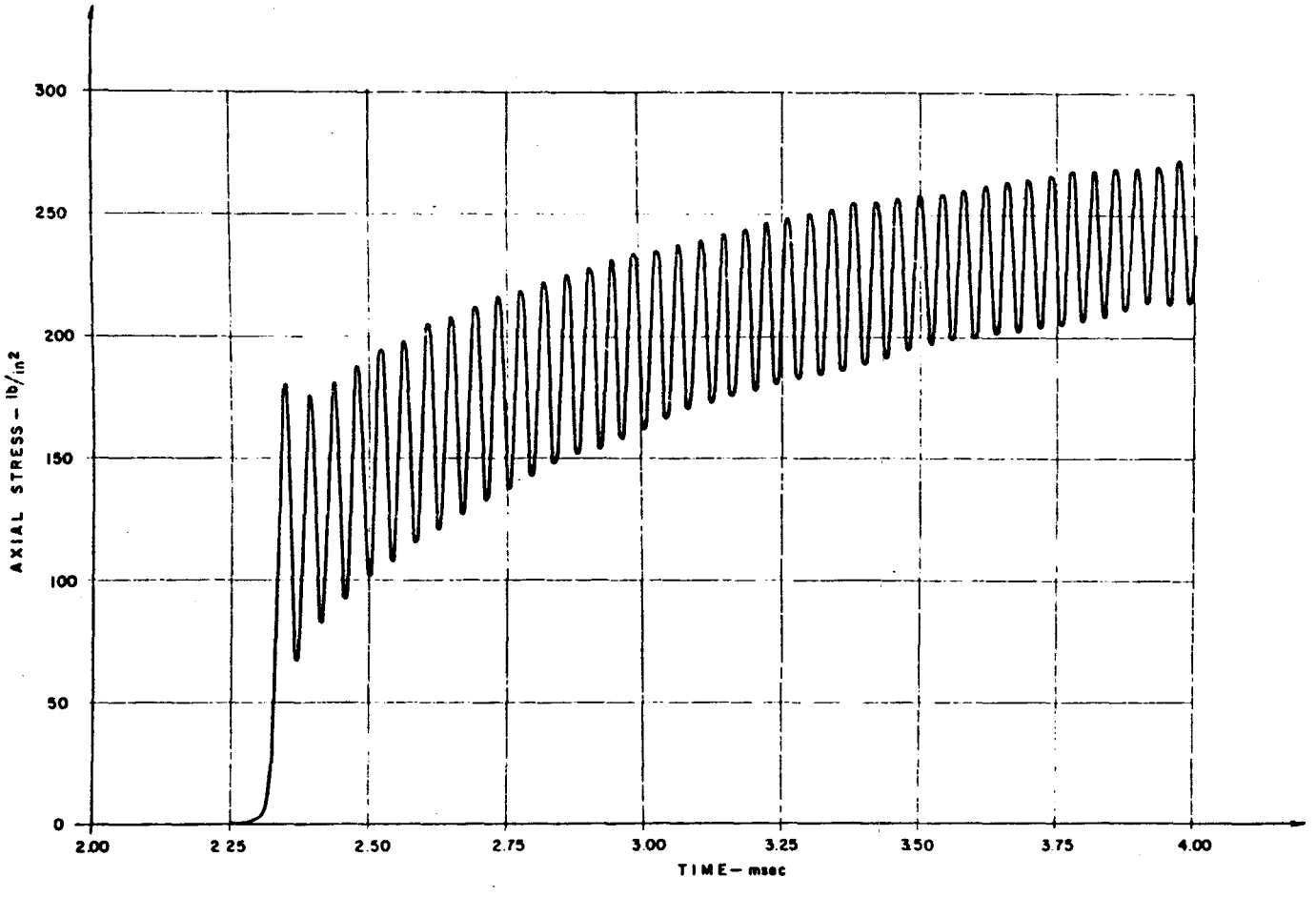

FIG. C-1 TIME HISTORY OF AXIAL STRESS AT $z = 25$ in FOR $C_0 = \infty$, $\Delta z = 0.125$ in, $\Delta t = 5 \times 10^{-3}$ msec MATERIAL CASE I ; LOADING, EQ. (XI -1)

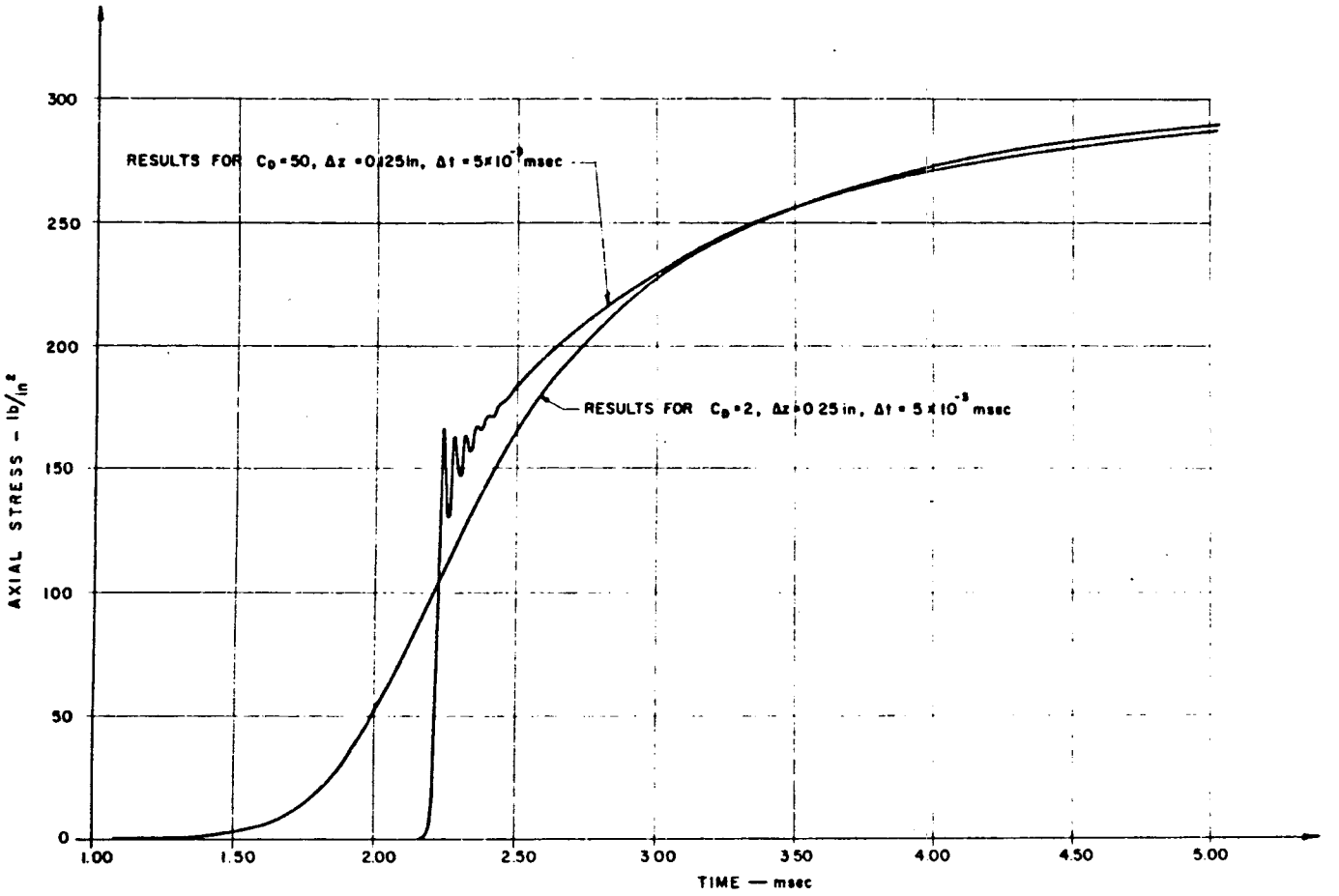

FIG. C-2 EFFECT OF THE PARAMETER C_D ON THE TIME HISTORY OF AXIAL STRESS AT $z = 25$ in
MATERIAL CASE I ; LOADING, EQ. (VI-1)

REFERENCES

[1] The Acceleration Response of a Stiff Cylinder Buried in Sand, Report in Preparation, U.S. Army Engineer Waterways Experiment Station, Vicksburg, Miss.

[2] Stoll, R.D. and Ebeido, I.A., Shock Waves in Granular Soil, Journal of the Soil Mechanics and Foundations Division, ASCE, Vol. 91, No. SM4, July 1965, pp. 107-125.

[3] Nelson, I and Baron, M.L., Development of Mathematical Material Models, Investigation of Ground Shock Effects in Nonlinear Hysteretic Materials, Report No. 1, Paul Weidlinger, Consulting Engineer, Contract No. DACA39-67-C-0048, U.S. Army Engineer Waterways Experiment Station, Vicksburg, Miss., March 1968.
A similar material prescription was used by Grigorian, S.S., On Basic Concepts in Soil Dynamics, PMM, Vol. 24, No. 6, 1960, pp. 1057-1072.

[4] Mindlin, R.D. and Herrmann, G., A One-Dimensional Theory of Compressional Waves in an Elastic Rod, Proc. First U.S. National Congress of Applied Mechanics, Chicago, Ill., June 1951, pp. 187-191.

[5] Mindlin, R.D. and McNiven, H.D., Axially Symmetric Waves in Elastic Rods, Journal of Applied Mechanics, ASME, Vol. 27, No. 1, March 1960, pp. 145-151.

[6] Skalak, R., Longitudinal Impact of a Semi-Infinite Circular Elastic Bar, Journal of Applied Mechanics, ASME, Vol. 24, No. 1, March 1957, pp. 59-64.

[7] Testa, R.B., Longitudinal Impact of a Semi-Infinite Circular Viscoelastic Rod, Columbia University, Office of Naval Research Project NR064-417, Technical Report No. 17, September 1963.

[8] Tapley, B.D. and Plass, H.D. Jr., The Propagation of Plastic Waves in a Semi-Infinite Cylinder of a Strain-Rate Dependent Material, Development in Mechanics, Vol. 1, Plenum Press, New York, 1961, pp. 256-267.

[9] Stoll, R.D. and Hess, M.S., Wave Propagation in a Stress-Relaxing Bar, Journal of the Engineering Mechanics Division, ASCE, Vol. 92, No. EM5, October 1966, pp. 25-42.

[10] Hunter, S.C. and Johnson, I.A., The Propagation of Small Amplitude Elastic-Plastic Waves in Pre-Stressed Cylindrical Bars, Proc., International Union of Theoretical and Applied Mechanics Symposium on Stress Waves in an Elastic Solid, Brown University, Providence, Rhode Island, 1963, Springer-Verlag, Berlin, 1964, pp. 149-165.

[11] Drucker, D.C. and Prager, W., Soil Mechanics and Plastic Analysis or Limit Design, Quarterly of Applied Mathematics, Vol. X, No. 2, 1952, pp. 157-165.

[12] Finlayson, B.A. and Scriven, L.E., The Method of Weighted Residuals - A Review, Applied Mechanics Reviews, Vol. 19, No. 9, September 1966, pp. 735-748.

[13] Drucker, D.C., A Definition of Stable Inelastic Material, Journal of Applied Mechanics, ASME, Vol. 26, No. 1, March 1959, pp. 101-106.

[14] Ames, W.F., Nonlinear Partial Differential Equations in Engineering, Academic Press, New York, 1965, pp. 453-460.

[15] Wilkins, M.L., Calculation of Elastic-Plastic Flow, Methods in Computational Physics, Vol. 3, Academic Press, New York, 1964, pp. 211-263.

[16] Richtmeyer, R.D. and Morton, K.W., Difference Methods for Initial Value Problems, Interscience Publishers, New York, 1967, 2nd Edition.

[17] King, W.W. and Frederick, D., Transient Elastic Waves in a Fluid-Filled Cylinder, Journal of the Engineering Mechanics Division, ASCE, Vol. 94, No. EM5, October 1968, pp. 1215-1230.

[18] Durbin, W.L., Steady Dynamic Stress-Strain and Wave Propagation Characteristics of Soils, United Research Inc., Contract No. DA-22-079-eng-373, Report No. 3, U.S. Army Engineer Waterways Experiment Station, Vicksburg, Miss.

[19] Dorris, A.F., Response of Horizontally Oriented Buried Cylinders to Static and Dynamic Loadings, U.S. Army Engineer Waterways Experiment Station, Report No. 1-682, Vicksburg, Miss., July 1965.

NUCLEAR WEAPONS EFFECTS DIVISION REPORTS

DISTRIBUTION LIST

Address	Normal No. of Copies
Army	
Chief of Engineers, Department of the Army, Washington, D. C. 20314	
ATTN: ENGME-S	1
ENGME	1
ENGCW-E	1
ENGCW-Z	1
ENGMC-E	1
ENGMC-EM	1
ENGMC-DE	1
ENGAS-I	1
ENGAS-I, Library	1
ENGNA	1
Chief of Research and Development, Headquarters, Department of the Army, Washington, D. C. 20310 ATTN: Director of Army Technical Information	3 copies of Form 1473
Chief of Research and Development, Department of the Army, Washington, D. C. 20310	
ATTN: Atomic Office	1
CRDES	1
Division Engineers, U. S. Army Engineer Divisions, Continental United States	Cy to ea
Commandant, U. S. Army Air Defense School, Fort Bliss, Tex. 79906	1
Commandant, U. S. Army Command & General Staff College, Fort Leavenworth, Kans. 66027 ATTN: Archives	1
Commandant, Army War College, Carlisle Barracks, Pa. 17013 ATTN: Library	1
Commanding General, Aberdeen Proving Ground, Aberdeen, Md. 21005 ATTN: Director, Ballistic Research Laboratories	4
Commanding General, The Engineer Center, Fort Belvoir, Va. 22060 ATTN: Assistant Commandant, Engineer School	1
Commanding General, U. S. A. Electronics Command, Fort Monmouth, N. J. 07703 ATTN: AMSEL-GG-DD	1
Commanding General, USA Missile Command, Huntsville, Ala. 35809	1
Commanding General, USA Munition Command, Dover, N. J. 07801	1
Commanding General, U. S. Continental Army Command, Fort Monroe, Va. 23351	1

Address	Normal No. of Copies
Army (Continued)	
Commanding General, U. S. Army Materiel Command, Washington, D. C. 20310 ATTN: AMCRD-DE-N	2
Commanding Officer, Picatinny Arsenal, Dover, N. J. 07801 ATTN: ORDBB-TK	1
Commanding Officer, U. S. Army Aviation Materiel Laboratories, Fort Eustis, Va. 23604	1
Commanding Officer, U. S. Army Combat Developments Command, Institute of Nuclear Studies, Fort Bliss, Tex. 79916	2
Commanding Officer, U. S. Army Mobility Equipment Research and Development Center Fort Belvoir, Va. 22060 ATTN: Technical Documents Center, Building 315	1
Commanding Officer, U. S. Army Nuclear Defense Laboratory, Edgewood Arsenal Edgewood, Md. 21040 ATTN: Technical Library	1
Department of the Army, CE Ballistic Missile Construction Office, P. O. Box 4187 Norton AFB, Calif. 92409	1
Director of Civil Defense, Office of the Secretary of the Army, Washington, D. C. 20310 ATTN: Mr. George Sisson (RE-ED)	2
Director, Nuclear Cratering Group, U. S. Army Corps of Engineers, Lawrence Radiation Laboratory, P. O. Box 808, Livermore, Calif. 94550	1
Director, U. S. Army Corps of Engineers, Coastal Engineering Research Center Washington, D. C. 20016 ATTN: Mr. T. Saville, Jr.	1
Director, U. S. Army Corps of Engineers, Ohio River Division Laboratories, 5851 Mariemont Avenue, Cincinnati, Ohio 45227	1
Technical Library USAMERDC, Bldg 314 Fort Belvoir, Va. 22060	1
Director, U. S. Army CRREL, P. O. Box 282, Hanover, N. H. 03755 ATTN: Mr. K. Boyd	1
Director, U. S. Army Construction Engineering Research Laboratory, P. O. Box 4005, Champaign, Ill. 61820 ATTN: Library	1

NWED Reports Distribution List

Address	Normal No. of Copies
Army (Continued)	
District Engineer, U. S. Army Engineer District, Omaha, 6012 U. S. Post Office and Court House 215 N. 17th Street, Omaha, Nebr. 68101 ATTN: MROGS-B	1
President, U. S. Army Air Defense Board, Fort Bliss, Tex. 79906	1
Superintendent, U. S. Military Academy, West Point, N. Y. 10996 ATTN: Library	2
U. S. Army Engineer Division, Missouri River, P. O. Box 103, Downtown Station Omaha, Nebr. 68101 ATTN: Mr. Ken Lane	1
Navy	
Commander-in-Chief, Pacific, FPO, San Francisco 94129	1
Commander-in-Chief, U. S. Atlantic Fleet, U. S. Naval Base, Norfolk, Va. 23511	1
Chief of Naval Operations, Navy Department, Washington, D. C. 20350 ATTN: OP-75 OP-03EG	 2 1
Chief of Naval Research, Navy Department, Washington, D. C. 20390 ATTN: Code 811	1
Commandant of the Marine Corps, Navy Department, Washington, D. C. 20380 ATTN: Code A04E	2
Commander, Naval Facilities Engineering Command, Navy Department, Washington, D. C. 20370 ATTN: Code 04 Code 03	 1 1
Commander, Naval Ordnance Systems Command, Washington, D. C. 20360	1
Commander, Naval Ship Engineering Center, Washington, D. C. 20360 ATTN: Code 6115	1
Commanding Officer, Nuclear Weapons Training Center, Atlantic Naval Base, Norfolk, Va. 23511 ATTN: Nuclear Warfare Department	1
Commanding Officer, Nuclear Weapons Training Center, Pacific, Naval Station, North Island San Diego, Calif. 92136	2
Commanding Officer & Director, Naval Electronics Laboratory, San Diego, Calif. 92152	1
Commanding Officer & Director, Naval Ship Research and Development Center Carderock, Md. 20007	1
Commanding General, Marine Corps Development and Education Command, Quantico, Va. 22134 ATTN: Director, Development Center	2

Address	Normal No. of Copies
Navy (Continued)	
Commanding Officer & Director, U. S. Naval Civil Engineering Laboratory Port Hueneme, Calif. 93041 ATTN: Code L31	2
Commanding Officer, U. S. Naval Civil Engineer Corps Officer School, U. S. Naval Construction Battalion Center, Port Hueneme, Calif. 93041	1
Commanding Officer, U. S. Naval Damage Control Training Center, Naval Base Philadelphia, Pa. 19112 ATTN: ABC Defense Course	1
Commanding Officer, U. S. Naval Weapons Evaluation Facility, Kirtland Air Force Base Albuquerque, N. Mex. 87117 ATTN: Code WEVS	1
Commanding Officer, U. S. Naval Weapons Laboratory, Dahlgren, Va. 22448 ATTN: TE	1
Commander, U. S. Naval Oceanographic Office, Suitland, Md. 20023	1
Commander, U. S. Naval Ordnance Laboratory, Silver Spring, Md. 20910 ATTN: EA EU E	 1 1 1
Commander, U. S. Naval Ordnance Test Station, China Lake, Calif. 93555	1
Director, U. S. Naval Research Laboratory, Washington, D. C. 20390	1
President, U. S. Naval War College, Newport, R. I. 02840	1
Special Projects, Navy Department, Washington, D. C. 20360 ATTN: SP-272	1
Superintendent, U. S. Naval Postgraduate School, Monterey, Calif. 93940	1
Underwater Explosions Research Division, Naval Ship Research and Development Center Norfolk Naval Shipyard, Portsmouth, Va. 23511	1
Air Force	
Air Force Flight Dynamics Laboratory, Wright-Patterson AFB, Dayton, Ohio 45433 ATTN: Mr. Frank Janik, Jr.	1
Air Force Institute of Technology, AFIT-L, Building 640, Wright-Patterson AFB, Ohio 45433	1
Commander, Air Force Logistics Command, Wright-Patterson AFB, Ohio 45433	2
Air Force Systems Command, Andrews Air Force Base, Washington, D. C. 20331 ATTN: SCTSW	1

Address	Normal No. of Copies
Air Force (Continued)	
Air Force Technical Applications Center, Department of the Air Force, Washington, D. C. 20333	1
Air Force Weapons Laboratory, Kirtland AFB, N. Mex. 87117	
ATTN: Library	2
WLDC	1
WLDC/R. W. Henny	1
Director, Air University Library, Maxwell AFB, Ala. 36112	2
Commander, Strategic Air Command, Offutt AFB, Nebr. 68113 ATTN: OAWS	1
Commander, Tactical Air Command, Langley AFB, Va. 23365 ATTN: Document Security Branch	1
Space and Missile Systems Organization, Norton AFB, Calif. 92409 ATTN: SAMSO (SMQNM)	1
Headquarters, USAF, Washington, D. C. 20330 ATTN: AFRSTG	1
Director, Air Research and Development Command Headquarters, USAF Washington, D. C. 20330 ATTN: Combat Components Division	1
Director of Civil Engineering, Headquarters, USAF, Washington, D. C. 20330 ATTN: AFOCE	1
Director, U. S. Air Force Project RAND, Via: U. S. Air Force Liaison Office, The RAND Corporation, 1700 Main Street, Santa Monica, Calif. 90406	
ATTN: Library	1
Dr. Harold L. Brode	1
Dr. Olen A. Nance	1
Other DOD Agencies	
Administrator, National Aeronautics & Space Administration, 400 Maryland Avenue, S. W. Washington, D. C. 20546	1
Assistant to the Secretary of Defense (Atomic Energy), Washington, D. C. 20301	1
Commandant, Armed Forces Staff College, Norfolk, Va. 23511 ATTN: Library	1
Commandant, National War College, Washington, D. C. 20310 ATTN: Class Rec. Library	1
Commandant, The Industrial College of the Armed Forces, Fort McNair Washington, D. C. 20310	1

Address	Normal No. of Copies
Other DOD Agencies (Continued)	
Commander, Test Command, DASA, Sandia Base, Albuquerque, N. Mex. 87115 ATTN: TCCOM, TCDT	2
Commander, Field Command, DASA, Sandia Base, Albuquerque, N. Mex. 87115	2
Defense Documentation Center (DDC), Cameron Station, Alexandria, Va. 22314 (NO TOP SECRET TO THIS ADDRESS) ATTN: Mr. Myer Kahn	20
Director, Defense Atomic Support Agency, Washington, D. C. 20301 ATTN: SPSS STAP	 5 2
Director of Defense Research and Engineering, Washington, D. C. 20301 ATTN: Technical Library Mr. Frank J. Thomas	 1 1
Director, Advanced Research Projects Agency, Washington, D. C. 20301 ATTN: NTDO	1
Director, Defense Intelligence Agency, Washington, D. C. 20301 ATTN: DIA-AP8B-1	1
Director, Weapons Systems Evaluation Group, Washington, D. C. 20305	1
Langley Research Center, NASA, Langley Field, Hampton, Va. 23365 ATTN: Mr. Philip Donely	1
Manager, Albuquerque Operations Office, USAEC, P. O. Box 5400, Albuquerque, N. Mex. 87115	1
Manager, Nevada Operations Office, USAEC, P. O. Box 1676, Las Vegas, Nev. 89101	1
National Aeronautics & Space Administration, Man-Spacecraft Center, Space Technology Division, Box 1537, Houston, Tex. 77001	1
National Military Command System Support Center, Pentagon BE 685, Washington, D. C. 20301 ATTN: Technical Library	1
U. S. Atomic Energy Commission, Washington, D. C. 20545 ATTN: Chief, Classified Tech Lib, Tech Information Service	1
U. S. Documents Officer, Office of the United States National Military Representative–SHAPE APO New York 09055	1
Other Agencies	
Aerospace Corporation, 1111 E. Mill Street, San Bernardino, Calif. 92408 ATTN: Dr. M. B. Watson	1
Agbabian-Jacobsen Associates, Engineering Consultants, 8939 South Sepulveda Boulevard Los Angeles, Calif. 90045	1

Address	Normal No. of Copies
Other Agencies (Continued)	
Applied Theory, Inc., 1728 Olympic Blvd, Santa Monica, Calif. 90404 ATTN: Dr. John G. Trulio	1
AVCO Corporation, Research and Advanced Development Division, 201 Lowell Street Wilmington, Mass. 01887 ATTN: Mr. R. E. Cooper	1
Battelle Memorial Institute, 505 King Avenue, Columbus, Ohio 43201 ATTN: Dr. P. N. Lamori	1
Bell Telephone Laboratories, Inc., Whippany Road, Whippany, N. J. 07981 ATTN: Mr. R. W. Mayo	1
The Boeing Company, P. O. Box 3707, Seattle, Wash. 98124 ATTN: Technical Library	1
Corrugated Metal Pipe Institute, Crestview Plaza, Port Credit, Ontario, Canada ATTN: Mr. W. A. Porter	1
Defence Research Establishment, Suffield, Ralston, Alberta, Canada	1
General Research Corporation, P. O. Box 3587, Santa Barbara, Calif. 93105 ATTN: Mr. Benjamin Alexander	1
Denver Mining Research Center, Building 20, Denver Federal Center, Denver, Colo. 80225 ATTN: Dr. Leonard A. Obert	1
Dynamic Science Corporation, 1900 Walker Avenue, Monrovia, Calif. 91016 ATTN: Dr. J. C. Peck	1
Edgerton, Germeshausen & Grier, Inc., 95 Brookline Avenue, Boston, Mass. 02129 ATTN: D. F. Hansen	1
Engineering Physics Company, 12721 Twinbrook Parkway, Rockville, Md. 20852 ATTN: Dr. Vincent J. Cushing Mr. W. Danek	1 1
General American Transportation Corporation, General American Research Division 7449 North Natchez Avenue, Niles, Ill. 60648 ATTN: Dr. G. L. Neidhardt	1
General Electric Company, Missile and Space Vehicle Department, Valley Forge Space Technology Center, Goddard Boulevard, King of Prussia, Pa. 19406	1
General Electric Company, TEMPO, 816 State Street, Santa Barbara, Calif. 93101 ATTN: Mr. Warren Chan (DASIAC)	1
Chief, Structural and Applied Mechanics Branch, Bureau of Public Roads, Federal Highway Administration, Washington, D. C. 20591 ATTN: Mr. F. J. Tamanini	1

Address	Normal No. of Copies
Other Agencies (Continued)	
IIT Research Institute, 10 West 35th Street, Chicago, Ill. 60616 ATTN: Dr. K. McKee	1
Kondner Research, Downes Road, Parkton, Md. 21120 ATTN: Dr. R. L. Kondner	1
Lockheed Missile and Space Company, Lockheed Aircraft Corporation, 111 Lockheed Way Sunnyvale, Calif. 94086 ATTN: Dr. R. E. Meyerott	1
Los Alamos Scientific Laboratory, P. O. Box 1663, Los Alamos, N. Mex. 87544 ATTN: Report Librarian	1
Ministry of Defense, MEXE, Christchurch, Hampshire, England ATTN: Dr. Philip S. Bulson Mr. Bruce T. Boswell	 1 1
The Mitre Corporation, Route 62 and Middlesex Turnpike, Bedford, Mass. 01730	1
Physics International Company, 2700 Merced Street, San Leandro, Calif. 94577 ATTN: Dr. Charles Godfrey Mr. Fred M. Sauer	 1 1
Research Analysis Corporation, Document Control Supervisor, McLean, Va. 22101	1
Dr. John S. Rinehart, Senior Research Fellow (R.2), IER/ESSA, Boulder, Colo. 80302	1
Sandia Laboratories, P. O. Box 5800, Albuquerque, N. Mex. 87115 ATTN: Classified Document Division for Dr. M. L. Merritt	1
Southwest Research Institute, 8500 Culebra Road, San Antonio, Tex. 78228 ATTN: Dr. Robert C. DeHart	1
Systems, Science and Software, P. O. Box 1620, La Jolla, Calif. 92037 ATTN: Mr. K. D. Pyatt, Jr.	1
TRW Space Technology Laboratories, One Space Park, Redondo Beach, Calif. 90278 ATTN: Dr. Millard Barton Mr. Fred Pieper Mr. J. L. Merritt	 1 1 1
URS Corporation, 1811 Trousdale Drive, Burlingame, Calif. 94010 ATTN: Mr. James Halsey	2
U. S. Department of the Interior, Geological Survey, Geologic Division, Branch of Engineering Geology, 345 Middlefield Road, Menlo Park, Calif. 94025 ATTN: Harold W. Olsen	1
Paul Weidlinger, Consulting Engineer, 110 East 59th Street, New York, N. Y. 10022 ATTN: Dr. M. L. Baron	5

Address	Normal No. of Copies
College and Universities	
University of Arizona, Tucson, Ariz. 85721	
ATTN: Dr. Donald A. DaDeppo, Department of Civil Engineering	1
Professor Bruce G. Johnston, Dept of Civil Engineering	1
Dr. George Howard, College of Engineering	1
University of California, Lawrence Radiation Laboratory, P. O. Box 808 Livermore, Calif. 94550 ATTN: Technical Information Division	2
University of Colorado, School of Architecture, Boulder, Colo. 80304 ATTN: Professor G. K. Vetter	1
University of Detroit, Department of Civil Engineering, 4001 West McNichols Road Detroit, Mich. 48221 ATTN: Professor W. J. Baker	1
University of Florida, Department of Mechanical Engineering, Gainesville, Fla. 32603 ATTN: Professor John A. Samuel	1
Florida State University, Department of Engineering Science, Tallahassee, Fla. 32302 ATTN: Dr. G. L. Rogers	1
University of Illinois, Urbana Campus, Department of Civil Engineering, Urbana, Ill. 61801	
ATTN: Professor N. M. Newmark	1
Professor S. L. Paul	1
Professor M. T. Davisson	1
Professor G. K. Sinnamon	1
Professor W. J. Hall	1
Professor A. J. Hendron, Jr.	1
Professor M. A. Sozen	1
Iowa State University of Science and Technology, Ames, Iowa 50010 ATTN: Professor Glen Murphy	2
Lehigh University, Bethlehem, Pa. 18015	
ATTN: Dr. J. F. Libsch, Materials Research Center	1
Dr. D. A. Van Horn, Department of Civil Engineering	1
University of Massachusetts, Department of Civil Engineering, Amherst, Mass. 01002 ATTN: Dr. M. P. White	1
Massachusetts Institute of Technology, Division of Sponsored Research, 77 Massachusetts Avenue, Cambridge, Mass. 02139	
ATTN: Dr. Robert J. Hansen	1
Dr. Robert V. Whitman	1
University of Michigan, Civil Engineering Department, Ann Arbor, Mich. 48104 ATTN: Professor Frank E. Richart, Jr., Consultant	1

Address	Normal No. of Copies
College and Universities (Continued)	
Dr. George B. Clark, Director, Rock Mechanics Research Group, University of Missouri at Rolla, Rolla, Mo. 65401	1
University of New Mexico, Eric H. Wang Civil Engineer Research Facility, Albuquerque, N. Mex. 87106 ATTN: Dr. Eugene Zwoyer	1
University of New Mexico, Eric H. Wang Civil Engineering Research Facility, P. O. Box 188 University Station, Albuquerque, N. Mex. 87106	2
Nova Scotia Technical College, School of Graduate Studies, Halifax, Nova Scotia, Canada ATTN: Dr. G. G. Meyerhof	1
Pennsylvania State University, University Park, Pa. 16802	
ATTN: Professor G. Albright, Dept of Architectural Engineering	1
Professor Richard Kummer, 101 Eng. A	1
Purdue University, School of Civil Engineering, Civil Engineering Building, Lafayette, Ind. 47907 ATTN: Professor M. B. Scott	1
Rensselaer Polytechnic Institute, Troy, N. Y. 12180 ATTN: Dr. Clayton Oliver Dohrenwend, Security Officer, Mason House	1
Rice University, Department of Civil Engineering, Houston, Tex. 77001 ATTN: Professor A. S. Veletsos	1
San Jose State College, Department of Civil Engineering, San Jose, Calif. 95114 ATTN: Dr. Franklin J. Agardy	1
University of Texas, Balcones Research Center, Austin, Tex. 78712 ATTN: Dr. J. Neils Thompson	1
Utah State University, Department of Mechanical Engineering, Logan, Utah 84321 ATTN: Professor R. K. Watkins	1
University of Washington, Seattle, Wash. 98105	
ATTN: C. H. Norris, Department of Civil Engineering	1
Dr. A. B. Arons, Department of Physics	1
Professor William Miller, Department of Civil Engineering, 307 More Hall	1
The George Washington University, Nuclear Defense Design Center, School of Engineering and Applied Science, Washington, D. C. 20006	1
Worcester Polytechnic Institute, Department of Civil Engineering, Worcester, Mass. 01609 ATTN: Dr. Carl Koontz	1
Northern Arizona University, Box 5753, Flagstaff, Arizona 86001 ATTN: Professor Sandor Popovics	1

UNCLASSIFIED

Security Classification

DOCUMENT CONTROL DATA - R & D

(Security classification of title, body of abstract and indexing annotation must be entered when the overall report is classified)

1. ORIGINATING ACTIVITY (Corporate author)	2a. REPORT SECURITY CLASSIFICATION
Paul Weidlinger, Consulting Engineer New York, New York	Unclassified
	2b. GROUP

3. REPORT TITLE

STRESS WAVES IN A SOIL-FILLED CYLINDRICAL SHELL

4. DESCRIPTIVE NOTES (Type of report and inclusive dates)

Final Report

5. AUTHOR(S) (First name, middle initial, last name)

John Kovarna and Hans H. Bleich

6. REPORT DATE	7a. TOTAL NO. OF PAGES	7b. NO. OF REFS
May 1970	104	19

8a. CONTRACT OR GRANT NO.	9a. ORIGINATOR'S REPORT NUMBER(S)
DACA39-67-C-0021 b. PROJECT NO.	
c.	9b. OTHER REPORT NO(S) (Any other numbers that may be assigned this report) U. S. Army Engineer Waterways Experiment Station Contract Report N-70-2
d.	

10. DISTRIBUTION STATEMENT

This document has been approved for public release and sale; its distribution is unlimited.

11. SUPPLEMENTARY NOTES	12. SPONSORING MILITARY ACTIVITY
Prepared under contract for U. S. Army Engineer Waterways Experiment Station, Vicksburg, Miss.	Defense Atomic Support Agency Washington, D. C.

13. ABSTRACT

An approximate solution to the problem of transient longitudinal wave propagation in a semi-infinite cylindrical body of elasto-plastic material restrained radially by a stacked-ring shell and subjected to a normal pressure at the end is obtained by a Galerkin technique using the radial coordinate as an expansion parameter. In order to get equations applicable to numerical computations the expansions are truncated to the leading term in each variable. This truncation creates a mathematical problem when elastic and plastic regions occur along the same radial line. A finite-difference scheme is used to solve the differential equations resulting from application and truncation of the Galerkin expansion. A special method for handling the boundary between elastic and plastic regions along the same radial line is developed in conjunction with this numerical solution. Numerical results of the finite-difference scheme are presented for several variations in such parameters as shell stiffness and material constants. For the purpose of evaluating the results of the truncation to the leading term in each expansion, the analogous problem is formulated for a linear inviscid fluid and solved twice, once with a truncation to the first term and once carrying two terms in each expansion. The numerical results are presented for these two solutions so that the change in the solution caused by the truncation can be evaluated.

DD FORM 1 NOV 65 1473 REPLACES DD FORM 1473, 1 JAN 64, WHICH IS OBSOLETE FOR ARMY USE.

UNCLASSIFIED

Security Classification

14. KEY WORDS	LINK A		LINK B		LINK C	
	ROLE	WT	ROLE	WT	ROLE	WT
Ground Shock						
Wave Propagation						
Soil Shell Interaction						